Université Grenoble Alpes

Mémoire de recherche

Pour l'obtention du diplôme

d'Habilitation à Diriger les Recherches
DE L'UNIVERSITE GRENOBLE ALPES

Présenté par

Maria Eletta NEGRETTI

préparée au sein du
Laboratoire des Écoulements Géophysiques et Industriels
LEGI UMR5519 (UGA/CNRS/Grenoble INP)

dans **l'École Doctorale**
Sciences de la Terre, de l'Environnement et des Planètes
(ED STEP)

The turbulent life of buoyancy driven flows

soutenue publiquement le **17 décembre 2021**
devant le jury composé de :

M. David Hurther
Directeur de Recherche, LEGI/CNRS, Univ. Grenoble Alpes, *Président*
Mme. Laurette Tuckerman
Directrice de Recherche, PMMH/CNRS, ESPCI Paris, *Rapporteur*
Mme. Claudia Cenedese
Directrice de Recherche, WHOI, Massachuttes, USA, *Rapporteur*
M. Koen Blanckaert
Professeur, Vienna University of Technology (TUW), *Rapporteur*
Mme. Florence Naaim-Bouvet
Ingénieure Chercheuse, ETNA/INRAE Grenoble, *Examinateur*
M. Pietro Salizzoni
Professeur, MFAE/LMFA Ecole Centrale de Lyon, *Examinateur*

«"O frati," dissi, "che per cento milia
perigli siete giunti a l'occidente,
a questa tanto picciola vigilia

d'i nostri sensi ch'è del rimanente
non vogliate negar l'esperïenza,
di retro al sol, del mondo sanza gente.

Considerate la vostra semenza:
fatti non foste a viver come bruti,
ma per seguir virtute e canoscenza".»

[…]

Noi ci allegrammo, e tosto tornò in pianto,
ché de la nova terra un turbo nacque,
e percosse del legno il primo canto.

Tre volte il fé girar con tutte l’acque;
a la quarta levar la poppa in suso
e la prora ire in giù, com’altrui piacque,

infin che ’l mar fu sovra noi richiuso».

(vv. 112-120, 136-142, Dante Alighieri, Divina Commedia, Inferno Canto XXVI)

Contents

Part I

Scientific coursus and curriculum vitae

Chapter 1

Summary of my scientific coursus

I earned my MS+BS in Environmental Engineering in 2003, including a supplementary year of courses done at the faculty of Physics and Mathematics of the University of Trento (Italy) chosen to deepen my knowledge in fundamental disciplines. I started my research activity in 2002 as an exchange student at the Karlsruhe Institute of Technology (KIT), in Germany. There, I came in contact with G.H. Jirka, who conducted fundamental research beside more applied environmental engineering problems. Fascinated in particular by laboratory experiments he conducted at that time in the field of shallow turbulent flows (jets and wakes), I decided to extend my exchange program to perform part of my master internship in his research group, performing a set of laboratory experiments on shallow turbulent wakes. I continued on this research topic in 2003 at the Department of Environmental Engineering under direction of M. Tubino, where I proposed to complete my master thesis initiated at the KIT with an analytical work consisting in extending the self-similar theory relative to turbulent wakes under conditions of shallow water flows. I have been awarded with the 'Ehrensenator Huber Price' for the best Master thesis at the KIT in 2004. This work resulted in 2 journal articles (`publications [80, 83]`).

Further motivated to continue in fundamental fluid mechanics, I started my PhD at the end of 2003 at the KIT under supervision of G.H. Jirka in the field of stratified flows, and more precisely on two-layer stratified exchange flows over topography as a physical model of sea straits. Herein, I became acquainted also with modern experimental techniques such as simultaneous PIV and LIF for velocity and concentration fields and theoretical work by means of linear stability analysis working closely with S.A. Socolofsky (Texas A&M University, USA). The main outcome concerned the identification of a pulsing phenomenon in the gravity flow that explained an anomalous behaviour observed in both oceanic field measurements and laboratory experiments. The PhD work has been published in 4 journal articles (`publications [84--86, 117]`). Parallel, as commonly done in the German system, I was largely involved in fund rising (German Science Foundation, 3 proposals written and accepted) and teaching duties (see chapter 2).

As a post-doc at the KIT in 2007, I wrote my own research proposal to the German Science Foundation (DFG) that was funded in a competitive process and would have supported me for the next three years. However, in early 2008, I decided not to accept this grant and to move on to the LadHyX group in Paris in order to work in a different, more physics-oriented scientific environment and learn more about fluid mechanical fundamentals. From 2008 to 2010 I started a post-doctorate at the LadHyX awarded with a Marie Curie Intra European Fellowship in FP7. The topic concerned stratified turbulence. I worked closely with P. Billant and performed both laboratory experiments and numerical

three-dimensional linear stability analysis. By means of the unique laboratory experiments of stratified turbulence, a direct energy cascade in the stratified turbulence regime has been demonstrated. I also showed that the gravitational instability is the dominant mechanisms for transferring energy from large to small dissipative scales in submesoscale eddies in stratified ambients.
This work is published in 2 journal articles (`publication [82? ]`).

During my stay at the LadHyX I did the CNRS competition to join the laboratory LEGI, which captivated my interest for its renowned expertise in geophysical fluid dynamics and sophisticated experimental installations. After my recruitment at LEGI in 2011, I started to work in the field of turbulent convection. Herein, I participated to the development of a new experimental technique to measure simultaneously the temperature and the velocity fields of a turbulent convective flow with high Rayleigh numbers, following two master students and then a PhD student, in collaboration with J.-B. Flor. It allowed for the simultaneous measurement of small and large-scale motions, and the local heat and momentum exchange by structures and plumes near walls within the highest precision reached to date for such large fields of view.

At the same time, I continued to work in the field of gravity currents. I demonstrated that different flow regimes can install as a function of the initial conditions at slope changes for gravity currents in spatial development that are very different from the generally assumed self-similar regime in ocean circulation models. Also, shallow water theory approach has been expanded including entrainment and bottom friction terms. A strong correlation between interface and bottom boundary layer has been reported and I demonstrated that this interaction causes local increase of bottom friction with important consequences on the further development of the flow. The effects of the bottom curvature on the stability of the boundary layer including effects of background stratification has been investigated as well and made object of a PhD which I co-supervise in collaboration with C. Brun and with the group MOST (G. Balarac).

Since 2018 I had the great opportunity to take the scientific responsibility of the Coriolis Rotating Platform. I am so directly involved in the various projects related to the transnational access, which enabled me to widen my research activities to a variety of fluid mechanical topics from fundamental geophysical fluid mechanics to environmental engineering problems but also to enhance and build up new international collaborations. Beside the scientific support in terms of design, performance of the experiments as well as contributing to the scientific data post-processing and analysis, this work also includes various administration duties such as proposal writing, fund rising, reporting and meetings attendance for the European and collaborative projects which strengthened my research management skills.

My recent research focus turned on geophysical turbulence, and in particular on the turbulence generated by rotating intruding downslope gravity currents within stratified ambients, to explore the contribution to the turbulence generation in the ocean induced by boundary layer processes. This topic will represent my main research activity in the upcoming years, with a close collaboration with the laboratory SHOM (Brest) and LA (Toulouse), concretized with an active SHOM contract over four years (2020-24) and with a ANR Astrid project to be submitted in the next call 2022.

Chapter 2

Curriculum Vitæ

Personal Information

	born the 5^{th} December 1978, italian nationality, 3 children (born 2012, 2014, 2015)
Languages	Italian (native), French and German (near-native), English and Spanish (very good), Greek (elementary)
Address	35 Avenue Alsace Lorraine, 38000 Grenoble (France)
Email	eletta.negretti@legi.cnrs.fr
Phone	+33 (0)7 70 28 61 43 (mob.),+33 (0)4 76 82 50 52 (prof.)

Current employment

2011–current	**Chargée de recherche CNRS (CRCN)** Laboratoire des écoulements géophysiques et industrielles LEGI UMR 5519, Grenoble, France
2018–current	**Scientific responsibility of Coriolis Rotating Platform, Grenoble** Organization and coordination of users venue, design and performance of experiments, support for data processing and analysis, fund rising reporting and meeting for access projects, organization of external visits
Research areas:	Gravity currents, geophysical turbulence, flow instabilities.

Education

2003–2007	**DOCTOR OF PHILOSOPHY**, Institute for Hydromechanics, Karlsruhe Institute of Technology (KIT), Germany (Full Marks), direction of GH Jirka, DZ Zhu.
1997–2003	**MASTER OF SCIENCE - LAUREA**, (Environmental Engineering), University of Trento, Italy, (Full Marks), direction of M Tubino, SA Socolofsky.
1992–1997	Studies at the Liceo Classico *A. Cantore*, Brunico (BZ), Italy (Full Marks).

Research experience

2008–2010	**POST-DOCTORATE (Marie Curie FP7 - CNRS)**, Laboratoire d'Hydrodynamique (LadHyX), École Polytechnique, Paris, France (P Billant, JM Chomaz) Numerical linear stability analysis of pancake-like vortices and experiments on forced stratified turbulence
2004–2007	**DOCTORATE (DFG)**, KIT Karlsruhe, Germany (GH Jirka, DZ Zhu) Title: Hydrodynamic instabilities and entrainment processes in two-layer density-stratified flows over a submerged sill. A physical model of sea straits. Experimental (PIV/PLIF) and theoretical study to investigate the influence of higher Reynolds numbers, of local enhanced bottom roughness and of a bottom slope on interfacial waves in two-layer stratified flows
10/2002–07/2003	**RESEARCH INTERNSHIP**, University of Trento, Italy (M Tubino, SA Socolofsky) Title: Analysis of the wake behind a circular cylinder in turbulent shallow water flows. Experimental design and measurements (LDA) to stabilize oscillating cylinder shallow wakes, analytical study and linear stability analysis of shallow turbulent wakes

Awards

2009	**Marie Curie Fellow**, Intra European Fellowships FP7 (PIEF-GA-2009-234782)
2004	**Ehrensenator Huber Preis**, Award for the best M2 Thesis 2003.
1997	**Premio Alto Adige**, for the best High School students 1997.

Professional and Teaching experience

Teaching

2004–2007	Research and Teaching assistant, IfH, University of Karlsruhe, Germany. Lecturer of the undergraduate course "Flow Measurements Techniques" (12h, 20 students) Teaching assistance of the undergraduate course "Hydromechanics" (60h, 120 students) Teaching assistance of the undergraduate course "Experimental Fluid Mechanics I" (50h, 30 students)
Supervision	**3** research internships, **19** Master thesis (M2), **3(+3)** PhD thesis, **1** Post-Doc.

Administration

2018–	Coordination of the Transnational acces to the Coriolis Rotating Platform within Euopean Projects
2003–2008	Coordination of the student exchange within the scope of the Double-Degree Program, University of Karlsruhe (Germany)-University of Trento (Italy)
2005–2007	Founding member of EWB - Engineers Without Borders, University of Karlsruhe

Organization of scientific meetings

2022	EUROMECH Colloquium 608, 'Gravity Currents' (postponed)
2014-	Organization of internal seminar series at LEGI-MEIGE
2006	Environmental Fluid Mechanics, Summer School at the IfH, KIT, Germany

Reviewing activities

2018	Reviewer, REPRISE-MIUR, Italy
2006-	Reviewer J. Fluid Mech., Phys. Fluids, Phys. Rev. Fluids, J. Hydr. Res.

Cooperations

F Dumas	Shom, Brest, France
F Auclair	Laboratoire d'Aerologie, Toulouse, France
C Adduce	University of Roma Tre, Rome, Italy.
A Rubino	University Ca' Foscari, Venice, Italy.
S Pierini	University Parthenope of Naples, Italy
A Pirro	INOGS, Trieste, Italy

Invited talks and Seminars

	"The turbulent life of downslope rotating gravity currents"
2019	Themes Conference Venice, Italy
	"Instability and mixing in turbulent stratified flows"
2017	Department of Applied Physics at Universitat Polytecnica de Catalunya, Barcelona, Spain
	"Gravity currents over complex terrain"
2015	Ecole Normale Superieure ENS, Lyon, France
	"Energy transfers in stratified turbulence"
2013	Karlsruhe Institute for Technology (KIT), Germany
	"Three-dimensional stability of a pancake vortex in a stratified fluid"
2010	Ecole Polytechnique Federale de Lausanne (EPFL), Lausanne, Switzerland
2010	Institut de Recherche des Phénomènes Hors Equilibre (IRPHE), Marseille (France)
2009	Laboratoire d'Hydrodynamique, (LadHyX), École Polytechnique, Paris, (France)
2009	Ecole Supérieure de Physique et de Chimie Industrielles (ESPCI), ParisTech, (France)
	"Three-dimensional structure of stratified turbulence"
2009	Institute for Hydromechanics (IfH), University of Karlsruhe
2008	Institut de Mécanique des fluides de Toulouse (IMFT), Toulouse, (France)
	"Hydrodynamic instabilities and entrainment in two-layer flows down a sill"
2008	Laboratoire d'Hydrodynamique, (LadHyX), École Polytechnique, Paris, (France)
2007	Coastal and ocean engineering division, Texas A&M University, College Station, USA
2006	Institute for Hydromechanics (IfH), University of Karlsruhe, Germany
	"On shallow wakes: an analytical study"
2006	Institute for Hydromechanics (IfH), University of Karlsruhe, Germany
	"Stabilization of cylinder shallow wakes"
2004	Dipartimento di Ingegneria Civile e Ambientale, University of Trento, Italy

Chapter 3

Publications

24 publications Rang A (2 of which submitted), **20** conference proceedings.

3.1 Refereed Journals Rang A

1. Wirth A and Negretti ME 'Non-intruding rotating gravity currents' submitted to *Ocean Modelling*.
2. Maggi MR, Adduce C and Negretti ME 'Lock-exchange gravity currents over a rough bottom' submitted to Special Issue Environmental Fluid Mechanics, October 2021.
3. Negretti ME, Tucciarone FL⋆ and Wirth A (2021) 'Intruding gravity currents and re-circulation in a rotating frame: Laboratory experiments' *Phys. Fluids* 33 (9), 096607,10.1063/5.0058629.
4. De Serio F, Armenio E, Badin G, Di Leonardo A, Hilel R, Liberzon D, Mossa M, Negretti ME, Pisaturo GR, Righetti M, Sommeria J, Termini D, Valran T, Vermeulen B, Viboud S (2021), 'Experiments on rotating jets interacting with vegetation' *Exp. Fluids*, 62, 218-33, 10.1007/s00348-021-03297-2.
5. Gacic M, Rubino A, Ursella L, Kovacevic V, Menna M, Malacic V, Bensi M, Negretti ME, Cardin V, Orlic M, Sommeria J, Viana Barreto R, Viboud S, Valran T, Petelin B, and Siena G. (2021) Impact of the dense water flow over the sloping bottom on the open-sea circulation: Laboratory experiments and the Ionian Sea (Mediterranean) example, *Ocean Sciences*, 17, 975-96, 10.5194/os-17-975-2021.
6. Mossa M, Hilel Goldshmid R, Liberzon D, Negretti ME , Sommeria J, Termini D, De Serio, F (2021) Quasi-geostrophic jet-like flow with obstructions, *J Fluid Mech*, 921, A12, 10.1017/jfm.2021.501.
7. De Falco MC⋆, Adduce C, Cuthbertson A, Negretti ME , Laanearu J, Malcangio D and Sommeria J (2021) Experimental study of uni and bi-directional exchange flows in a large scale rotating trapezoidal channel, *Selected as Featured Article of Phys. Fluids*, 35(1), 014102, 10.1063/5.0039251.
8. Dagaut J⋆, Negretti ME , Balarac G and Brun C (2021), Laminar to turbulent Görtler instability transition *Phys. Fluids*, 33(1), 014102.
9. De Falco MC⋆, Adduce C, Negretti ME and Hopfinger EJ (2021) On the dynamics of quasi-steady gravity currents flowing up a slope. *Adv. in Water Res.*, 147, 103791.
10. Rubino A, Gacic M, Bensi M, Kovacevic V, Malacic V, Menna M, Negretti ME, Sommeria J, Zanchettin D, Viana-Barreto R, Ursella L, Cardin V, Civitarese G, Orlic M, Petelin B, Siena G (2020) Multiannual Oceanic Surface Circulation Rever-

sals Without Wind Influence: an Experimental Evidence, *Scientific Reports, Nature.*

11. Martin A⋆, Negretti ME, Ungarish and Zemach T (2020), On the propagation of a continuously supplied gravity current head down bottom slopes, *Phys Rev Fluids*, 5, 054801 .
12. Zemach T, Ungarish M, Martin A* and Negretti ME (2019), On gravity currents of fixed volume that encounter a down-slope or up-slope bottom *Phys Fluids* 31, 096604.
13. Martin A⋆, Negretti ME and Hopfinger EJ (2019), Development of gravity currents on slopes under different interfacial instability conditions, *J Fluid Mech* 880,180-208.
14. Kostaschuk R, NasrAzadani MM, Wei T, Chen Z, Meiburg E, Negretti ME, Best J, Peakall J and Parsons DR (2018), On the causes of pulsing in turbidity currents *J Geophys Res Earth Surf* 123(11), 2827-43.
15. Negretti ME and Flor JB and Hopfinger EJ (2017), Development of gravity currents on rapidly changing slopes, *J Fluid Mech* 833, 70-97.
16. Caudwell T⋆, Flor JB and Negretti ME (2016), Convection at an isothermal wall in an enclosure and establishment of stratification, *J Fluid Mech* 799, pp 448-75.
17. Augier P Billant P Negretti ME and Chomaz JM (2014) Experimental study of stratified turbulence forced with columnar dipoles, *Phys Fluids* 26, 046603.
18. Negretti ME and P Billant (2013) Stability of a Gaussian pancake vortex in a stratified fluid, *J Fluid Mech* 718, pp 457-80.
19. Weitbrecht V, Seol DG, Negretti ME, Detert M, Kuehn G and Jirka GH (2011) PIV measurements in environmental flows *J Hydr Res* 5(4), pp 231-45.
20. Negretti ME Socolofsky SA and Jirka GH (2008) Linear stability analysis of inclined two-layer stratified flows *Phys. Fluids* 20, 094104.
21. Negretti ME, Zhu DZ and Jirka GH (2007) The effect of enhanced bottom roughness in two-layer exchange flows over a sill, *Dyn of Oceans and Atm* 45, pp 46-68.
22. Negretti ME, Zhu DZ and Jirka GH (2007) Barotropically induced interfacial waves in two-layer exchange flows over a sill, *J Fluid Mech* 592, pp 135-54.
23. Negretti ME Vignoli G Tubino M and Brocchini M (2006) On shallow wakes : an analytical study, *J Fluid Mech* 567, pp 457-75.
24. Negretti ME Socolofsky SA and Jirka GH (2005) Stabilization of cylinder wakes in shallow water flows by means of roughness elements : an experimental study *Exp. Fluids* 38, 403-14.

3.2 Articles in preparation

25. Pierini S, De Ruggiero P, Negretti ME, Sommeria J, Schiller-Weiss I, Weiffenbach J and Dijkstra H 'Laboratory experiments reveal self-sustained intrinsic oscillations in ocean relevant rotating fluid flows' in submission stage for Nature.
26. Shi H⋆, Negretti ME, Chauchat J, Blanckaert JK, Lemmin U. and Barry DA 'Unconfined Plunging Process of a Hyperpycnal River Flowing into a Lake: Laboratory Experiments and Numerical Modelling' in preparation for *Water Resour. Res.*
27. Negretti ME, Martin A⋆ and Naaim-Bouvet F 'On the propagation of the front speed of lock released density clouds' in preparation for *Env. Fluid Mech.*
28. Johnson H, Cuthberson A, Adduce C, Negretti ME and Sommeria J 'Morphological implications for two-layer stratified rotating exchange flows' in preparation for J. Hydraulic Research.
29. Maggi MR, Negretti ME and Adduce C 'On the formation of ripples in downslope

gravity currents over a sediment floor' in preparation for Env. Fluid Mech.

3.3 Refereed Conference Proceedings

- Maggi MR, Adduce C and Negretti ME Lock-exchange gravity currents propagating over roughness elements, 2nd IAHR YPN Congress Online, Nov-Dec 2021.
- Negretti ME, Tucciarone F, Wirth A and J Sommeria The turbulent live of oceanic gravity currents, THEMES November 2019, Venice, Italy.
- Negretti ME, Martin A and Hopfinger EJ, Spatially developing gravity currents, EGU 7-12 April 2019, Vienna, Austria.
- Negretti ME, Wirth A and Sommeria J, The turbulent life of downslope intruding rotating gravity currents, THEMES 26-29 November 2019, Venice, Italy.(in press)
- M Gacic, A Rubino, Negretti ME, G Civitarese, M Bensi, V Kovacevic, V Cardin, G Siena, R Viana Barreto, B Petelin, J Sommeria, T Valran, S Viboud, L Ursella and M Menna (2019) A rotating tank model of the North Ionian gyre inversions produced by dense water flows, EGU 7-12 April 2019, Vienna, Austria.
- V. Kovacevic, M. Bensi, G. Civitarese, M. E. Negretti and A. Rubino (2019) Northern Ionian Circulation inversions: simulations in the Coriolis Rotating Platform (Legi, Grenoble), CIESM Congress, 7-11 October, Cascais, Portugal.
- Gacic M, Rubino A, Negretti ME, Civitarese G, Bensi M, Kovacevic V, Cardin V, Siena G, Viana Barreto R, Petelin B, Sommeria J, Valran T, Viboud S, Ursella L and Menna M (2019) A rotating tank model of the North Ionian gyre inversions produced by dense water flows, 6th Hydralab Meeting, 20-25 May, Bucharest, Romania.
- De Serio F, Armenio E, Badin G, Di Leonardo A, Hilel R, Liberzon D, Mossa M, Negretti ME, Pisaturo GR, Righetti M, Sommeria J, Termini D, Valran T, Vermeulen B, Viboud S (2019), Jets interacting with vegetation in the rotating LEGI platform, EGU General Assembly, Vienna, 7-12 April 2019
- De Serio F, Armenio E, Badin G, Di Leonardo A, Hilel R, Liberzon D, Mossa M, Negretti ME, Pisaturo GR, Righetti M, Sommeria J, Termini D, Valran T, Vermeulen B, Viboud S, Jet interacting with vegetation in a rotating basin (2019), Proceedings of the HYDRALAB+ Joint User Meeting, Bucharest, 21-25 May 2019.
- Negretti ME, Martin A and Hopfinger EJ, Gravity currents over complex topography, IUTAM/AMERIMECH SYMPOSIUM Dynamics of Gravity Currents 25-27 September 2017, Santa Barbara UCSB, US.
- Negretti ME Flor JB and Hopfinger EJ, On gravity currents over changing topography, VIIIth ISSF, San Diego CA, US, August 2016. 26. Negretti ME Flor JB and Hopfinger EJ, Gravity currents over concave slopes, EuroMech 567 Turbulent Mixing in Stratified Flows, DAMTP Cambridge, March 2015.
- Negretti ME and Billant P, Three dimensional stability of a pancake vortex in a stratified fluid, Int Symposium on Strat. Flows ISSF Rome, August 2011.
- Negretti ME and Billant P, Linear stability of a pancake vortex in a stably stratified fluid, APS DFD, Long Beach California, November 2010.
- Negretti, ME and Billant, P Stability of a pancake vortex in a stratified fluid EuroMech Colloquium 519 Mixing and dispersion in flows dominated by rotation and buoyancy, Rolduc (The Netherlands), 20-23 June 2010.
- Negretti, ME and Billant, P Three dimensional stability of a pancake vortex in a stably stratified fluid, Workshop/summer school on waves and instabilities in geophysical and astrophysical flows, Porquerolles (France) 25-31 May 2009.

- Augier, P, Negretti, ME, Billant, P and Chomaz, JM Experiments on forced stratified turbulence Advances in Turbulence XII, Springer Proceedings in Physics 132, Ed. by B. Eckhardt, 397-400 2009.
- Negretti, ME, Hagan, K and Jirka, GH Experiments on pulsating surges in a two-layer downslope flow, Fifth International Symposium on Environmental Hydraulics, Tempe (Arizona) 2007.
- Negretti, ME, Socolofsky, SA and Jirka, GH Linear stability analysis of spatially accelerating stratified shear flows, 32nd IAHR Congress, Venice, Italy, 2007.
- Negretti, ME, Jirka, GH and Zhu, DZ Combined PIV PLIF measurements in stratified exchange flows over a submerged sill, International Symposium on Stratified Flows, Perth, Australia 2006.
- Negretti, ME, Weitbrecht, V, Zhu, DZ and Jirka, GH Experiments on stratified exchange flows past a submerged sill, 31st IAHR Congress, Coex Seoul, Korea, 2005.
- Negretti ME, Vignoli G Scia turbolenta su acqua bassa, XXI Convegno di Idraulica e Costruzioni Idrauliche, Trento, Italy, 2004.

Chapter 4

Supervision of students and research management

4.1 Supervision of Post-Doc, PhD and M2 internships

3 research internships, **19** Master thesis (M2), **3(+3)** PhD thesis, **1** Post-Doc.

From 2011 to 2015 I co-supervised with J.-B. Flor the Master and then the PhD thesis of Tobit Caudwell. Tobit Caudwell pursuits his career in a self-created start-up of scientific consulting in the domain of energy efficiency.

From May 2017 to July 2020 I closely supervised the post-doctoral fellow financed by the Labex Tec21, Antoine Martin, from which a fruitful collaboration developed with a total of four articles published. At present, he has a permanent position within a R&D group in Minatec Grenoble as a data scientist.

Since the end of 2017 I co-supervise (with C. Brun and G. Balarac) the PhD thesis of Jeremie Dagaut focusing on the Görtler instabilities. He will defend his PhD in December 2021. The results from his PhD thesis give enough material to pursuit the research topic with my colleagues and is detailed in 12.1 in the Perspetives part of this manuscript.

Further I co-supervised the PhD thesis of Maria Chiara De Falco from the University of Roma Tre with C. Adduce, on the topic of 'Uni and bi-directional exchange flows, propagating over complex boundaries', which has been successfully concluded on January 26, 2020. She was visiting LEGI within a Hydralab+ Project from January to July 2018. I trained her in the experimental techniques of PIV and LIF. Back to her University, we worked closely on further experiments she conducted in Rome on gravity currents propagating up a slope. She left the academic career in March 2021 and works currently in a private company (TELECOM) as a data scientist.

Since I am at LEGI, I supervised 13 master thesis M2 on the topics of turbulent convection (2), gravity currents (4), geophysical turbulence (6) and shallow jets (1).

In 2018 I took the responsibility of the Coriolis Rotating Platform, so I was also involved in several visits to the infrastructure of High Schools, TIPE works, and other local and national events such as 'Fête de la Science' or 'Journées de l'OSUG'.

I participated to the review process of several articles submitted to the Journal of Fluid Mechanics, Physics of Fluids, Physical Review Fluids and Journal of Hydraulic Research (with an average of 4 per year since my PhD).

I am the principal organiser, with P. Linden (DAMPT, Cambridge UK) of an Euromech Colloquium (https://euromech.org/colloquia/colloquia-2020/608) on gravity currents. It was initially planned for June 2020 at LEGI and now postponed to a date after the Pandemic situation has stabilized, presumably in 2022.

4.2 Research management

After my PhD, I managed the European project of the Marie Curie Fellowship that supported my post-doctorate at the LadHyX. Since my arrival at LEGI, I managed 2 research projects funded by the LabEx OSUG and one project funded by the LabEx Tec21 for three years. From 2014 I am responsible for the organisation of the internal seminar series of the team MEIGE.

A list of all funded research proposals is given in the following

Funded research proposals (10):

1. 2004 - Zhu, DZ (PI), Negretti, ME and Jirka, GH 'Hydrodynamic instabilities and entrainment in stratified two-layer exchange flows over a sill' **German Science Foundation, DFG Ji 18/12-1**, 70%, 2yrs, 250kE.

2. 2006 - Negretti, ME (PI) and Jirka, GH, 'Hydrodynamic instabilities and entrainment in stratified two-layer arrested flows over a sill' **German Science Foundation, DFG Ji 18/12-2**, 100%, 2yrs, 250kE.

3. 2008 - Negretti, ME (PI), Billant, P., 'Three-dimensional structure of stratified turbulence', **FP7 Marie Curie Intra European Fellowships, PEOPLE-IEF, 3DZZI, Proposal Number 234782**, 100%, 2yrs, 300kE+OH.

4. 2008 - Negretti ME (PI), P. Linden, 'The fluid mechanics of natural building ventilation' **German Science Foundation, DFG NE1184/2-1**, 100%, 2yrs, 160kE.

5. 2011 - Negretti ME, 'Gravity currents over complex terrain' **UJF SMINGUE**, 70%, 10kE.

6. 2012 - Negretti ME, 'Gravity currents over topography', **UJF SMINGUE**, 70%, 12kE.

7. 2013 Negretti ME (PI), Brun, C - 'Gravity currents over complex terrain', **Labex-OSUG2020**, 3yrs, 70%, 16kE.

8. 2014 - Flor J.-B. (PI), Negretti ME, 'Turbulent convection for energy efficient buildings **AGIR SMINGUE**, 3yrs, 40%, 25kE.

9. 2017 - Negretti ME (PI), Ungarish M 'Gravity currents over complex terrain' **LabEx Tec21**, 3 yrs, 70%, 160kE.

10. 2021 - Wirth A (PI), Negretti ME, Auclair F., 'The turbulent life of intruding downslope gravity currents', 50%, **SHOM Nr.20CP03**, 4yrs, 80kE.

4.3 Scientific direction of the Coriolis Rotating Platform

At the end of 2017, the direction team of the LEGI changed and J. Sommeria became the new director. He was the scientific responsible of the Coriolis Rotating Platform since 1999. Starting from 2018, I have been then asked to take on this role.

The scientific support of the Coriolis Rotating Platform consists of the conception and design of the experiments in close discussion with the users, in assisting and surveying the experiments and in the primary data management and post-processing to produce data files that can be further exploited by the external users. This latter task also includes ad-hoc calibrations and new developments of the existent softwares (e.g. UVMAT) for PIV/LIF and also for the data processing from other instrumentation such as probes and acoustic doppler devices. I further participate in the discussion and physical interpretation of the results as well as in the redaction of the articles.

Beside the scientific support, the coordination of the Coriolis Rotating Platform also includes the organization of the external users venues and meetings and their training in the specific softwares and data management/treatment tools. I also coordinate and mediate the technical and instrumentation support team for the experiments, supervising the work of technicians and of the two engineers who have the technical responsibility of the Coriolis Rotating Platform: S. Viboud and T. Valran. Herein, I was also involved in supporting the tenure of a new CNRS position of the additional engineer (T. Valran) in 2018, for an enhanced technical support of the Coriolis Rotating Platform. Also, I coordinate the continuous technical maintenance of the Platform leaded by S. Viboud, including the constant optimization and possible automation of the instrumentation devices.

The scientific direction also includes various administration duties such as proposal writing and reporting for the national and international research agencies.
Since 2020, the 25 years long support from the European Union in the frame of the Hydralab Consortium has stopped. New perspectives to perpetuate the future administrative and financial support of the Coriolis Rotating Platform need to be conceived. This will be further discussed in section 14 in the perspective part of this manuscript.

I am also regularly contacted by local, national and international mediating institutions for interviews or interventions for scientific vulgarization to the broad audience. As an example, in 2021 I was directly involved in the production of an international documentary 'Odyssey: Behind the Myth' (for more details see https://www.kepach.it/film/odyssey/) to reproduce the flow conditions through the Strait of Messina and in general the phenomenon of Maelstrom. As already mentioned, I am also involved in several visits to the infrastructure of High Schools, higher education institutions, companies as well as TIPE works and other local and national events such as 'Fête de la Science' or 'Journées de l'OSUG'.

The transnational access projects I have coordinated since 2018 are listed below.

Coordinated transnational access projects (4 Hydralab+, 2 external)

- 2018 - `H+ -CNRS-05 18ADDUCE` - *The dynamics of bi-directional echange flows: implications for morphodynamic change within estuaries and sea straits.* University of Roma Tre, Politecnico di Bari (Italy), Talinn University (Estonia), University of Dundee (UK). `Publication` [22].
- 2018 - `H+ -CNRS-06 18JEVERB` - *Jets interacting with Vegetation in Rotating Basin,*

Politecnico di Bari, University of Palermo, University of Bolzano/Trento (Italy), Technion IIT (Israel). `Publications` [23, 78].

- 2018 - `H+ -CNRS-07 18CROPEX` - *The Adriatic-Ionian Bimodal Oscillating System (BiOS)*, INOGS Trieste, University Ca' Foscari Venice (Italy), NIB Piran (Slovenia). `Publications` [34, 96].
- 2019 - `H+ -CNRS-08 19GAPWEBS` - *Laboratory modeling of gap-leaping and intruding western boundary currents under different climate change scenarios*, Parthenope University Naples (Italy), Utrecht University (The Nederlands). `Publication` [92].
- 2020 - `20LEMAN` - *Three-dimensional hyperpycnal plunging currents as a model of the Rhone inflow into Lake Geneva*, EPFL Lausanne (Switzerland) (15kE). `Publication` [102].
- 2021 - `21CYPROSS` - *Barotropic Rossby waves in a homogeneous and a nearly stratified rotating flow*, INOGS Trieste (Italy), MIO Marseille (France) (15kE).

Part II

Research accomplished

Chapter 5

Introduction

Variations in temperature, salinity and/or sediment concentration cause variations of fluid density in the vertical direction. The resulting flow stratification, which typically occurs in environmental and geophysical flows, leads to qualitative and quantitative modifications of the flow patterns by buoyancy. Vertical mixing of mass and momentum are strongly reduced by the buoyancy due to the stable stratification but they are still possible. Stratified flows can support two main types of fluid motions [95]: on the one hand there are internal gravity waves [106] which propagate to restore the gravitational (buoyant) equilibrium, similarly to the ocean's surface waves. On the other, quasi-horizontal motions with vertical variations can develop due to the buoyancy. The research I accomplished concerned this latter flow type.

When buoyancy driven flows encounter topography, a downslope dense current, i.e. gravity current, is created. Its motion is then sustained by buoyancy and deviated by the topographic slope. Gravity currents are key processes that affect ocean, atmospheric and coastal circulation.

Gravity currents may be generated from a finite volume release, or can have a continuous supply of a buoyancy flux. Examples of the first type are avalanches ([45], [94], see figure 5a), volcanic eruptions [44] (figure 5b) or turbidity currents (figure 5c) such as those generated on continental shelf and coastal regions in the nearshore, where the breaking of large waves enhances sediment suspensions that may propagate off-shore and contribute to the erosion of coastal regions. Katabatic winds are also an example of an intermittent gravity flow and are important in determining the local air circulation in several regions. In mountain areas, the dynamics of the atmospheric boundary layer is dominated by downslope currents, which are decoupled from the usually weak synoptic winds due to abrupt changes in topography. Under stable winter conditions a significant buoyancy jump can exist in enclosed mountain valleys, which may act as a barrier to vertical mixing. Bad air quality develops and pollutants emitted by traffic, heating/cooling systems and industry transported by katabatic winds are mainly trapped at low heights with serious consequences on the human health. In Antarctica and Greenland katabatic winds are directly responsible for cooling the ocean surface water at the polynya [67] and open sea and play an important role for the deep water formation.

In oceanic gravity currents, or overflows, the density differences are induced by temperature and/or salinity differences. This can drive a flow in the connecting channel or strait. One of the best known examples of such flow happens at the Strait of Gibraltar [30]. While the density difference between these two water bodies is about 2kgm^{-3}, it drives a flow of over 1 sverdrup in each direction with the heavier Mediterranean sea water

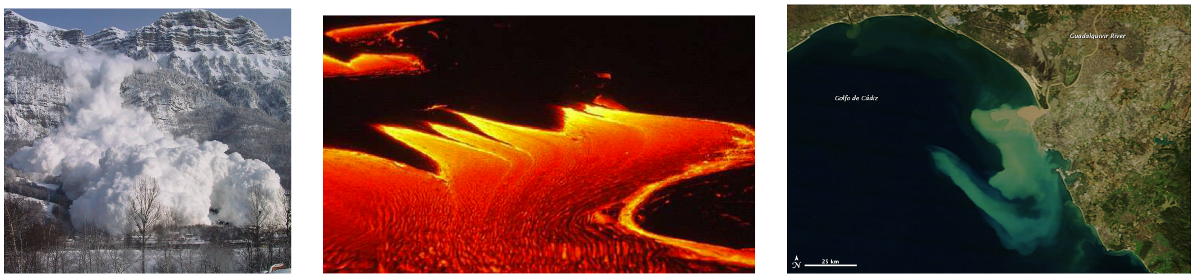

(a) (b) (c)

Figure 5.1: (a) The Guadalquivir River empties into the Gulf of Cádiz along Spain's southwestern coast. In November 2012, the river yielded a heavy load of sediment to the gulf. The Moderate Resolution Imaging Spectroradiometer (MODIS) on the Terra satellite captured the image in natural color. (b) Image of a snow avalanche in Switzerland (from Swiss Confederation National Platform of Natural Hazards). (c) Picture of a lava eruption from Etna Volcano (Sicily, Italy) taken by Tom Pfeifer.

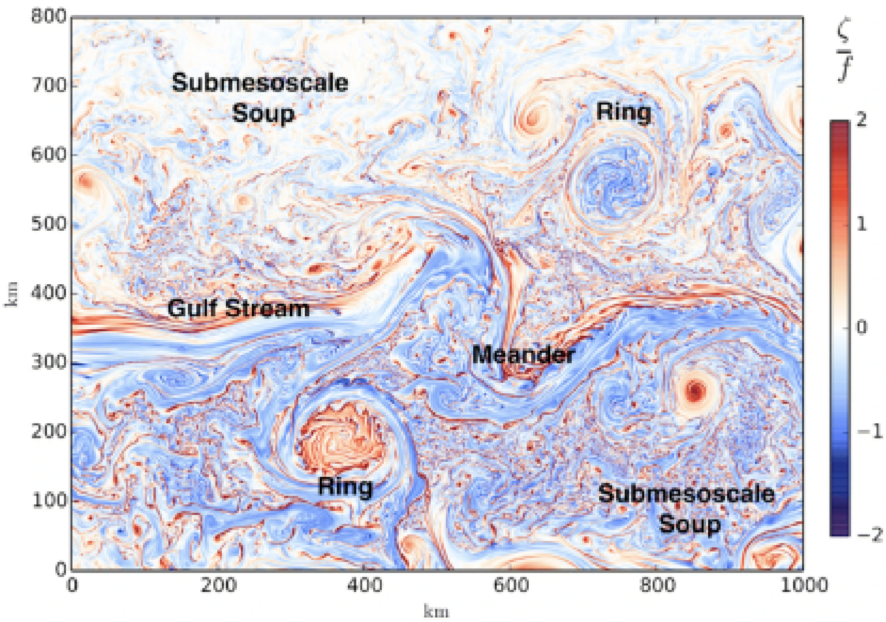

Figure 5.2: Vertical vorticity normalized by the Coriolis parameter f at the surface in the wintertime of the Gulf Stream, after separation from the western boundary in a nested-subdomain simulation [41]. Notice the meandering Gulf Stream in the center, the northern warm anticyclonic and southern cold cyclonic mesoscale rings, and the nearly ubiquitous submesoscale features of many different types, including the typical open-sea 'soup' away from strong mesoscale currents.

flowing under the lighter Atlantic Ocean water.

In the ocean, the dense currents descend the continental slope for long distances before encountering the ocean bottom or interleaving at their level of neutral buoyancy. During the descent, they entrain the surrounding ambient water and sediment from the bottom. One example is given by the North Atlantic Deep Water (NADW) formed in the Nordic Seas [26]. Its water properties are strongly influenced by entrainment occurring at the Denmark Strait [51] and along the descent on the continental slope. These key processes occur in very localized regions (cf. figure 5) and are so rapid that a full resolution of their dynamics is out of reach for ocean circulation numerical models. Hence, the overflows need to be correctly represented in those general ocean circulation models [**?**].

In specific oceanic regions, as e.g. semi-enclosed basins, intense air-sea fluxes modify the temperature and salinity of the surface water leading to a buoyancy loss and the formation of deep water which will subsequently descend to depth, slowly mixing with surrounding waters to eventually return to the surface after many centuries. This global overturning circulation, commonly referred to as the great conveyor belt, is a key component of the climate system, transporting heat, freshwater, carbon and nutrients across the world; and acting as a buffer of anthropogenic perturbations by storing excess heat and carbon dioxide in the abyssal layers of the ocean for several centuries.
Oceanic gravity currents are hence a fundamental part of the thermohaline circulation.

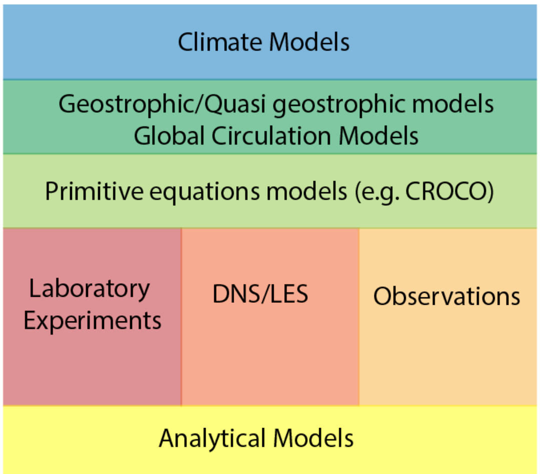

Figure 5.3: Schematic picture of the different approaches.

Oceanic gravity currents are of large scale and are much slower ($1\,\mathrm{m\,s^{-1}}$) as compared to finite volume released gravity currents such as snow or submarine avalanches or, in general, turbidity currents. They typically have characteristic time scales that exceed one day, and thus the Coriolis effect may become also important. The primary effect of the Earth's rotation on these flows is to deviate them in a preferential direction. The combination of buoyancy and rotation effects give rise to a large variety of instability phenomena (shear, front, gravitational, baroclinic/barotropic instabilities, inertial and internal waves) and induces the formation of mesoscale and submesoscale vortices. A typical example of submesoscale vortices produced by large scale oceanic currents is given by those produced by the Gulf Stream as given in figure 5.

The dynamics of gravity currents involves processes over a wide variety of scales and it is impossible to explicitly resolve them in the numerical models of today or the near future of the ocean dynamics [55]: bottom viscous boundary layers are only a few meters

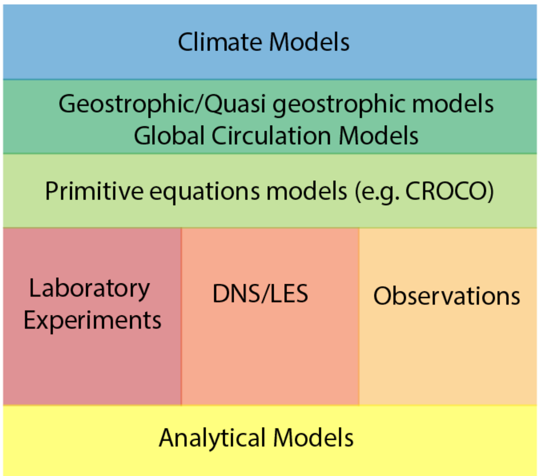

Figure 5.4: (a) Aerial view of simulated overflow. Iceland is on the right margin, and Greenland is at the top. Yellow/red/black coloring (in increasing order) indicates the thickness of the overflow layer of dense water, with the greatest thickness in the northern basin reservoir. Green represents the coastline. (b) Thickness from the combined 1996-1998 Poseidon/Aranda data set. From [51].

thick, possibly including role vortices, covered by a possibly unstable Ekman-layer of a few tenths of meters thickness. At the upper boundary of the gravity current there can be an unstable interfacial Ekman-layer, Kelvin-Helmholtz or Holmboe instabilities [55, 84–86, 120, 121]. Several such physical mechanisms, not all completely understood, allow the energy to be transferred from mesoscale quasi-geostrophic motion to the very small scales where irreversible mixing can take place. But energy may also be transferred from the submesoscales to the larger geostrophic scale (cf. sketch in figure 5.5). Consequently, the entrainment, and often the overflows themselves need to be parametrized. It has been known for more than two decades that a small modification of vertical turbulent diffusivity in a circulation model has a major impact on the thermohaline circulation [12], [20].

Ellison and Turner [28] and Turner [112] were the first to investigate this phenomenon experimentally, in the case of a current flowing into a homogeneous ambient medium, without rotation and down a slope. They derived a model for the bulk properties of the flow, based on measurements of various quantities and proposed various relations to estimate entrainment as a function of the slope or the bulk Richardson number that are still largely employed. A number of studies succeeded trying to find more sophisticated relations to evaluate entrainment [6, 7, 14, 60]. In situ measurements, well resolved numerical simulations (DNS), as well as experimental studies, are then necessary to provide the necessary information (e.g. turbulent fluxes) to build robust parametrizations for entrainment, and turbulent diffusivities. In order to obtain a valid parameterization from a laboratory experiment however, there is also a need for a model that extrapolates the parameterization to oceanic conditions.

Ocean dynamics, as any natural system, is complex because of the (non) linear interaction between different processes. This complex system needs therefore to be decomposed into the relevant physical processes to be studied separately, in order to understand their role in the system. This requires not only a wide scientific knowledge and experience, but also creativity and intuition.

Understanding the physical processes using idealized laboratory experiments, fine resolved direct numerical simulations, observations and analytical models, permits us to build reliable primitive equation models (such as the emerging CROCO model) to finally be able to exploit idealized models such as geostrophic or quasi-geostrophic models (e.g. climate models or global ocean circulation models).
The tools which permit nowadays to realize a (simplified) idealized physical model are both resolved numerical simulations (DNS, LES) and laboratory experiments. The main difference between them is that while laboratory experiments represent a 'real' physical phenomena and modern experimental techniques allow nowadays to have high quality quantitative measurements of the main fluid characteristics, numerical simulations are built on a (mathematical) numerical model, whose correspondence to reality needs to be necessarily validated using observational or laboratory experimental data. Observational data taken directly from the 'real' physical system, have however the drawback of being limited in space and time and of including all processes, i.e. observations do not permit us to isolate the relevant physical processes governing the investigated natural system. On the other hand, laboratory experiments also give limited information compared to a numerical simulation: while the measurement techniques of the velocity fields are nowadays well established (2D/3D PIV), the simultaneous measurement of the scalar field (density, suspended particles or chemicals) still remains a technical challenge. In contrast, once validated, numerical simulations give access to all relevant variables and permit us to study a much wider parameter range (geometry, non-dimensional numbers), which may become prohibitively demanding for laboratory experiments.

Hence, it crucial to combine the different complementary methods (laboratory experiments, observations, numerical simulations and theoretical modelling) to build robust and consistent models that can correctly represent the key small-scale processes in large-scale ocean circulation and climate models.

This represents the main goal of my future research: to interact actively and constantly with those who develop numerical models for the geophysical fluid dynamics furnishing the necessary data to build robust and reliable numerical/theoretical models and parametrizations and to collaborate closely with colleagues who have access to observational data. The easy access to the Coriolis Rotating Platform makes LEGI an ideal environment for this scope, enabling us to perform unique experiments that can approach dynamical similarity with geophysical flows and giving the opportunity to come into contact with international research groups with complementary competencies.

The contract with the SHOM (20CP03, PI LEGI: A. Wirth) signed in January 2021 is a first concretization of this scope: their interest in the development of the CROCO model in particular for what concerns the validation under non-hydrostatic conditions, (such as encountered in overflows) and who have observational data to compare with both experimental and numerical data. This project opens new collaborations with the LA (F Auclair) and with LEGOS (Yves Morel) in Toulouse, to set-up a national network for the common objective of building a robust numerical model able to better represent sub-grid scale processes under non-hydrostatic conditions.

The core of my research since my PhD focuses on gravity currents over complex terrain using laboratory experiments coupled with analytical modelling and linear stability analysis. More recently, I started to study rotating intrusive gravity currents to understand their contribution to the turbulence production in the ocean. The main contribution of my past research is summarized below.

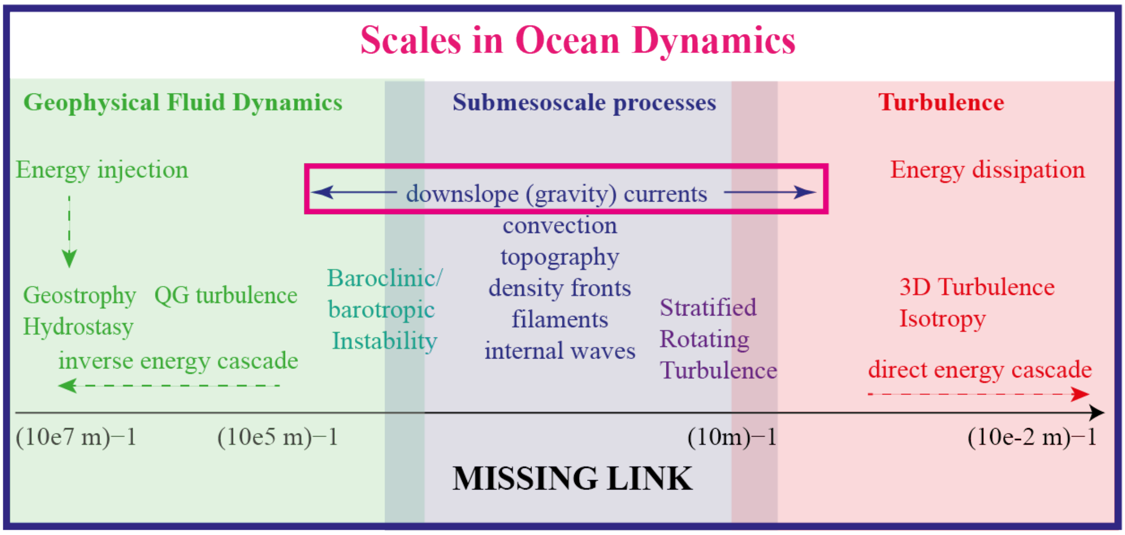

Figure 5.5: Sketch of the ocean scales.

5.1 Research activities after the PhD: an overview

My research following my PhD focused mainly on buoyancy driven flows, and concerned the fields of

1. turbulent convection,
2. gravity currents and
3. geophysical turbulence.

The first topic was particularly interesting for the research politic of the laboratory LEGI and was linked to my recruitment. In particular, the laboratory was interested in initiating the new research axis of turbulent convection for building ventilation at the interface between the geophysical and the energetic teams of LEGI.

For political reasons and due to the poor perspectives of financial support, after conclusion of the PhD thesis of Tobit Caudwell in 2016, my investment within this research topic shifted towards gravity currents over complex terrain that received more local support from the LabEx OSUG and LabEx Tech21. This work was carried out in collaboration with Jan-Bert Flor, Emil Hopfinger and Christophe Brun. It started to evolve into the geophysical turbulence topic since the last three years, linked to my previous work during the post-doctorate.

Starting from January 2018 I was given the opportunity to take the scientific responsibility for the transnational access at the Coriolis Rotating Platform within the European consortium 'Hydralab +' from which active and fruitful collaborations started (INOGS, Trieste, University of Rome, Univ. Partenope Naples, EPFL Lausanne, TU Vienna) that opens wide perspectives of collaborations with international groups that have access to observational data and/or have a large experience with numerical codes of geophysical flows. During the last three years I followed closely six Hydralab+ research projects, in which I was actively involved not only during the designing phase and performance of the experiments, but also for the data analysis, interpretation and discussion of the results and redaction of articles. I further realized two transnational access projects with the

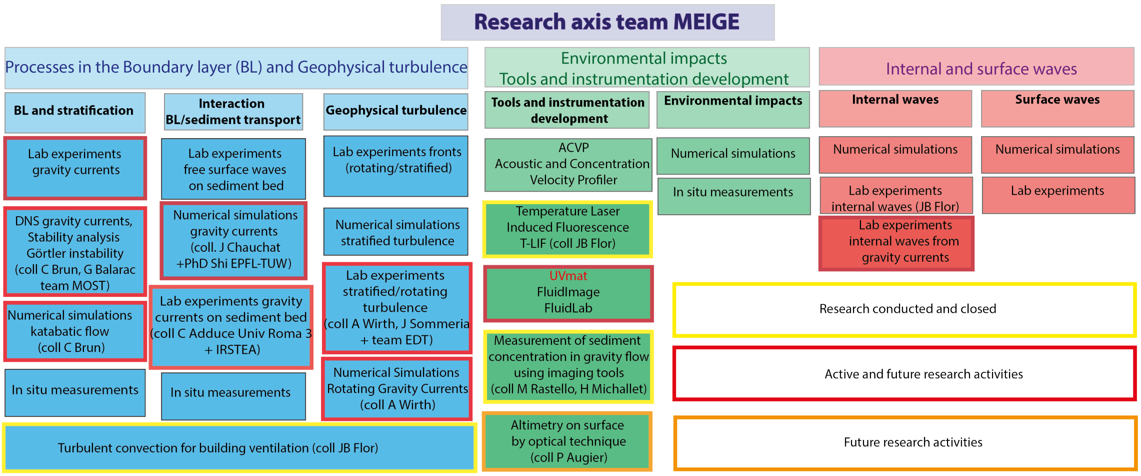

Figure 5.6: Organigram of the research activities of the team MEIGE at LEGI. Red boxes highlight my present research activities orange boxes enclose future research not started yet, while the yellow boxes represent the research finalized during the considered report period and not active at the present time.

./figs/timeaxeNew.png

Figure 5.7: Timeline of my research activity performed and planned in the future. The different colors indicate the four research axis: Turbulent Convection (blue), Gravity currents over complex terrain (green), Geophysical turbulence (red) and the access to the Coriolis rotating platform (yellow). The projects and the non-permanent staff are written in the corresponding colors.

EPFL (Switzerland) and INOGS (Italy) in 2020 and 2021, respectively. Hence, I include in the following also the research that has been accomplished within these collaborations.

Figure 5.6 gives an overview of my research activities within the team MEIGE at LEGI. The main accomplishments of my research are described further below, while for the detailed results the reader is referred to the journal articles given for each topic. An overview of the topics of the research accomplished and the future research perspectives are given in figure 5.7.

Chapter 6

Turbulent convection

Since the research topic was new to me and at LEGI, the first works on this topic concerned the development of an experimental facility appropriate for studying turbulent convective flows in competition with stratified conditions and to study the interaction between the small plumes generated at the kinetic and thermal boundary layers and the Large Scale Circulation that have been seen to develop in a convective cell (figure 6).

A particularity of this tank was the possibility to regulate the temperature on the lateral walls, which permitted to study non-adiabatic effects in turbulent convection and asymmetric heating.

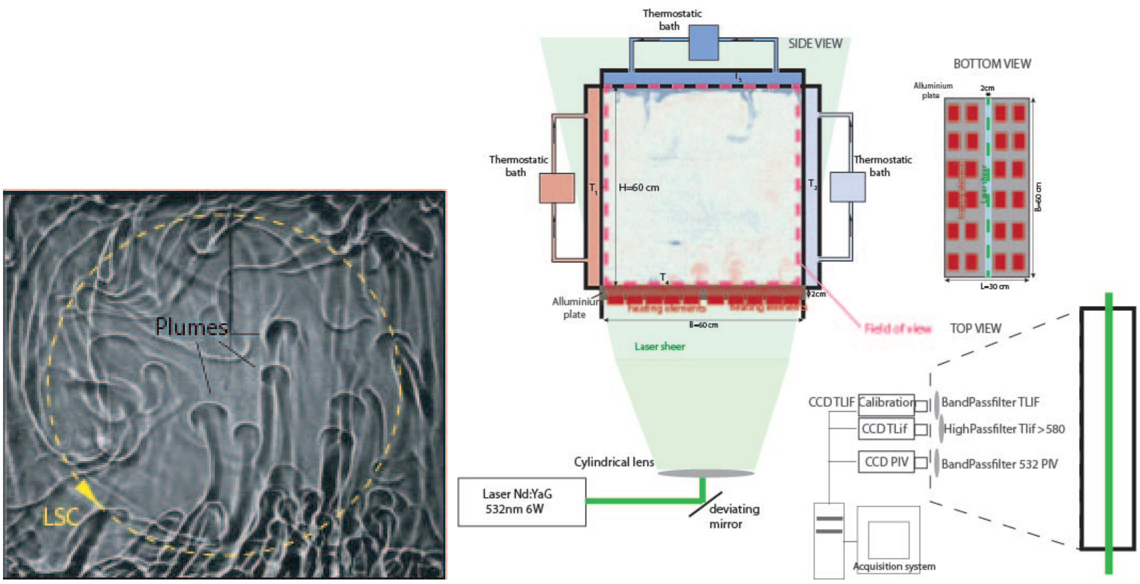

Figure 6.1: (Left) Shadowgraph visualisation of the different structures in turbulent convection ($Ra \sim 10^8$, $Pr \sim 10^2$): the convective plumes released from the cooled/heated surfaces and the large scale circulation (LSC) which can be recognized by the preferential direction assumed by the plumes (from [36]). (Right) Sketch of the experimental set-up for the study of turbulent convection available at the LEGI.

I contributed to the initial development of a new experimental technique to measure simultaneously the velocity field using PIV (Particle Image velocimetry) and the temperature field in a two-dimensional plane. This technique takes advantage of the different emission spectrum of fluorescein dye with temperature (TLIF). Preliminary tests using different fluorescent dyes, laser distributions and two different cameras have been per-

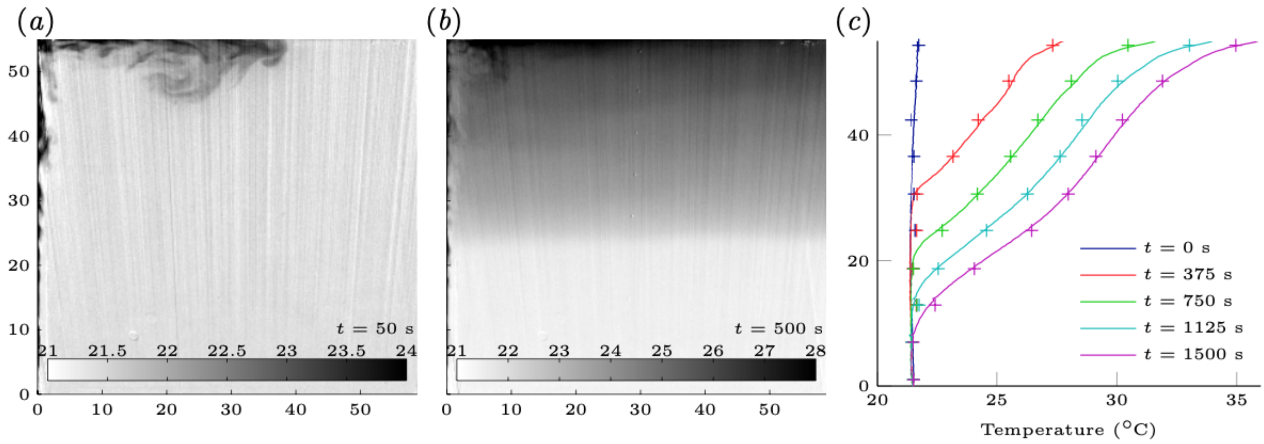

Figure 6.2: Examples of TLIF results. Gray levels represent temperature in Celsius degrees, axes are in centimetres. (a) Temperature field at the beginning of the experiment ($t = 50\,\mathrm{s}$). (b) Temperature field when stratification is established ($t = 500\,\mathrm{s}$). Remaining striations due to temporal variations in laser light did not affect the results. (c) Stratification profiles taken at different times, averaged over 10 s with probe measurements (+) and T-LIF measurements (solid lines).

formed within a master thesis (M2) by L. Rakatomalala in 2011. The development of the technique continued with the M2 thesis of Tobit Caudwell, who then continued with a PhD; within his PhD work, a very high precision in the measurements of the temperature field using the TLIF technique has been achieved (0.2 °C) over a very long experimental duration of several hours, which was never achieved in turbulent convection measurements (figure 6.2). This research was done in collaboration with Jan-Bert Flor, DR2 at LEGI. A research article for the Journal of Fluid Mechanics with results of simultaneous PIV and T-LiF measurements and considering a vertical lateral distributed heat source has been published in 2016 (`publication [13]`). The research focused on the understanding of the temporal entrainment behaviour of the lateral plume rising from the lateral heating within a rectangular cavity (cf. figure 6.3a), as well as the different roles played by the laminar and turbulent boundary layer within the rising plume (cf. figure 6.4). The wall plume was found to have an inner layer close to the heated boundary with a laminar transport of hardly mixed fluid which causes a relatively warm top layer and an outer layer with a transition from laminar to turbulent at a considerable height. The measured entrainment coefficient has been found to be dramatically influenced by the increase in stratification of the ambient fluid (cf. figure 6.3).

To model the flow, the entrainment model of [76] has first been adapted to the case of an isothermal wall. Differences due to their boundary condition of a constant buoyancy flux turned out to be small.

Next, to include the laminar-turbulent transition of the boundary layer, a hybrid model has been constructed which is based on the similarity solutions reported by Worster and Leitch [123] for the laminar part and the entrainment model for the turbulent part. Finally, the observed variation of the global entrainment coefficient, which is due to the increased presence of an upper stratified layer with a relatively low entrainment coefficient, has been incorporated into both models. All models have shown reasonable agreement

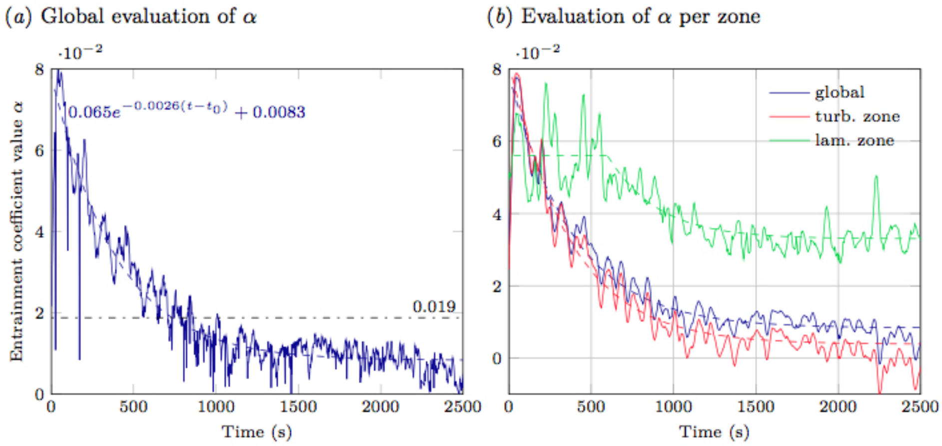

Figure 6.3: (a) Experimental entrainment coefficient for the entire plume against time, with the average value (dash-dotted line) and exponential fit (dashed line) with t_0 taken at 30 s for the onset time of the plume. (b) Entrainment coefficient for the turbulent part of the plume (red), the laminar part (green) and total plume (blue) with the respective exponential fits. The data has been averaged over 20 s.

with the experimental measurements for the volume, momentum and buoyancy fluxes as well as for the evolution of the stratification in the interior. In particular the introduction of the variable entrainment coefficient has improved all models significantly.

Observations gave access to dynamics and patterns within the stratified medium, and to the turbulent plume structure in interaction with the ambient stratification. Using the obtained results, a precise description of the initial and long term evolution of the stratification generated by a rising plume at a heated wall has been given. A model derived from plume theory of Morton et al. [76] has been adapted to the case of a constant temperature boundary condition. The detailed experimental data allowed to compare each of the key variables (volume, momentum and buoyancy fluxes) with the model predictions to highlight its strengths, weaknesses and limits. Since the interior in these flows is heated so that the buoyancy of the wall plume decreases, also the entrainment coefficient has shown to decrease. Including a varying entrainment coefficient and considering the wall shear stress, both estimated from the experimental measurements (see figure 6.3b), a significant improvement of the theoretical model has been achieved.

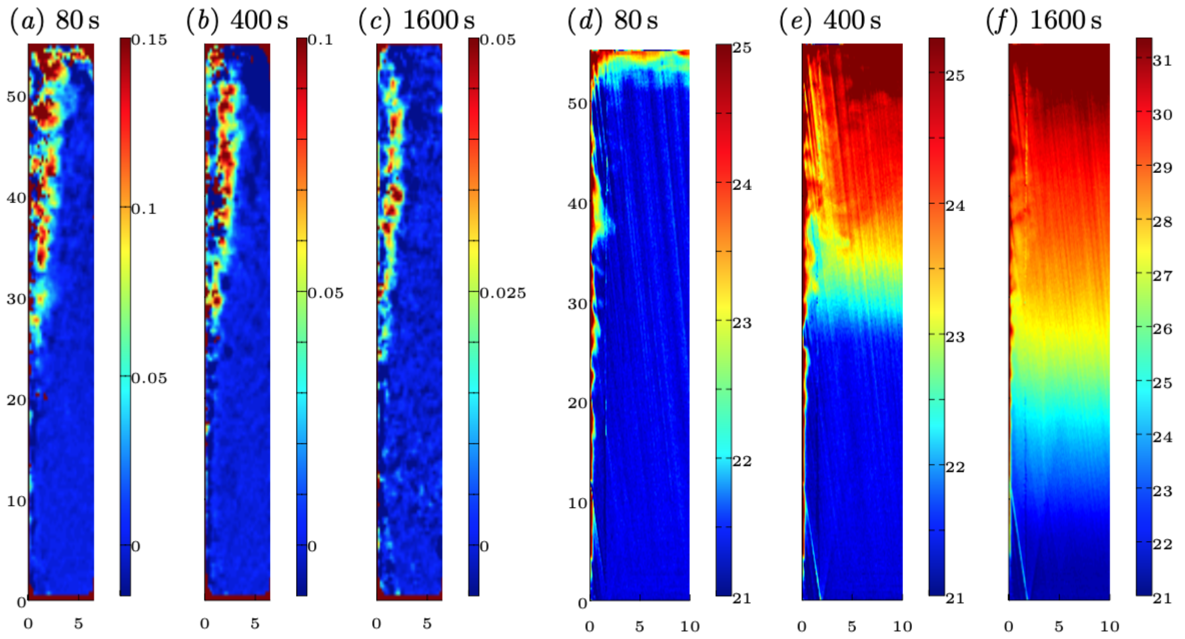

Figure 6.4: (a)-(c) Reynolds tensor $u'_x u'_z$ ($cm^2 s^{-2}$) and (d)-(f) temperature (C) in the plume region at respectively t = 80, 400 and 1600 s after the start of the forcing. Axes are in centimetres.

Chapter 7

Gravity currents

7.1 Contribution to non rotating gravity currents

Laboratory studies of gravity currents have been essential in the understanding of the dynamics of gravity currents. Most of these studies focused on gravity currents on horizontal or slightly inclined boundaries, where the head is an essential feature of the flow [103]. The first experiments of the steady layer gravitational flow down slopes were conducted by Ellison and Turner [28] who also developed the, now classical, similarity theory of these flows (see also Turner [112]) and since then, there has been a very large amount of studies on various horizontal and downslope gravity currents under different boundary conditions, however mostly assuming self-similarity and a constant value of the Richardson number.

The initial developing region of the current before reaching the constant Richardson number conditions was investigated by Pawlak and Armi [90], who studied experimentally the development of an accelerating current on linear inclines. Turbidity currents on slopes can also accelerate due to sediment entrainment [89]; Rastello and Hopfinger [94], but the flow preserves similarity and an equilibrium state because accelerations are weak. However, when there are more complex terrain conditions (such as rapid slope changes, curvature or enhanced bottom roughness) the current may undergo to stronger accelerations or decelerations and this may affect the global characteristics of the gravity current (height, speed, momentum and buoyancy fluxes) and interfacial and bottom boundary layer instabilities with related drag terms (entrainment and bottom friction), which can vary spatially and temporally very strongly.

These questions represented the core of my research on non-rotating gravity currents. An overview is illustrated schematically in figure 7.1 and the main accomplishments are summarized below, subdivided into three areas:

1. Rapidly changing slopes (`publications` [21, 53, 68, 69, 87, 125]). In these situations, the gravity current is not in the commonly assumed equilibrium regime and the current development and classical entrainment laws are not valid anymore. This is supported in observations as in the Romanche Fracture Channel in the South Atlantic Ocean [113] or plunging flows from rivers into lakes or oceans [35, 53].

2. Enhanced bottom roughness (`publications` [49, 65, 66]). Herein, the aim is to better understand and quantify the interaction between the bottom boundary layer and the sheared interface through enhanced bottom roughness (fixed and interaction with bottom sediments) in gravity currents, including sediment transport and morphological aspects.

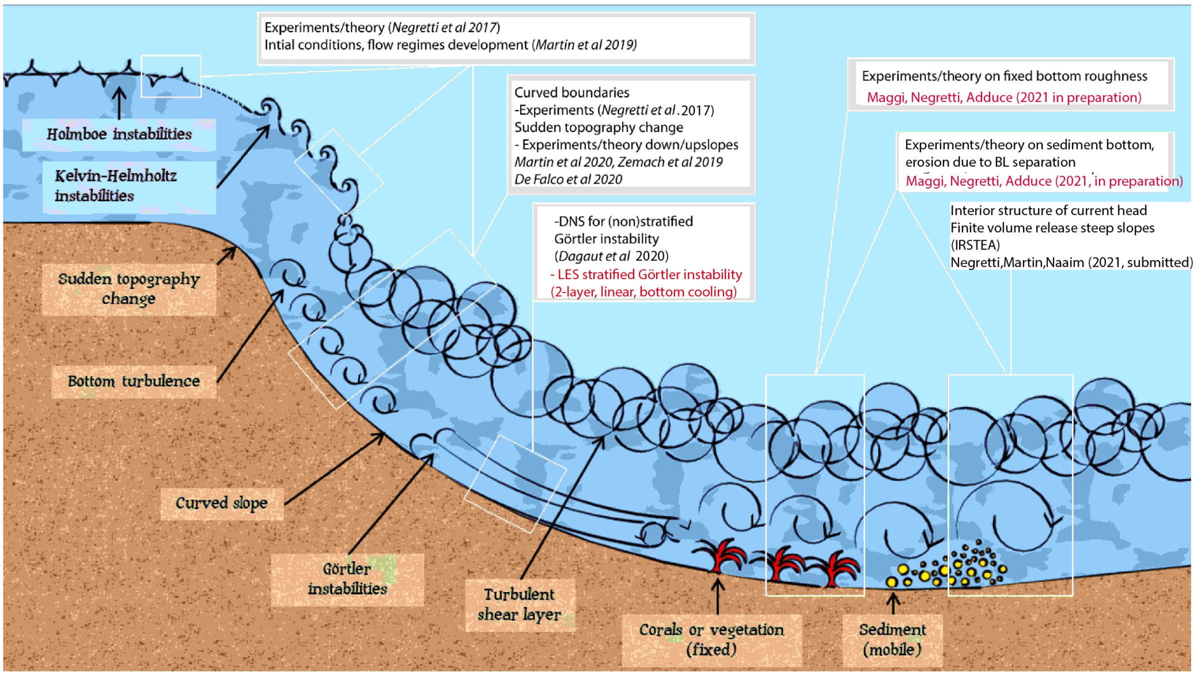

Figure 7.1: Overview of the research on non-rotating gravity currents over complex terrain.

3. Effects of the flow curvature on the dynamics of gravity currents (`publication` [87]). In particular, in collaboration with C. Brun and G. Balarac, the possible conditions of existence of the Görtler instability in a stratified flow are investigated. Note that for this topic, we started with the non-stratified problem (Blasius boundary layer) to better characterize the transition to stratified conditions (`publication` [19]). Results on the stratified boundary layer on curved slopes are presently processed [18].

In the following, essential conclusions on the research accomplished in these three areas will be presented.

7.1.1 Spatial Development

We considered first a gravity flow moving from a horizontal boundary onto a concave slope, producing two effects: first the sudden slope change, and, second a smooth topography variation induced by the concave bottom.

The sudden change in boundary slope and the consequent acceleration has shown to give rise to a transition from a stable subcritical current with a large Richardson number to a Kelvin-Helmholtz (KH) unstable current. The interface thickness and shear across the interface at the start of the slope are crucial for the nature of the gravity current downhill. They determine, together with the acceleration down the slope, the flow instability and the size of the KH billows, and therewith the flow evolution. We can summarize the main results on the spatial development as follows.

(i) When a gravity current with an initially thick and stable interface (high interfacial Richardson number) on a horizontal or nearly horizontal boundary moves onto a steep slope, it is first stable, and then, as a consequence of shear instabilities at the interface and Kelvin-Helmholtz billows, undergoes a cycle of accelerations and decelerations and does not reach the constant equilibrium velocity within the distance x_c of approximately $30h_0$ considered, where h_0 is the initial depth of the gravity current (cf. figure 7.2(a,b,c)). Subsequently, it evolves towards a state of collapsed Kelvin-Helmholtz billows on top of the accelerating dense gravity current. Different regimes have been reported depending on slope angle and on the initial velocity and density profiles, characterized by the Richardson number $J_i = \delta_i g_0'/\Delta u_i^2$, where δ_i, Δu_i and g_0' are, respectively, the velocity interface thickness, the maximum velocity difference and reduced gravity at the beginning of the slope (cf. figure 7.2(a,b,c)). For $J_i > 0.7$ and the larger slope angle, the flow strongly accelerates, reaches a maximum at the beginning of Kelvin-Helmholtz instability, then decelerates and re-accelerates again. For $0.3 < J_i < 0.6$, instability occurs earlier and velocity oscillations are less. When $J_i \leq 0.3$ the increase in velocity is smooth. This latter case is the commonly assumed case for classical downslope plume theory [28, 112]. The magnitude of velocity oscillation depends on the combined effect of J_i and slope angle, expressed by an overall acceleration parameter $\overline{T_a} = \frac{\delta_i}{U_i}\frac{U_c - U_i}{x_c}$, which, to first order, is given by $J_i \sin\theta$, where U_c and x_c are, respectively, the velocity and position at instability onset. The velocity increases smoothly up to equilibrium state when $\overline{T_a} \leq 0.06$ and exhibits an irregular behaviour at larger values of $\overline{T_a}$. This evolution is quite different from the flow over a weir, accelerating on a slope, as investigated by [90], where the current has from the beginning a thin unstable interface. The value of the Richardson number at the sill, and in particular the shear thickness, are thus important for the initial flow development on the slope.

(ii) The spatial development on a concave boundary, more representative of natural slopes, is very similar to that on a constant slope boundary, so that it is rather the sudden slope change that causes the observed different behaviour in the development of the gravity flow.

(iii) By solving numerically the depth integrated governing equations, the gravity flow velocity, depth and buoyant acceleration in the flow direction has been well predicted for all the performed experiments over the full measured domain. The numerical results for the experiments with $J_i > 0.3$ predict that the current requires a distance of at least $x_n \approx 40h_0$ to reach a normal state of constant velocity, which is much larger than the distance $x_n \approx 10h_0$ required in the case of a current with $J_i \leq 0.3$ that is commonly assumed for downslope currents (cf. figure 7.2(d,e,f)).

(iv) The first Kelvin-Helmholtz billows cause boundary layer separation and reattachment, which lead to a large boundary friction coefficient which is of the order of the interfacial drag due to entrainment. Dye visualizations have shown the continuous formation of billows in the bottom boundary layer coupled with the development of the large Kelvin-Helmholtz billows at the interface. Hence bottom friction may become very large and cannot be neglected, and, more importantly, is directly related to the entrainment at the interface (cf. figure 7.2(c)). These results are given in `publications` [68, 87]).

This latter point motivated the collaboration with R. Kostashuck and E. Meiburg, who observed wall boundary layer separation related to the interfacial instability activity in their in situ observations and numerical simulations, respectively, of pulsing plunging flows.

Several different mechanisms have been ascribed to the generation of velocity pulsing observed in continuous turbidity currents entering lakes and reservoirs, including Rayleigh-Taylor instabilities that are related to surface lobes along the plunge line where the river enters the receiving water body and interfacial waves such as Kelvin-Helmholtz instabilities. Through a stability analysis for inclined flows [85] compared against laboratory experiments, direct numerical simulations, and field data from Lillooet Lake, Canada, and Xiaolangdi Reservoir, China, an improved understanding of the formative mechanisms for velocity pulsing has been achieved. Both Rayleigh-Taylor and Kelvin-Helmholtz instabilities are shown to be prevalent in turbidity currents depending on initial conditions and topography, with plunge line lobes and higher bulk Richardson numbers favoring Rayleigh-Taylor instabilities. Other interfacial wave instabilities (Holmboe and Taylor-Caulfield) may also be present. These results are given in `publication [53]`.

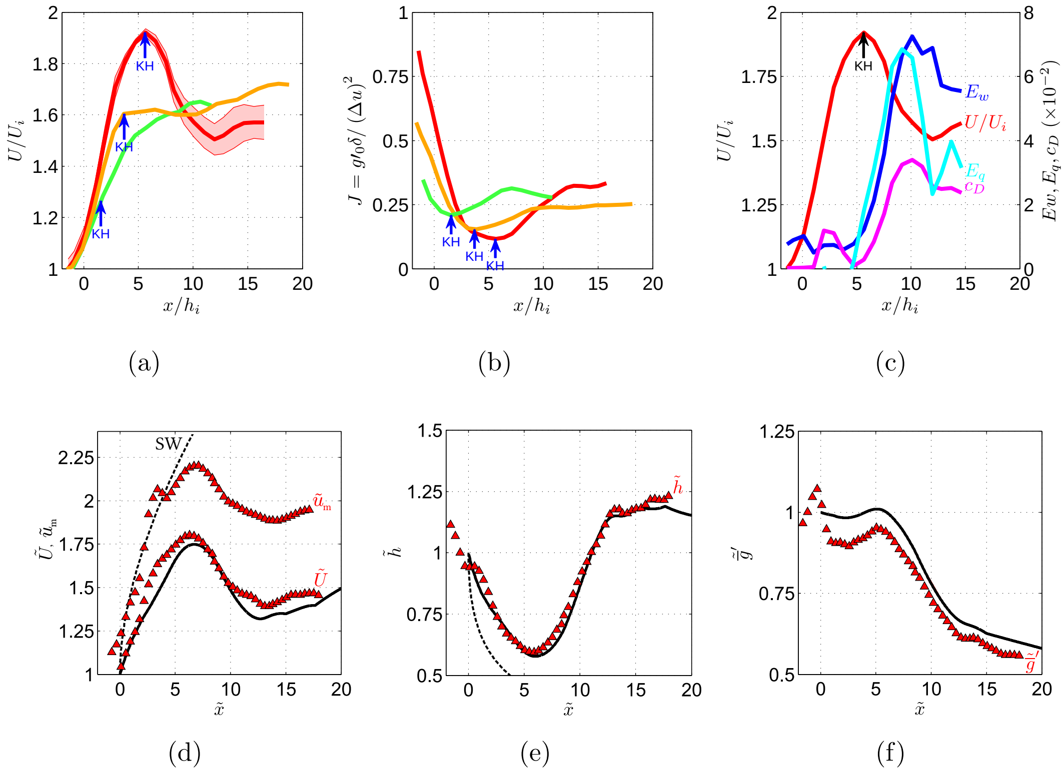

Figure 7.2: a) Depth integrated velocities for the three regimes identified and (b) relative interfacial Richardson number for a slope of 15 degrees. The regimes are classified based on the acceleration parameter: the larger T_a, the more oscillating are the basic characteristics of the gravity current. (c) Drag terms in the downstream direction. (d,e,f) Comparison between experimental data and the numerical solution of the theoretical model (continuous line) and the classical shallow water model (dashed line) for velocity, depth and buoyancy anomaly.

7.1.2 On the gravity current head

The theoretical development in the above summarized studies was based on the depth integrated momentum equations that enabled to study the steady tail of a continuously supplied gravity current, *after* passage of the initial gravity current head. Beside the tail characteristics, environmental flows are often represented by the gravity current head, such as submarine currents, powder snow avalanches or dust storms [103].

Downslope currents (`Publication` [69]) A combined theoretical-experimental investigation of the downslope propagation of a gravity current sustained by a source has been performed in collaboration with Marius Ungarish (IIT Haifa, Israel). Considering the different initial conditions for the experiments discussed in the previous section 7.1.1,

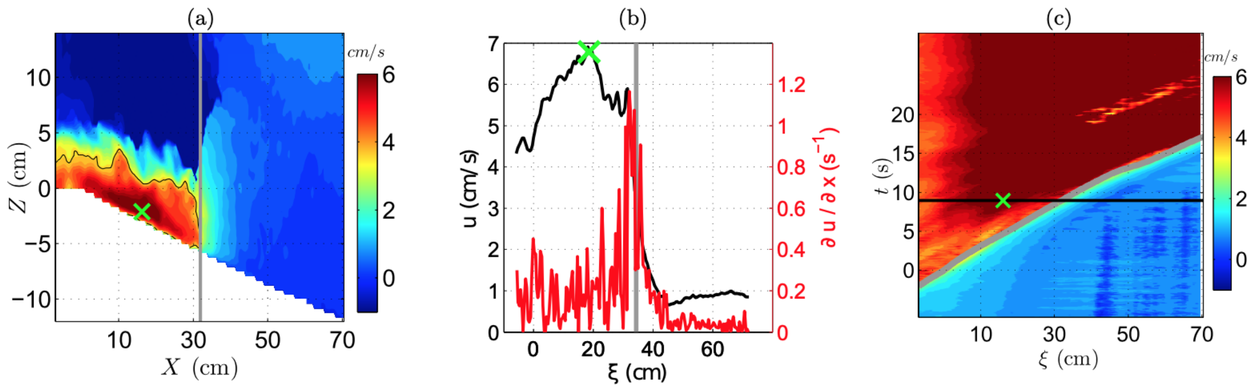

Figure 7.3: (a) Instantaneous ($t = 9$ s) along-slope velocity for a linear slope of 10° (*Exp. 6*), $u = U$ (black contour). (b) Instantaneous free stream velocity with ξ (black) and spatial derivative of the free stream velocity (red). (c) Hovmöller diagram of the free stream velocity with ξ and t, time position of the snapshot (horizontal black line). Nose position (grey line). The green cross represents the maximum velocity in the head as reported in [87].

we focused on the case of a current with a stable interface and critical with a Froude number $F = 1$ at the slope begin. The equations that govern the nose propagation and speed has been derived using a shallow-water model, in which the nose represented a jump matched to characteristics emitted at the ridge. This provided a self-contained prediction for the speed of propagation and position of the nose (cf. figure 7.3). The predicted speed showed to increase with time and distance from the ridge. Since the interfacial Richardson number decreases with the distance from the ridge in the tail behind the nose, appearance of instabilities at a certain travelled distance determines the domain of validity of the obtained shallow water solution. A good agreement was reported with various experiments with different initial conditions at the ridge and slope angles (both constant or and changing with distance from the ridge, cf. figure 7.4). An important result that emerged is that the nose velocity is always less than the maximum velocity within the current head, which corresponds to the speed of the characteristics released at the ridge that catch on the current head (cf. figure 7.3).

Further developments of the the Shallow Water (SW) theoretical model for finite volume released currents has been extended including entrainment and drag. When this quantities have been added to the shallow-water balances (using an off-the-shelf closure for the entrainment coefficient and a constant drag coefficient), the shallow water extended model (SWE) can also predict the experimentally observed accelerating-decelerating regimes in the downslope current (see `publication` [125]).

Upslope currents Within the PhD framework I co-supervised of MC De Falco, the dynamics of gravity currents propagating up a slope has been investigated by experiments performed at the University of Roma Tre (cf. figure 7.5) and a novel theoretical analysis based on self-similarity theory. The developed theoretical model, using the depth averaged momentum equation, provided new physical insight into the importance of the different driving forces and accounts for the gravity component along the slope, whose effect increases with both the slope angle and the ratio of ambient fluid to current depth. The height of the current is assumed to decrease linearly with up-slope distance and the spatial rate of decrease is determined from the theory, using the measured up slope distance at which the current stops. This current shape parameter is found to depend on

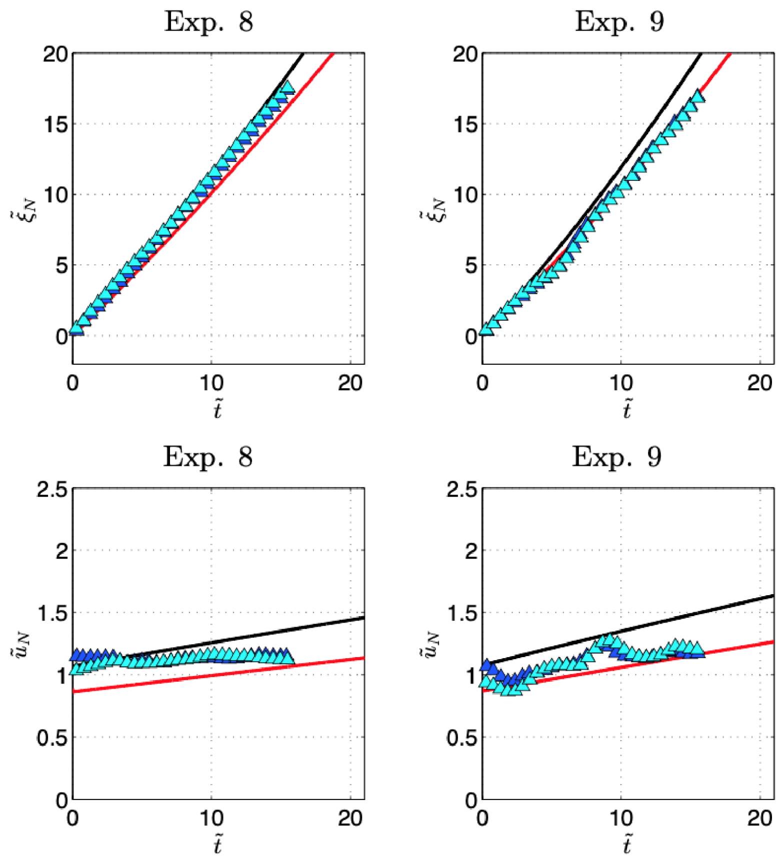

Figure 7.4: Nose position (top panels) and nose velocity (bottom panels) for one of the performed experiments. Model solution (continuous lines) and experiments (symbols) obtained from a threshold on the free stream velocity (blue triangles) and from the maximum spatial derivative of the free stream velocity (cyan triangles). The theoretical nose speed $\tilde{u}_N$ and position $\tilde{\xi}_N$ are computed using different Froude number conditions at the nose (black and red lines).

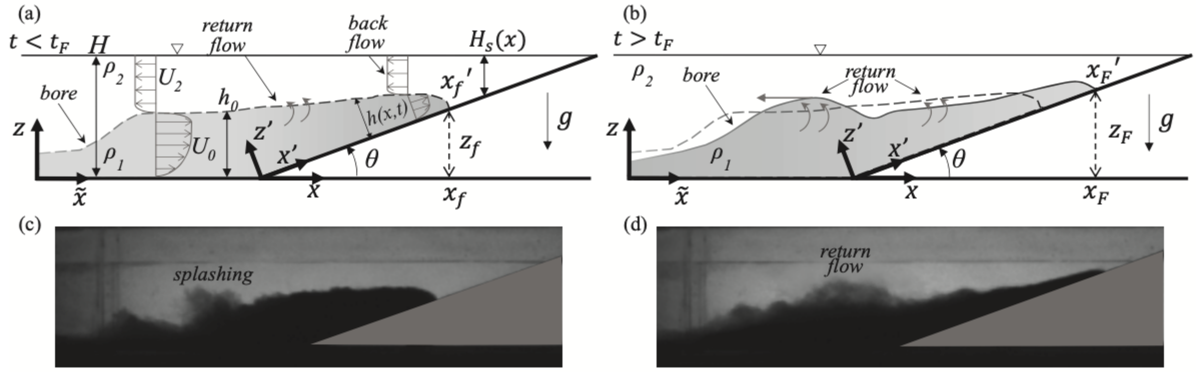

Figure 7.5: Schematic representation of the interaction with the inclined bottom and snapshots of the experiment with a slope of $S = 0.36$ and $\phi = 1$. (a) and (c) $t < t_F$ at time $t = 7\,\mathrm{s}$, (b) and (d) $t > t_F$ at time $t = 13\,\mathrm{s}$, where t_F is the time at which the current front comes to a stop at $x'_f = x'_F$. The dashed line in (b) represents the interface of the dense current shown in (a).

the slope only. The theory is capable of well predicting the front velocity of all performed experiments indicating that the theory remains valid up to slopes ≈ 1, although some splashing occur already for slopes > 0.5. The good agreement between theory and experimental results, confirms the validity of treating the gravity current development as a space dependent problem when flowing up to slopes ≈ 1 (see `publication` [21]).

Interior structure More recently, the downslope propagation of a finite volume released gravity current over steep slopes has been investigated at INRAE using combined PIV/LIF measurements delivering detailed information of both velocities and concentrations inside the current head.

The gravity currents have been generated using saline solutions released from a reservoir by the opening of a gate within a quiescent fresh water ambient with a constant total water depth within the channel.

The evolution of the head down the slope includes three stages: a first one in which the cloud accelerates fed by its tail with increasing buoyancy. A large scale recirculation vortex develops at the back of the cloud which has shown to be hydrostatically unstable that causes separation of the tail from the head. Consequently, the buoyancy (and lateral surface) of the cloud stop increasing [70]. In this latter stage, a large dilution of the head takes place with consequent deceleration of the current.

Experiments were focused on the deceleration phase of the buoyancy cloud at a distance $x \ll 10H_0$ from the initial volume reservoir. Results relative to the global quantities characterizing the buoyancy cloud such as the head speed, the buoyancy and the lateral surface are in agreement with previous studies, predicting in the later development stage of the buoyancy cloud the loose of buoyancy and lateral surface.

The combined velocity and density measurements showed the complex turbulent structure of the cloud (cf. figure 7.6). The back of the buoyancy cloud is gravitationally unstable with the associated Thorpe scale larger than at the front of the cloud. Large patches of ambient fluid are engulfed into the cloud, especially at the back of the head due to a large scale recirculation vortex, that causes convectively unstable structures within the head and subsequent intense dilution. Smaller scale instabilities at the limiting edge between the head and the ambient fluid also contributes to local mixing and dilution.

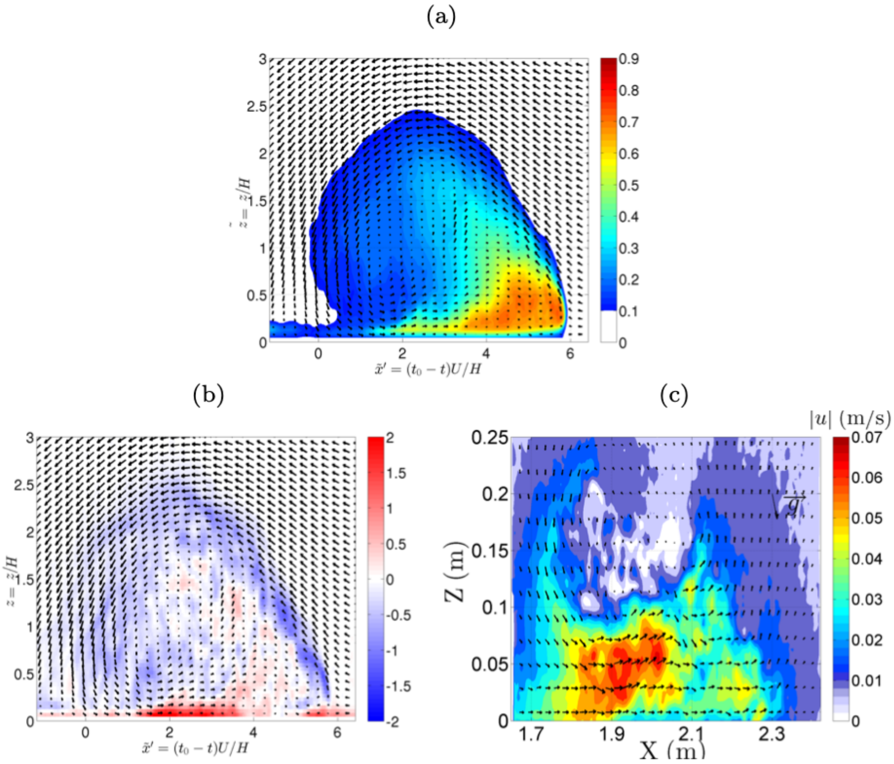

Figure 7.6: (a) Mean structure of the buoyancy cloud for $\Delta\rho/\rho|_i = 5 \times 10^{-3}$. Density $\langle \Delta\rho/\rho \rangle$ (color) and velocity $\langle \vec{u} \rangle - \langle \vec{u}_B \rangle$ in the buoyancy cloud referential with $\langle \vec{u}_B \rangle$ the velocity of the gravity center of the buoyancy (black arrows). (b) Mean vorticity of the buoyancy cloud for $\Delta\rho/\rho|_i = 5 \times 10^{-3}$.(c) An example of an instantaneous PIV/LIF field.

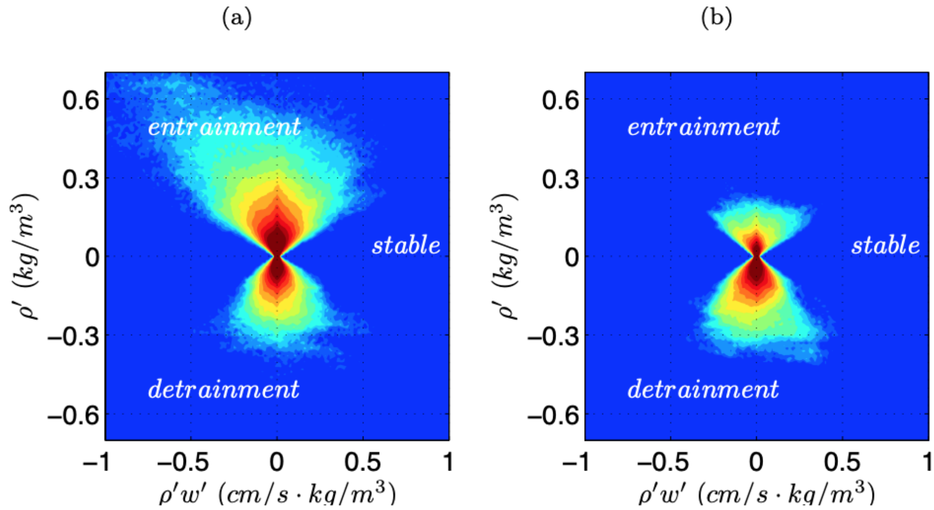

Figure 7.7: 2D PDFs of the density flux versus density fluctuations. (a) For an increase of A/A_0. (b) For a decrease of A/A_0.

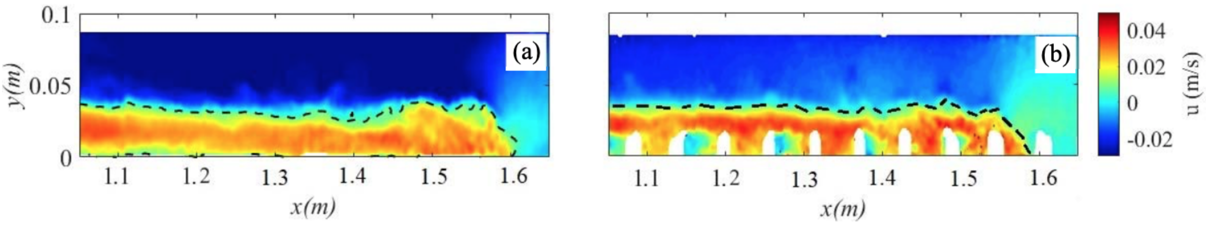

Figure 7.8: Streamwise velocity field after the current has travelled 1.6m for a smooth run (a) and rough run with the height of the elements being 2.5 cm at $t = 23$ s and $t = 26$ s, respectively. The strong recirculation patterns and the enhanced velocity just above the roughness elements close to the interface with the ambient fluid are evident in (b).

Using the combined velocity and density data and by averaging the buoyancy cloud along its descent, turbulent fluxes have been estimated revealing that the usual parameterization laws based on the assumption of a constant turbulent diffusivity or a constant turbulent mixing length does not work properly for such highly spatially inhomogeneous structures. The initial development region has shown to produce intense entrainment, while the final stage is characterized rather by detrainment (cf. figure 7.7). Additional studies are needed to find the appropriate turbulent closure for these flows. These results are given in a paper (`publication` [81]) which has been submitted in October 2021.

7.1.3 Interaction with the bottom

Further experiments to explore the effect of regular/irregular bottom roughness elements on the propagation and mixing properties of lock-release gravity currents including both the slumping and inertial regimes have been conducted. PIV experiments in longitudinal, transverse sections and specific zoomed areas behind the obstacles have been performed and preliminary results show a combined role of current characteristics and friction Reynolds number that together dictate the mixing processes and extent of dilution in density currents over roughness, very different from smooth bottoms.

Figure 7.8 shows the instantaneous maps of the streamwise velocity, for two of the runs performed when the current reaches almost the limit of the visualization window. The frontal region of the current loses definition and the forward speed of the current decreases as the height of the roughness increases. By continuity the ambient fluid above the dense current decelerates too, and this deceleration seems to be related to the LEGO Bricks height, the larger the height the larger the deceleration. Furthermore, figure 7.8 shows some alternate recirculation areas, with clearly negative velocity values between the LEGO structures, absent in the smooth case. The data are processed within the PhD thesis of M.R. Maggi at the University of Roma Tre. These results are given in an article in preparation for a special issue in Environmental Fluid Mechanics `publication` [65]).

The subject of gravity currents over rough bottoms (fixed roughness elements and sediment bed) will be part of my future research perspectives and are detailed in section 12.2 in the Perspectives Part of this manuscript.

7.1.4 Curved boundaries

The effects of curved boundaries on the development of a the gravity current has been investigated experimentally [87]. Through comparison of currents on concave and straight

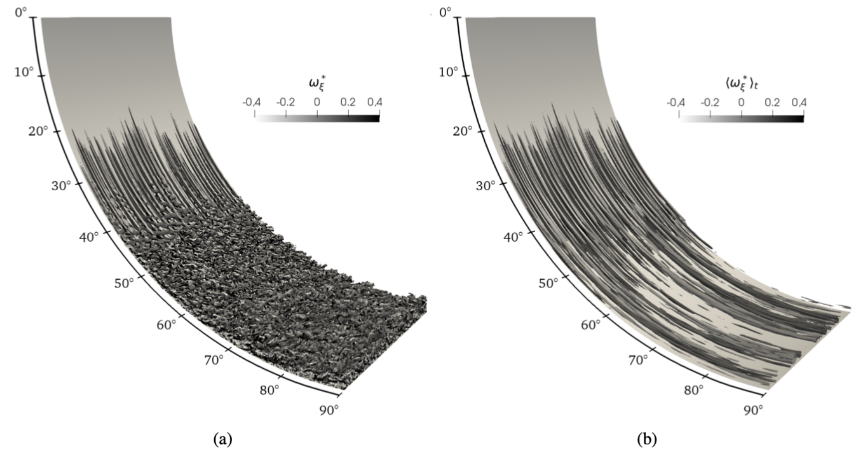

Figure 7.9: Three-dimensional views of iso-contours of the normalized Q-criterion $Q^* = QR^2/U_\infty^2 = 1$, computed from the instantaneous flow velocity field (a) and the mean flow velocity field (b) colored by the instantaneous non-dimensional vorticity $\omega^*_\xi = \omega_\xi\delta_0/U_\infty$ and the mean non-dimensional streamwise vorticity $\langle\omega^*_\xi\rangle_t = \langle\omega_\xi\rangle_t\delta_0/U_\infty$. Streamwise streaks structures (Görtler vortices) are visible in the non-linear region of the instability ($22° < \phi < 42°$), and persistent in the turbulent region (b).

slopes, the downhill deceleration on concave slopes reveals to have no quantitative influence, without formation of centrifugal instabilities: the dynamics is entirely dominated by the initial acceleration and ensuing shear instabilities induced by the sudden slope change. Specific experiments need to be designed to explore the onset of such instabilities in stratified flows.

Instead, the problem of the effects of a curved boundary on the development of a (non) stratified boundary layer has been tackled using numerical simulations which is the core of the PhD thesis of Jeremie Dagaut that I co-supervise, with C Brun and G Balarac (LEGI). This work is motivated by previous observations and realistic numerical simulations of the atmospheric boundary layer, that the so-called Görtler instability can arise due to a local unbalance between the centrifugal force and the radial pressure gradient. Prior of investigating the effects of a background stratification on the Görtler instability, highly resolved Large-Eddy Simulations of a boundary layer flow over a concave wall has been performed using a Blasius inflow profile and both with and without turbulence and wavelength forcing. Figure 7.9 gives a 3D view of of iso-contours of the normalized Q-criterion $Q^* = QR^2/U_\infty^2 = 1$, computed from the instantaneous flow velocity field obtained from a simulation without initial turbulence and wavelength forcing, with the inlet Reynolds and Görtler numbers $Re_{\theta_0} = 1,175$ and $G_{\theta_0} = 75$, respectively. Transition to turbulence is then induced by the natural development of the Görtler instability and a developed turbulent region was reached at the end of the computational domain, with maximum $Re_\theta = 1,800$ and $G_\theta = 140$.

In this case, the developed flow over a concave wall exhibits steady large scale vortical structures that induce a spanwise heterogeneity of the mean flow properties even in the developed turbulent region, with a first clear wavelength in the initial development region $\lambda_1 = 0.385\delta_0$ and a second clear wavelength $\lambda_2 = 1.55\delta_0$ in the turbulent region.

The predictions of both the most amplified wavelength along with the associated spatial modes obtained by extending the linear stability analysis of [32] to a wider parameter

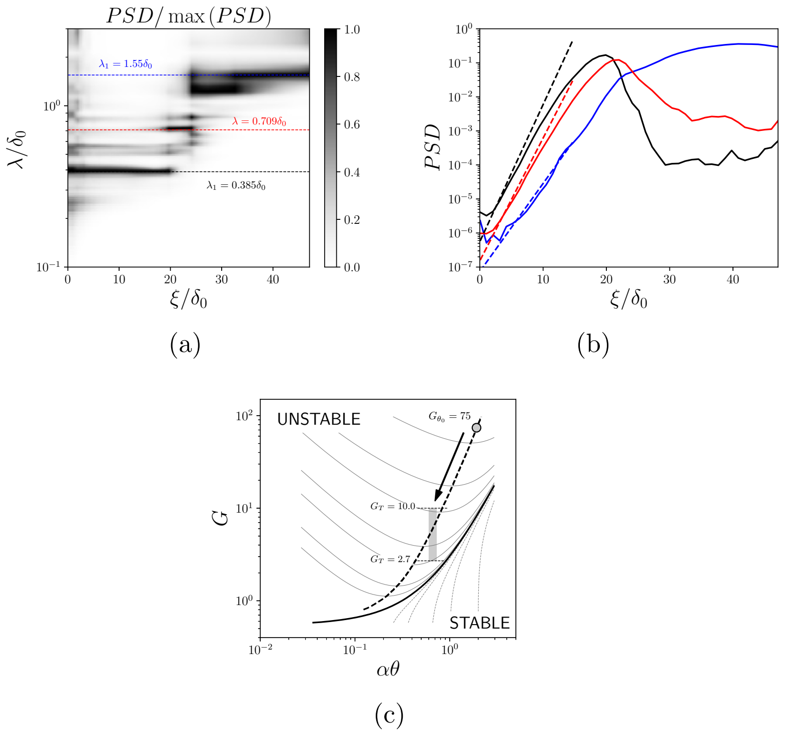

Figure 7.10: (a) Spectrogram from a spatial FFT in the spanwise direction on the wall-normal disturbance velocity $\langle v \rangle_t'$ normalized by the local maximum amplitude. Two dominant wavelengths emerge in the different development regions: $\lambda_1 = 0.385\delta_0$ (linear region, black dotted line), $\lambda_2 = 1.55\delta_0$ (turbulent region, blue dotted line) and an intermediate wavelength $\lambda = 0.709\delta_0$ (red dotted line); (b) respective streamwise evolution of the power spectral densities (solid lines) with the theoretical growth from LSA (dashed lines). (c) Curves of constant non-dimensional amplification rates $\beta\theta Re_\theta$. The black thick solid line and thick dashed lines correspond to the stability limit and the curve of maximum amplification rate, respectively. Present LES results are highlighted by the grey box, considering the turbulent Görtler number $G_T = U_\infty\theta/\nu_t(\theta/R)^{1/2}$.

domain of G_θ and the non-dimensional wavelength Λ well compare to the computed wavelength and the spanwise averaged spatial modes in the linear region for λ_1. The dominant wavelength λ_2 in the turbulent domain is well predicted with the LSA if a turbulent Görtler number is considered, in which the kinematic viscosity ν is replaced by the turbulent viscosity ν_t, as proposed by [109] (see figure 7.10). Also, the spatial modes associated with λ_2 converge with a low scatter in the turbulent region.

The skin friction coefficient $\langle C_f \rangle_t$ increases locally up to a factor 3.5 in the non-linear region of dominance of λ_1 and up to a factor of 1.4 in the developed turbulent region for the downwash location of the λ_2 Görtler instability (cf. figure 7.11), very different from the homogeneous distribution of $\langle C_f \rangle_t$ reported previously in the literature, in which no Görtler vorticies develop in the turbulent region because the estimated turbulent Görtler number is close or even below the neutral stability curve. The high value of initial Re_θ induces non-linear effects that act primarily on the first appearing Görtler wavelength λ_1 damping its growth, so that the skin friction coefficient C_f slightly exceeds the flat plate turbulent prediction for the second dominant wavelength λ_2 at the end of the computational domain, and no overshoot of C_f is reported in the region of dominance of λ_1. Additional simulations we performed with a smaller initial $Re_{\theta,0}$ are in agreement

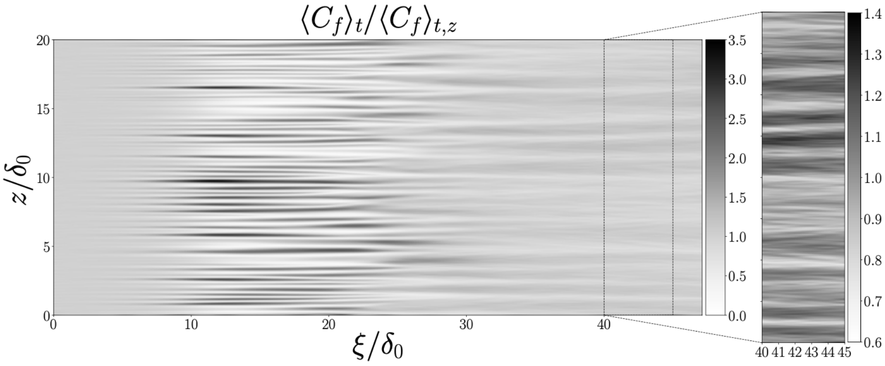

Figure 7.11: Curved wall colored by the mean skin friction coefficient $\langle C_f \rangle_t$ normalized by the local spanwise averaged skin friction coefficient $\langle C_f \rangle_{t,z}$. The zoomed area in the inset ($40 < \xi/\delta_0 < 45$) highlights the persistence of the heterogeneity in the fully turbulent region.

with previous studies with an overshoot of C_f for the first dominant Görtler wavelength with respect to the turbulent plate predictions. These results are given in the journal `publication` [19]).

The next step of this research topic is to explore the influence of a background stratification on the onset and development of the Görtler instability and is part of the PhD Thesis of J Dagaut. Together with my colleagues C Brun and G Balarac, we will pursuit on this research topic (see 12.1).

7.1.5 3D plunging of dense currents

A collaboration has recently started with A. Barry (EPFL), interested in performing experiments at the Coriolis Rotating Platform simulating the Rhone river hyperpycnal inflow into the lake Geneva. Upon entering the water body, the dense river water is known to plunge towards the bottom, and to continue subsequently as an underflow. Knowledge on the plunging process and the plunging mixing coefficient mainly stems from laboratory experiments in highly simplified configurations with a constant width that constrains the riverine inflow. It is qualitatively known that the plunging entrianment is up to an order of magnitude larger in configurations that are not geometrically confined by sidewalls or the bottom [4, 107], such as typically found in natural lakes. Surprisingly, the flow and entrainement processes in such unconfined configurations have never been investigated to date.

The team of Barry has recently established a research project on the plunging process in unconfined configurations to finance detailed field measurements campaigns on the plunging Rhone inflow into Lake Geneva that have already been performed for a variety of hydraulic conditions by the group of Barry, and are still on-going. Parallel, numerical simulations using OpenFoam are being performed in collaboration with my colleague J. Chauchat. The aim of the proposed work is to elucidate the turbulent flow and mixing processes in the plunging area and their dependence on the control parameters by performing a systematic series of laboratory experiments at the Coriolis Rotating Platform, to be compared to the numerical simulations and the observational data.

The experimental set-up consisted in a shallow horizontal channel (1/50) that entered the ambient on an unbounded slope of angle 8°. The superposition of the longitudinal and

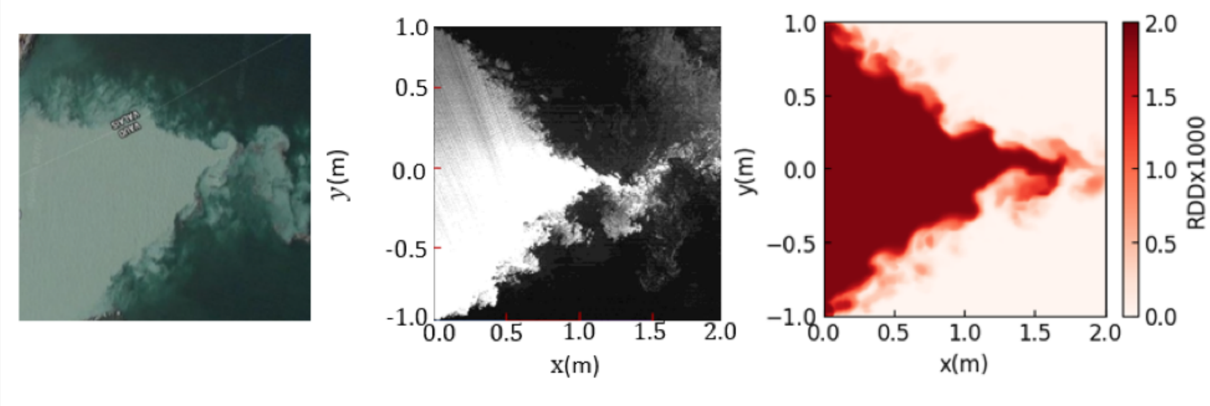

Figure 7.12: Surface shapes of the plunging flow (a) A satellite image of the Rhone River mouth from Google map; (b) Experimental surface image with Rhodamine tracer; (c) Numerical model results showing contours of relative density difference RDD. The densimetric Froude number in the laboratory and numerical experiments is $Fr = 3$ while in the Rhone River $Fr = 10$.

transverse velocity vectors results in a flow pattern that produces a converging velocity (and density) contour on the surface (see figure 7.12) and causes the near bottom cross-section to be much wider than the surface triangle and also wider than the river mouth. It has also been proven that the initial densimetric Froude number is the main parameter which dominates the surface triangle shape. In contrast to 2D hyperpycnal currents, which plunge at one single longitudinal distance, this 3D current progressively plunges at its surface triangular edge. Along this edge, vertical middle-scale vortices are generated by the shear stress between the hyperpycnal current and ambient water (figure 7.12). Because of these vortices, the turbulent intensity in these near-edge areas are 5 times that of the upstream open channel flow, indicating that these coherent structures contribute significantly into the mixing and entrainment during the plunging process. Moreover, the current's core part detaches from the bottom bed due to the angle between the inlet flow velocity and bottom slope, then reattaches again under the effects of negative buoyancy, establishing a detachment area with large density but small velocity inside the plunging current. A further interesting point under investigation is the presence further downstream the surface triangle of localized buoy. The mechanism that produced the localized rising of heavier water is still not understood and represents one significant difference to confined hyperpycnal currents.

These experiments have been financed by the EPFL (15,000Euros) with a PhD (Haoran Shi) which I co-supervise, who came in September/October 2020 to assist the experiments for 6 weeks. He is working on the experimental data and numerical simulations. It is planned to submit a collaborative research project (PRCI) to further finance the research topic in collaboration with the groups at EPFL (Switzerland) and at TUW (Austria) see section 13.2.

7.2 Contribution to rotating gravity currents

7.2.1 Rotating downslope intruding gravity currents

Experiments on rotating downslope intruding gravity currents have been performed at the beginning of 2019 at the Coriolis Rotating Platform (TUBE I). A novel axisymmetric configuration was conceived and an instantaneous image taken during a PIV experiment is shown in figure 7.13. The experiments have been realized using saline solutions to generate the gravity current injected at 32 points equally spaced on the Coriolis Rotating Platform's circumference at the top of an inclined boundary, shaped as an inverted cone, with circular cross section (cf. figure 7.13). This configuration with axisymmetric injection provided a long experimental duration of several hours (200 rotational days) which was aimed at capturing the long term evolution of the gravity current and of the so created turbulent environment in the central deep area (see also chapter 11). The vorticity was thus produced continuously and naturally during the development of the gravity current without imposing any length scale. The ambient reservoir was discrete-layered. The velocity fields have been measured by PIV and an ADVP was mounted on an axis on the slope along a radial section to resolve the thin Ekman boundary layer. The variations parameters were the injected buoyancy flux and the background rotation rate.

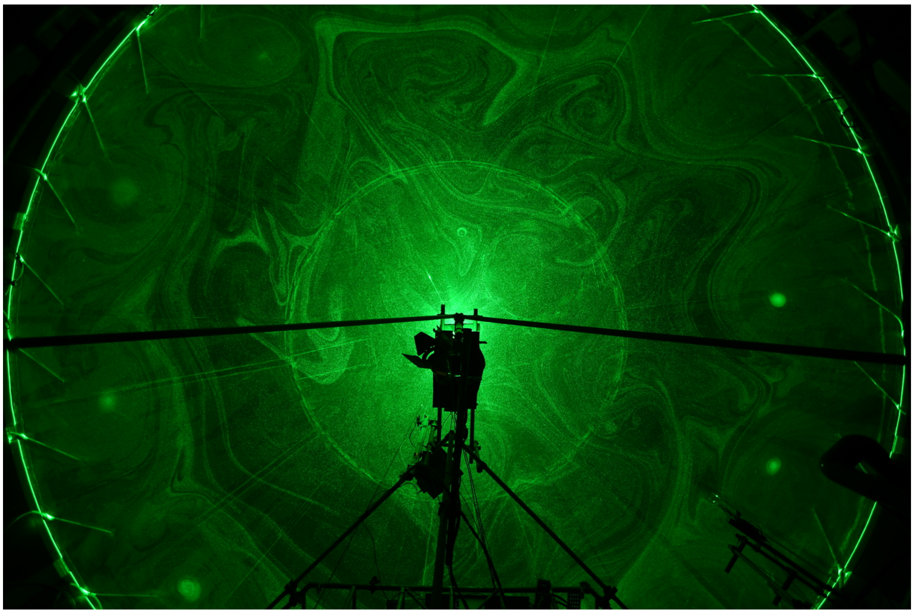

Figure 7.13: Instantaneous image of the PIV field of view at the top layer $z/H = 0.9$ at $t/T = 10$ with cyclonic vortices in the outer area evident from particles concentrated in their core. The horizontal scale is $13m$, the vertical scale 9 m.

With this experimental set-up, once the flow rate was switched on, heavier fluid with respect to the ambient started to exit the 32 pipes (cf. figure 7.13) and a gravity current set in. With the given inclination of the pipes, the current was quickly deviated to the right subject to a geostrophic adjustment, resulting in a main velocity component in the azimuthal direction. Wirth [119] demonstrated that in a 2D setting the current has a dual structure consisting of a thick vein, governed by geostrophy and with an Ekman layer at the bottom, and a thin friction layer at the downslope side of the vein. For a detailed description of the structure of a rotating downslope gravity current it is referred to Wirth [119] and references herein.

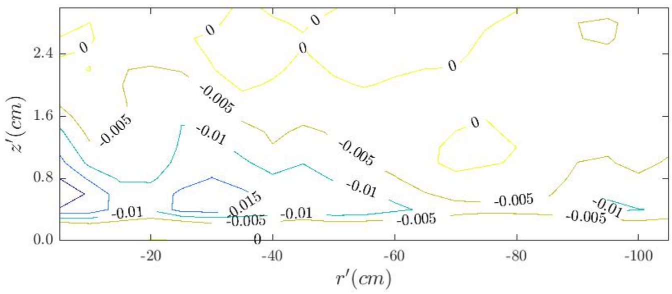

(a)

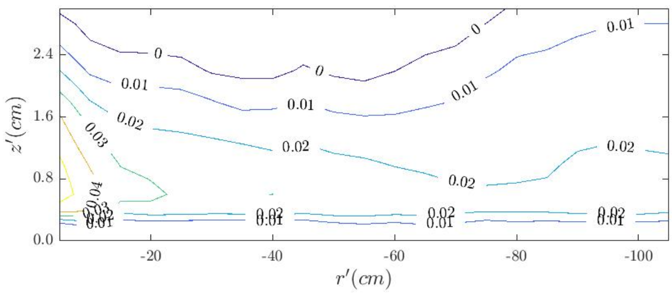

(b)

Figure 7.14: Time averaged velocity contour plots for experiment *B1* over $t/T = 50$ for the two velocity components v' (a) and u' (b).

The scalings of the rotating gravity current proposed in the literature [56, 119] has been verified using the ADVP velocity data captured 1.1 m from the tank edge. Time averaged velocity contour plots relative to one experiment and averaged over $t/T = 50$ are shown in figure 7.14 for the along-slope and radial velocity components v' (a) and u' (b) respectively, with the vertical and radial axis normal and parallel to the slope. For the along slope velocity component v', part of the vein can be clearly distinguished in the region $0 < r' < 20$ cm and $0 < z' < 2.5$ cm, with v' being the dominant velocity with maximum values of $5\,\mathrm{cm\,s^{-1}}$. The radial velocity u' is predominant in the thin layer $0 < z' <$ over the full spanned radial coordinate, which is in good accord with the prediction of the friction layer $\delta_f \approx 0.9$ cm.

After looking to the gravity current structure, focus was concentrated on the surface baroclinic vortices generated by the gravity current.

Past studies [17, 29, 56, 77, 108] have reported the formation of cyclonic vortices in the ambient water above the current. They inferred their formation to two main processes: the geostrophic adjustment process and the Ekman drainage. In the first case, if the fluid above the current is not moving with respect to the current layer, the upper layer is captured by the current following it like a Taylor column. Using the thermal wind relation and the conservation of potential vorticity Lane-Serff and Baines [56] derived a velocity in the upper layer with the sign varying with f, thus cyclonic. In the second case, the cyclonic vorticity is induced in the upper layer by Ekman drainage due to entrainment into the downslope flowing friction layer. The former mechanism occurs on a short time scale while the latter is a process that acts during the whole experiment; both concur to reduce the thickness of the gravity current.

After the initial adjustment phase lasting $t/T \sim 10$ the surface cyclonic vortices have formed and are organized as displayed in figure 7.13, that shows a top view of a raw PIV image of one of the performed experiments, with the core of the vortices highlighted by white spots of concentrated PIV particles. These vortices persist until the end of the experiment duration, for all experiments performed.

From the long time series and analyzing the time variability the characteristics (dimension, speed and vorticity) of the surface baroclinic vortices has revealed to be quasi-steady and ergodic over the considered experiment duration (up to 150-210 rotational days depending on the experiment).

The evaluated size of the surface vorticies $\mathcal{R}_{obs}$ of our experiments are given in figure 7.15a compared to the theoretical Rossby deformation radius $\mathcal{R}_{th} = \sqrt{g'h_*}/f$ (solid red line). The relation proposed by Lane-Serff and Baines [56] and that proposed by Decamp and Sommeria [24] are given as well by the blue and grey shaded regions in figure 7.15a. Since the study of Lane-Serff and Baines [56] was realized in a much smaller installation and therefore with a smaller Reynolds number, with the maximum size of the vortices being one order of magnitude less than the values reported in the present study, this relation do not fit our experimental data. Our data agree better with the relation proposed by Decamp and Sommeria [24], which however still overestimates the reported values.

Lane-Serff and Baines [56] also defined an important length scale to measure the viscous drainage $Y = Q/(v_g \delta_E)$ (where $\delta_E = 2\delta_f$ if the Ekman layer), which gives the length needed for the current to drain through the friction layer. Small values of Y represent strong viscous effects.

One significant difference in the present study is the distributed axisymmetric injection, while in previous studies the injection was realized through a single source. One aspect that has not been discussed in those studies is the eventual presence of topographic Rossby waves, induced by the sloping boundary, which represents a topographic β-plane. Comparison of both the predictions of the wavelength and phase speed of topographic Rossby waves to the experimenta data reveal a good agreement hence suggesting that in our configuration, the size of the surface vortices and their phase speed is not only determined by the Rossby deformation radius, the viscous drainage Y/L_g or the velocity U as suggested by Lane-Serff and Baines [57] and Decamp and Sommeria [24], respectively, but they are also influenced by the topographic Rossby wave, explaining why our results in figure 7.15(a) do not fit with the observations of previous studies. Probably, in Lane-Serff and Baines [57] and Decamp and Sommeria [24] the effect of the topographic β-plane was negligible.

Lane-Serff and Baines [56] argued that the formation of the baroclinic vortices in the upper layer is favored when the depth in the upper ambient layer is reduced, and related this to a vortex stretching mechanism for which the water column is sucked by the current of typical width $\mathcal{R}$ over a depth of order $s\mathcal{R}$. They defined as stretching parameter the ratio between this distance and the total depth above the current in the upper ambient water h_*, i.e. $\Gamma = s\mathcal{R}/h_*$.

Figure 7.15c gives the relative influence of the stretching parameter Γ and the viscous drainage $Y/\mathcal{R}$, that has been classified into three areas by Lane-Serff and Baines [56] based on their experimental data: the so called 'eddy region' above the dashed line, a region without eddies, below the solid line and an overlap region between these two areas that represents a transition region with possible formation of vortices.

Most of our experiments lay in the overlap region as given by the symbols in figure 7.15b, even if in our experiments the baroclinic vortices are clearly developed in all cases.

The eddies form as a result of the stretching of fluid columns in the overlying fluid, which Lane-Serff and Baines [56, 57] explained to be produced by three processes. Two of these are due to the initial adjustment of the flow. The third process depends on

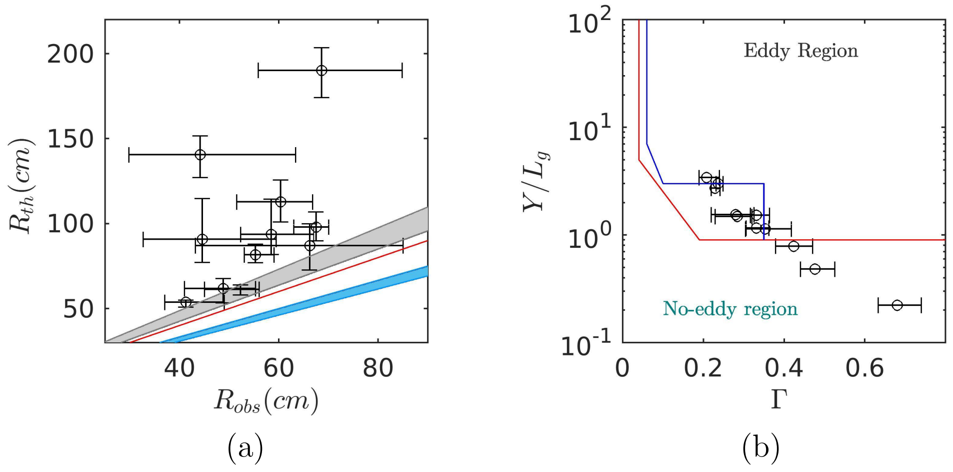

Figure 7.15: Baroclinic vortices averaged characteristics for all the experiments performed. (a) Theoretical Rossby deformation radius $\mathcal{R}_{th}$ versus the observed radius $\mathcal{R}_{obs}$. (b) Viscous drainage Y/L_g versus the stretching parameter Γ. The blue and red continuous lines represent the limit between the eddies formation region and the no-eddies region, along with the overlap region, as proposed by Lane-Serff and Baines [56].

stretching of the fluid column by Ekman drainage from below and operates continuously. These processes are collectively represented by the parameters Γ (the stretching parameter) and Y/L_g (the viscous drainage scale). However, to compare between different laboratory experiments and then extrapolate the results to oceanographic situations, the similarity between the laboratory experiments and the oceanographic scenarios should be approached in terms of the turbulent eddy dissipation as well. For the Coriolis tank, we estimate values of the normalized tubulent eddy diffusivity of the order of 10^{-2}, while for the real ocean context we estimate values of 10^{-3}. The small-scale installation in Lane-Serff and Baines [56] may have damped the formation of such vortices with relevant viscous drainage. The values from oceanic data are smaller than the experimental tank due to weak shear and strong stratification combined with large Richardson numbers.
Hence, we expect the limit of the transition region of vortex formation to be shifted so that vortices develop for lower values of the viscous drainage Y/L_g.
These results are given in `publication` [88]).

These experiments served also to monitor the turbulence that was produced in the central deep area under different initial stratification conditions (homogeneous and 2-layer stratified). Preliminary results are summarized in section 8.2 further below.

7.2.2 Rotating exchange flows and implications for morphodynamical aspects

This research topic was related to the transnational access to the Coriolis Rotating Platform of the group leaded by C. Adduce, (University Roma Tre, Italy) and in collaboration with A Cuthberson (University of Dundee, UK) and Yannek Laanereau (Talinn University, Estonia). The aim of the experiments was to determine the effects of both the rotation and the tides on the lateral distribution of the counter-flowing water masses and of an erodible bottom to investigate the changes in the channel morphology.

The experiments were targeted at obtaining detailed synoptic velocity fields for these

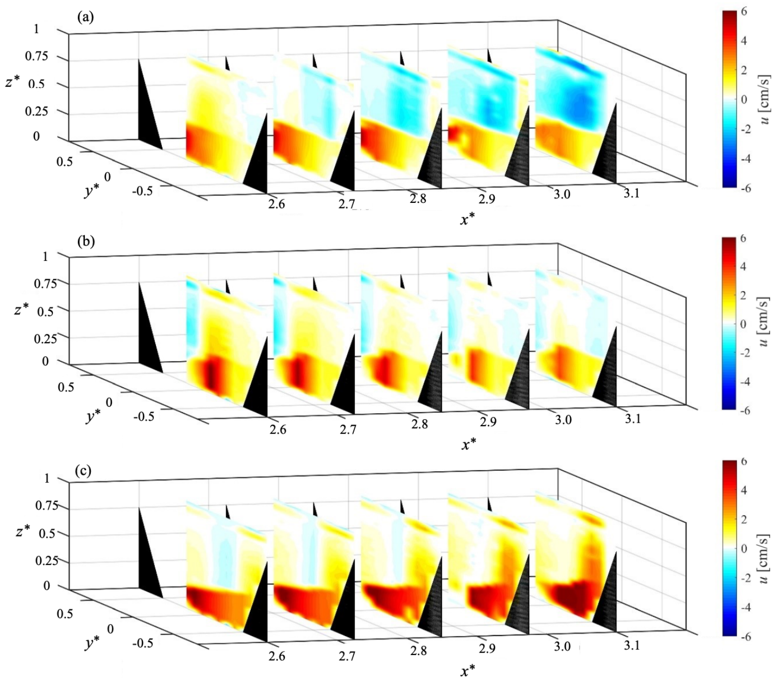

Figure 7.16: 3D Cross channel colormap of the time averaged, along-channel velocity component $u(y,z)$ of an experiment with $q^* = 0$ (with the bottom layer only moving) and $f = 0.2\,\mathrm{s}^{-1}$, for successive PIV scans at (a) $t = 0$, (b) $t = 6\,\mathrm{min}$ and (c) $t = 2\,\mathrm{min}$.

flows from PIV measurements across the flume, as well as density profiles measured at specific transverse locations by micro-conductivity probes. Under non-rotating conditions, the velocity fields highlight the role of the upper fresh water flow in reducing the dense layer thickness, which was also accompanied by an increase of the shear layer thickness induced by the increase of the relative magnitude of fresh and saline inflow q^*, representing the tidal effect. In rotating conditions, in agreement with previous studies, the Burger number Bu is the main governing non-dimensional parameter characterizing the dynamics of stratified rotating exchange flows. For $Bu > 0.7$ the Coriolis acceleration caused the geostrophic adjustment of the outflowing dense saline layer to the right hand channel side wall. By contrast, for $Bu < 0.5$, the exchange flows are characterized by time and space variability and baroclinic instability in the outflowing dense layer (cf. figure 7.16). In particular, in the bi-directional runs with $Bu < 0.5$, the interface slope of the dense outflowing layer deviated from the evaluated geostrophic slopes indicating the presence of ageostrophic motion, due to the baroclinic instability.

Details of this study are given in `publication` [22].

An additional set of experiments has been performed over a sediment bed. Herein, we were able to reconstruct the bed morphology (see figure 7.17) by use of a calibrated camera and performing laser bed scans, within a large domain of $3\,\mathrm{m} \times 1\,\mathrm{m}$ giving information about the bed elevation within less than 10% error. These results are still under processing.

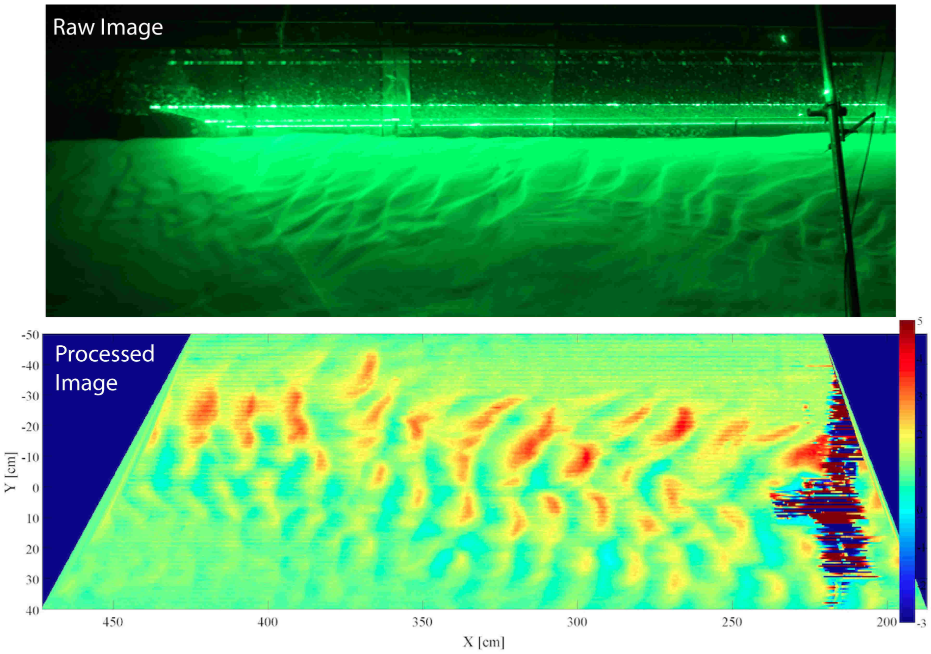

Figure 7.17: Reconstruction of the bed morphology in a rotating stratified bi-directional flow.

7.2.3 The Adriatic-Ionian Bimodal Oscillating System

This research was performed within the transnational access to the Coriolis rotating Platform of the group led by M. Gacic (INOGS, Italy) and in collaboration with A. Rubino (University Ca' Foscari, Italy).

The sense of rotation of the sub-basin-wide upper circulation in the Northern Ionian Sea (NIG, Northern Ionian Gyre) is a possible driver for deviating fresh surface Atlantic waters on their way toward the Cretan Passage to the east and toward the Adriatic Sea to the north. The reversals of this circulation on a decadal time scale (named BiOS mechanism) are known as impacting on marine physics and biogeochemistry and potentially influencing near-term regional climate predictability in the Eastern Mediterranean. They also influence the salt content of the adjacent basins, the Adriatic Sea, and Levantine basin. The salt content in turn, influences the density of the intermediate and deep waters. The BiOS mechanism acts out-of-phase in the Adriatic and in the Levantine basin: when the NIG is anticyclonic, the flow of the AW towards the Levantine is deviated northward, and mixes with adjacent waters (see figure 7.18). So, it dilutes more the upper Adriatic waters, and less the Levantine basin. When the NIG is cyclonic, the Atlantic Water flows directly eastward toward the Cretan Passage and dilutes more the Levantine basin and less the Adriatic basin. At the same time, the Levantine Intermediate Waters and Cretan Intermediate Waters flow westward in the intermediate layer. Whilst it has been suggested that local wind forcing cannot explain such variability, aspects of the alternative hypothesis indicating that NIG reversals mainly arises from an internal ocean feedback mechanism alone remain largely debated.

Using the results of the physical experiments performed at Coriolis we were able to demonstrate that the main observed feature of BiOS, i.e., the switch of polarity of the near-surface circulation in the NIG, can be induced by a mere injection of dense water on a sloping bottom. Hence, BiOS is a truly oceanic mode of variability and abrupt polarity changes in circulation can arise solely from extreme convective events. These results are

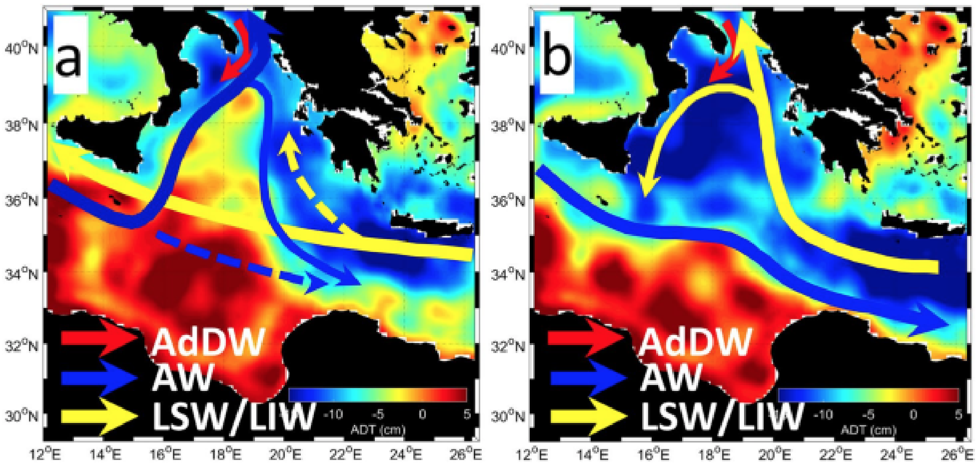

Figure 7.18: Schematic representation of the geostrophic circulation in the North Ionian Gyre region. (a) anticyclonic phase. (b) cyclonic phase. The background maps are annual averages of Absolute Dynamic Topography (ADT) in 1996 and 2003, respectively. AdDW: Adriatic Deep Waters, AW: Atlantic Waters, LSW: Levantine surface waters, LIW: Levantine Intermediate Waters. Adapted from Menna et al.

given in `publication` [96]). A further journal article `publication` [34]) gives details about the flow on the slope area and the flow in the central deep area, comparing results of the different performed experiments with various injection rates and times and initial conditions in the receiving water ambient.

./figs/Rubinoetal.png

Figure 7.19: Normalized vorticity (vorticity divided by the Coriolis parameter (10^{-4}, 10^{-1}, 10^{-1} for panels a, b, and c, respectively). (a) Surface geostrophic vorticity observed in the Northern Ionian area during the year 2012. (b) Spatially averaged vorticity field in the upper layer within the central portion of the laboratory tank for two different experiments: Solid lines represent the normalized vorticity from the experiment at different depths (in cm) from the free surface, dotted colored lines represent the same normalized vorticies for a second experiment, similar to the first, but with an injection of dense water having density $\rho = 1019.5\,\mathrm{kg\,m^{-1}}$ at day 57 and with a larger flow rate ($2\,\mathrm{l\,s^{-1}}$). (c) Near-surface spatially averaged vorticity field within the central portion of the tank as simulated by the numerical frontal model. The vertical lines indicate the onset and the end of the dense-water injection. Please note the different temporal scales in the abscissae between oceanic conditions on one hand and, physical and numerical models on the other. Grey line in (c) represents the vorticity change computed from the theoretical expression.

Chapter 8

Geophysical turbulence

8.1 Stratified turbulence

I worked on this research topic first during my post-doctorate at the LadhyX with P. Billant and J.-M. Chomaz.

Many open questions remain in explaining the dynamics of turbulence in the presence of stratification. Because buoyancy inhibits vertical motions, stratified turbulence is highly anisotropic and generally organized into quasi-horizontal layers as observed in the atmosphere [16] in the oceans [30?] and in lakes [46, 111]. Several experimental and numerical studies have confirmed the spontaneous formation of horizontal layers [37, 93, 97, 115]. However, the origin and role of these layers in stratified turbulence is still not well understood.

The typical vertical thickness of these layers has been shown to be very small ($\sim U/N$, with U being the horizontal characteristic velocity and N being the Brunt-Väisäla frequency). Strongly stratified fluids do not have a two-dimensional dynamics even if vertical motions are small [8]. As a consequence, strongly stratified turbulence is not similar to two-dimensional turbulence with an inverse energy cascade for the turbulent energy spectrum as conjectured previously [61, 95?]. Recent numerical studies have confirmed that the dynamics of strongly stratified turbulence is three-dimensional, with a direct energy cascade from large horizontal scale to small scale vortices [10, 52, 63, 64, 95, 115]. A direct energy cascade has been also found in the atmosphere [62? ?].

Geophysical flows are characterized by a large range of spatial and temporal scales with a complex and unsteady three-dimensional character. Very little is known about the physical mechanisms underlying the direct cascade of energy to small scales in stratified turbulence. When the Reynolds number is very large, the vertical shear between the horizontal layers leads to secondary instabilities (like Kelvin-Helmholtz instabilities [25]) which in turn initiate small-scale three-dimensional motions.

This motivated the experiments conducted at the LadHyx: in order to check the advanced hypothesis of direct cascade associated with a $k_h^{-5/3}$ horizontal kinetic energy spectrum in stratified turbulence, specially designed experiments have been performed. The flow was generated by 12 vortex generators (flaps) placed on the side of a large stably and linearly stratified tank ($2m$x$1m$). The interaction of the randomly produced vortex pairs created a statistically stationary turbulent flow with a low Froude number and a buoyancy Reynolds number of order unity. The velocity measurements in vertical cross-sections showed clearly that the flow organizes itself into horizontal layers (see figure 8.1a). When the buoyancy Reynolds number was increased by increasing the injection

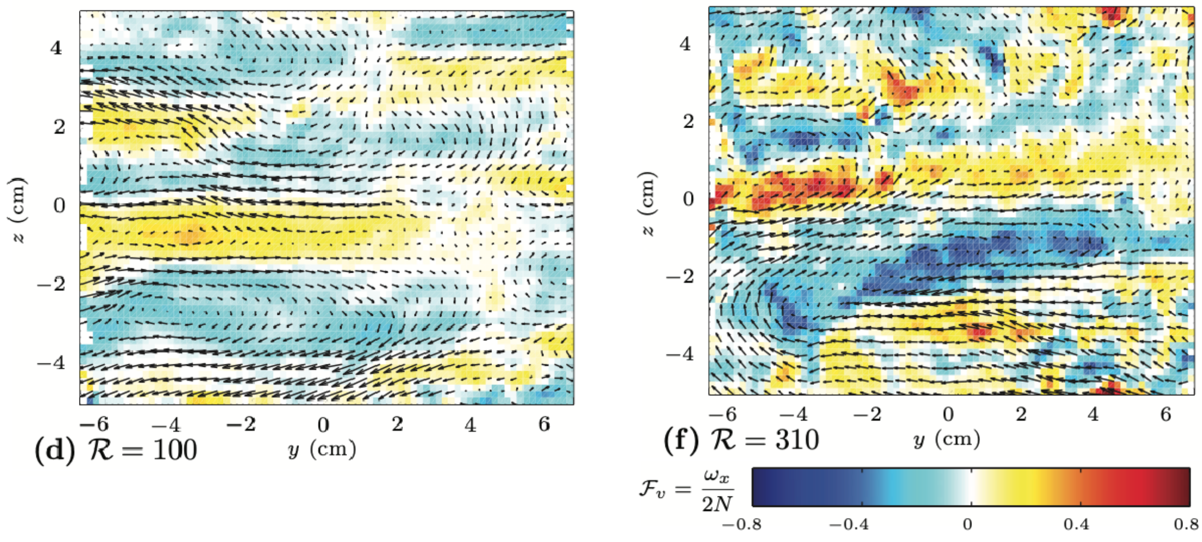

(a) (b)

Figure 8.1: Vertical cross-sections of the velocity in the quasi-stationary regime for a buoyancy Reynolds number $\mathcal{R} = 100$ (a) and $\mathcal{R} = 310$ (b). The colors show the local vertical Froude number $\mathcal{F}_v$, vectors represent the velocity field. The formation of horizontal layers is evident and the onset of shear instabilities between the layers in (b).

rate of energy, also the development of shear instabilities and the increase of the number of overturning events was reported, as evident from figure 8.1b. Consistently with the governing scale laws for which the waves-vortices separation is dynamically meaningless, the divergent and rotational part of the horizontal velocity fields were of the same order of magnitude. These results yielded the prediction of the vertical scale selected by the instabilities as a function of the relevant non dimensional numbers such as the Froude and the Reynolds numbers. `publication` [5]).

A second important issue concerned a possible mechanism for dissipation of turbulent kinetic energy by submesoscale vortices, such as "pancake" vortices, characterized by a very small aspect ratio. Many examples of such vortices exist in the ocean (Spirals, Meddies, Swoddies) and the atmosphere (high and low pressure cells).

One peculiar feature of pancake vortices is a high vertical shear due to their characteristic shape. They also present an anomalous pressure and density structure in their core. Both these features interplay to to form secondary instabilities, like the shear and the gravitational instabilities, important since they are known to cause significant vertical mixing and entrainment by re-initiating three-dimensional motions. In order to better characterize the conditions of onset and evolution of secondary instabilities, the stability of a single pancake vortex has been investigated numerically as a function of its vertical thickness and the Froude and Reynolds numbers.

Numerical results have revealed that reducing the vertical aspect ratio has a destabilizing effect on the vortex stability. Applying the general criteria for each of the most probable instabilities (Kelvin-Helmholtz and the gravitational instability), it has been shown that the dominant mechanisms is related to the anomalous density structure which pancake vortices exhibit in their core. This procedure led us to obtain the stability boundaries in the relevant parameter space and so to calculate the critical aspect ratios for each instability: surprisingly, the Kelvin-Helmholtz instability appears for much lower aspect

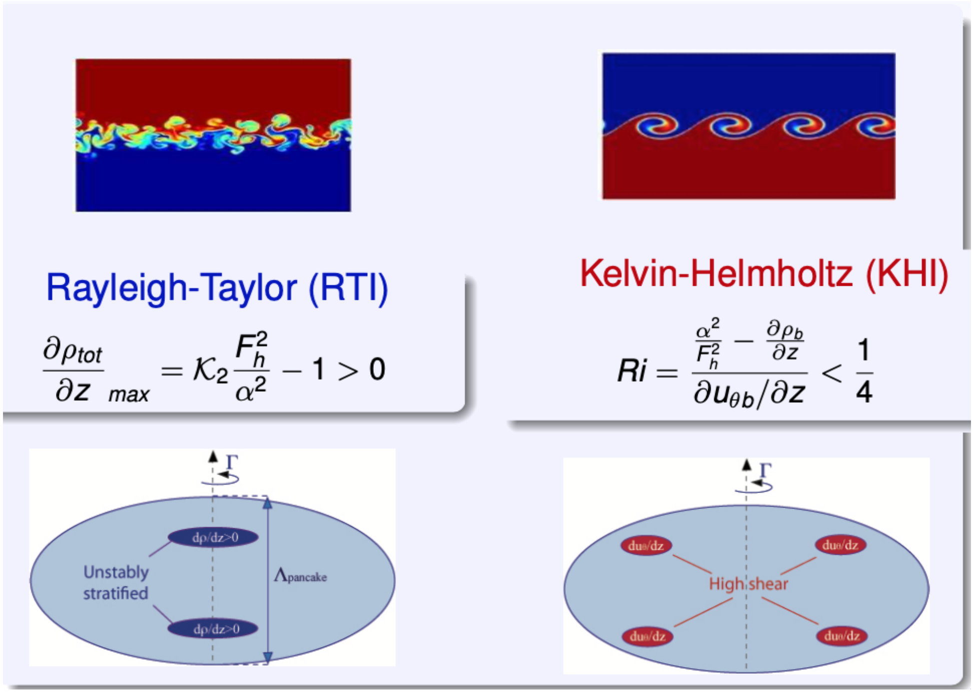

Figure 8.2: Possible small scale instabilities that may arise within a pancake vortex: the Kelvin-Helmholtz instability due to high shear regions and the Rayleigh Taylor instability due to unstable stratified regions. The relative instability conditions are given.

ratios as compared to the gravitational instability (figure 8.2). The comparison of the numerical results with the classical gravitational stability theory (viscid and inviscid) revealed an excellent agreement. The investigation on the effects of the horizontal Froude number demonstrated that reducing the vertical scale has the same effect as decreasing the background stratification. In order to better explain the properties of the gravitational instability developing in the pancake vortex, the linear stability of an unstably stratified fluid in solid body rotation has been considered. In the axisymmetric case the derived dispersion relation could be solved analytically and two types of solutions were found: neutral wave solutions for large vertical wavenumbers (or small unstable stratification) and unstable solutions for small vertical wavenumbers. This is a new interesting result since in the stably stratified case only neutral wave solutions are possible. Results have been finally generalized to any vertical and radial velocity profile.

These results are given in `publication` [82]).

8.2 Stratified and rotating turbulence

Since 2018, I started to work on rotating gravity currents.

Motivated by recent studies suggesting that vorticity in the ocean may have a substantial contribution from boundary layer processes, ([41], [114], [3]), the main idea is to evaluate and characterize the contribution to the turbulence and vorticity production in the ocean induced by boundary layers produced in intruding rotating gravity currents.

While previous studies on rotating gravity currents considered one source to generate the gravity flow, mostly bounded in a channel, and concentrated on the generation of surface baroclinic vortices [15, 27, 29, 48, 50, 56, 60, 100] or, more recently, on the topographic

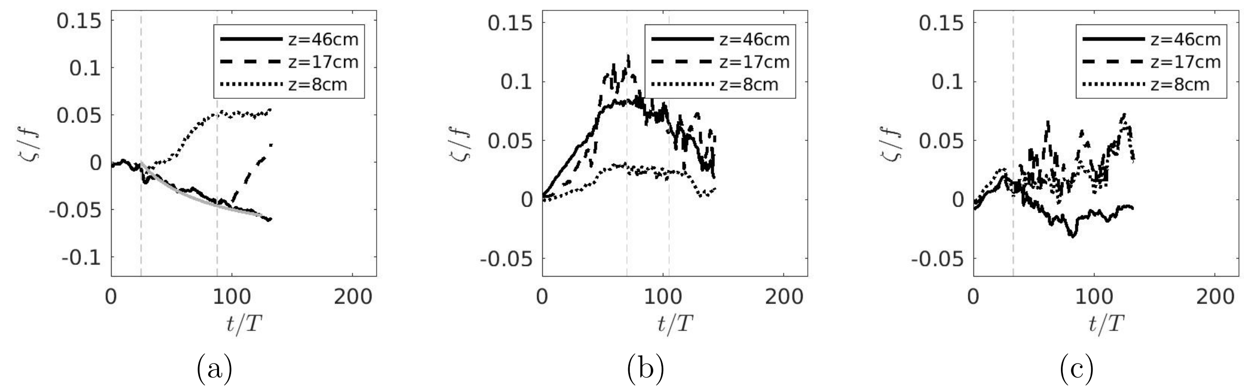

Figure 8.3: Normalized averaged vorticity ζ/f in the central deep area ($r < R_0 = 250\,\mathrm{cm}$) versus time for experiments H (a), I (b) and B (c) with $T = 90\,\mathrm{s}$ at the top layer (solid lines), at the intermediate layer (dashed lines) and the bottom layer (dotted lines). The vertical dashed grey lines are the instants at which the conductivity probe registers a conspicuous salt intrusion.

generated submesoscale vortices [3, 41, 114], the first set of experiments was conceived to explore the long term evolution of the gravity current, monitoring at the same time the subsequent evolution of the global circulation and vorticity produced in the ocean interior by intruding gravity currents, induced by the detachment of the boundary layers. The experiments conducted at the Coriolis Rotating Platform in 2019 demonstrated that a large range of scales can be produced and their evolution can be observed over a long experimental duration (up to 210 rotational days).

In particular, a novel axisymmetric gravity current configuration was conceived in order to create a quasi-steady gravity current and thus to monitor the flow evolution over a very long duration as described in section 7.2.1. Another novelty of this set up consist in considering the intrusion of the gravity current into a stably stratified background which mimics oceanic intrusions [105, 124]. Moreover, it enabled also a better control of the turbulence that is generated by the saline intrusion in the central deep area, as compared to previous studies that used moving grids [47, 54, 93] or random operating flaps ejecting dipoles[5]. This experiment leads to a sustained turbulence production (no turbulence decay) without imposing a characteristic length scale. Another advantage of this set-up is that since the geometry is almost homogeneous along concentric circles, it allows for averaging along this direction, which in turn enables the definition of an averaged large scale circulation.

The variation parameters in the performed experiments were the rotation rate and the initial stratification. In particular, we distinguished a homogeneous case H leading to a bottom gravity current, an intrusive case I with the injection density being between the top and bottom two-layer stratified ambient densities, and a bottom intrusive case B with the injection density very close to that of the bottom layer of the two-layer stratified ambient in the central deep area.

The global circulation induced by the gravity currents - intruding or following the slope until the bottom of the central deep area (I and B, respectively) - reveals to be very different.

Dense (bottom) gravity currents into a homogeneous ambient H turns cyclonically along the slope and induce a global cyclonic circulation in the salty layer while filling the bottom of the central deep area, whereas the fresh ambient water layer turns anticyclonically because of the compression and consequent outward movement in the top layer (cf.

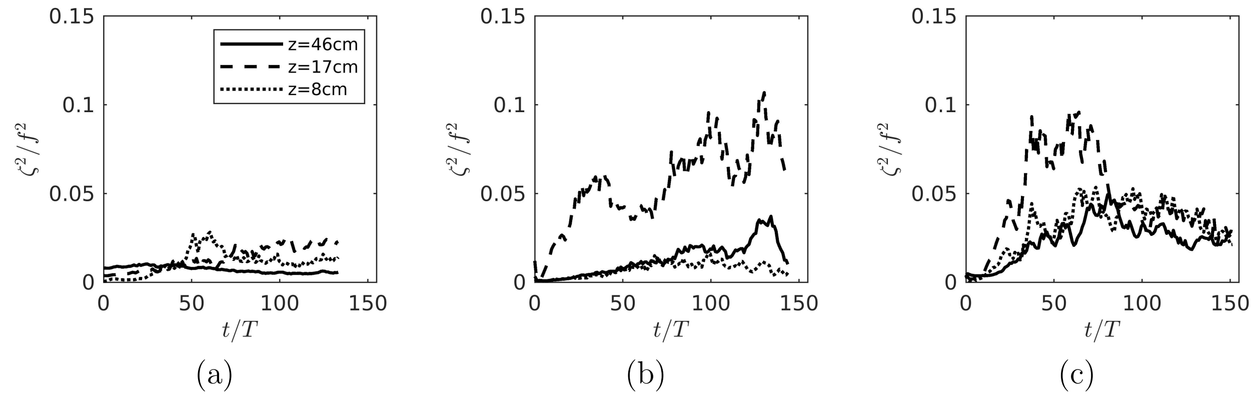

Figure 8.4: Temporal evolution of the normalized enstrophy $\langle \zeta^2(t) \rangle_{\theta,r}/f^2$ averaged in the central deep area within $0 < r/R_0 < 1.1$ at $z = 49$ cm (solid lines), $z = 16$ cm (dashed lines) and $z = 8$ cm (dotted lines) for the experiments *H* (a), *I2* (b) and *B1* (c).

figure 8.3a). Intrusive gravity currents *I* produce at the intrusion location an upward movement that creates a region of anticyclonic circulation on the slope area and a global cyclonic circulation in the central deep area, for all layers considered. As the intrusion propagates into the central deep area creating a third layer, the cyclonic circulation in the top and bottom layers decreases due to compression of the layers (cf. figure 8.3b). In the bottom intrusive cases *B* with an injection density close to the initial bottom ambient layer density, the global circulation is more similar to the homogeneous case as the intrusion takes place in the entire bottom layer, hence stretching it, while compressing the top layer, inducing hence a cyclonic and an anticyclonic global circulation, respectively (cf. figure 8.3c).

Intrusive *I* and bottom intrusive *B* cases were revealed to produce strong turbulent environments in the central deep area at intermediate and bottom layers, in contrast to the dense current which follows the slope until the bottom of the central deep area, where the vorticity in the central deep area remains constant at low values throughout the experiment at all levels. This is shown in figure 8.4, which shows the time evolution of the normalized enstrophy ζ^2/f^2 for the three experiments *H*, *I* and *B* (a,b,c, respectively) at three different depths: one representative of the surface layers (continuous line), one at the intermediate level (dashed line) and one at the bottom (dotted line). For experiment *H*, the enstrophy remains almost constant throughout the experiment at each level, while this is not the case in the intrusive and in the bottom cases, where we have a conspicuous increment of enstrophy in the intermediate layers.

This can be also seen from visualizations as given in figure 8.5, which shows two instantaneous pictures made using Rhodamine injections in the injected saline solutions that reached the pycnocline level at two different times during the experiment: the first after 40 rotational days, the current starts intruding with the boundary layer characterized by small scale instabilities and detaching, with an ejection event in form of a dipole. After 120 rotational days, the same level has become fully turbulent, with a large range of scales.

One important question that remains unanswered is whether submesoscale turbulence in the ocean interior can be created by frictional processes that occur in the boundary layer, with structures that detach from the bottom slope and form coherent vortices, as recently investigated in the studies of Molemaker et al. [74], Vic et al. [114], Wenegrat et al. [118] and Gula et al. [41]. The detachment and propagation mechanisms, still unknown, are likely to be induced by baroclinic and barotropic instabilities and take the

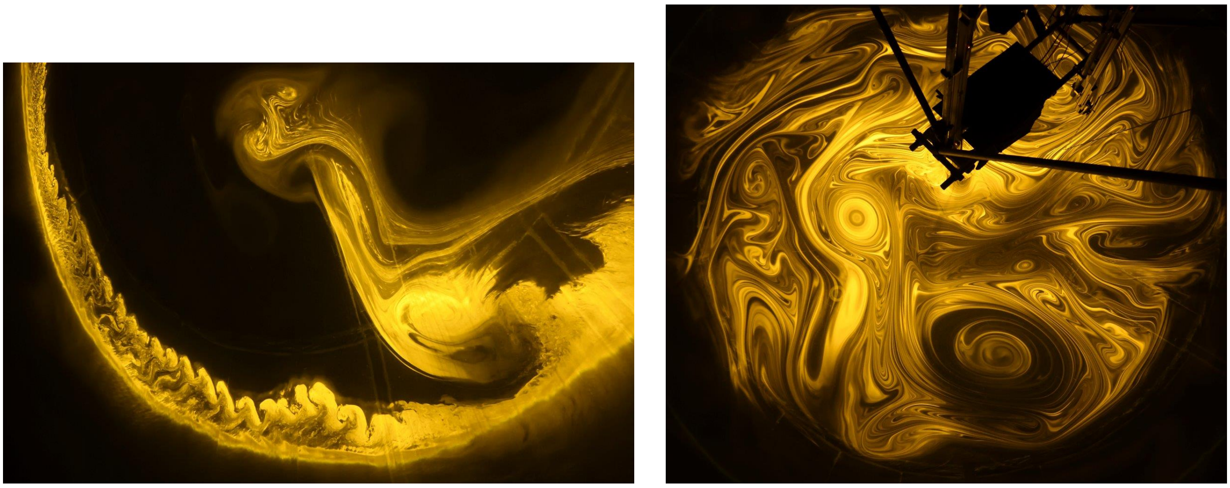

(a) (b)

Figure 8.5: Top view of the pycnocline layer of preliminary experiments at the Coriolis Rotating Platform using fluorescent dye injections. (a) After 40 days dipole ejection and the detaching frictional boundary layer into the quiescent ambient are evident and (b) after 120 days the environment has become fully turbulent with formation of coherent vortices.

form of dipoles, with their own propagation speed induced by mutual advection (Akuetevi and Wirth [3] and figure 8.5). Frictional effects are present in both intrusive and bottom gravity currents. However, the main difference between these two cases is that in the former the boundary layer can detach and freely develop in the ambient water interior, carrying with it the small-scale turbulent structures present in the boundary layer. The size of these turbulent structures begins at the order of the Ekman layer thickness or smaller, and they may then evolve into larger structures, which we call 'submesoscales', that remain smaller than the Rossby deformation radius ($1m$). In the bottom gravity current case, the current always remains attached to the bottom slope and fills the central deep area, so that in this case the small scale turbulent structures remain 'trapped' in the boundary layer and cannot freely develop into the interior. In this case, a global circulation is induced in the central deep area, but the vorticity remain low throughout the experiment in all layers.

These results suggest that the global circulation in the central deep area and in particular the formation of submesoscale vortices of different size and sign is closely related to boundary layer processes that can be transmitted into the ambient interior only in intrusive-type currents (experiments I and B) and not in cases where the current follows the slope until the bottom of the central deep area as in experiment H, with important consequences on the mixing and re-stratification processes that take place in the ocean interior.

These questions motivated a second experimental campaign in the Coriolis Rotating Platform in spring 2021 (TUBE II), representing the core of the PhD work that will be undertaken by the student recruited in October 2021, Sevan Retif.

This project will represent my main research activity for the upcoming years and is further detailed in the chapter 11.

Chapter 9

Other research

9.1 Turbulent jets

In 2017 I investigated the possible existence of self-similar analytical solutions for a turbulent jet in shallow water conditions, continuing the work I initiated during my master project `publication` [83]) in which I obtained self-similar analytical solutions for shallow wakes.

In the work of the M2 student F. Afolabi which I supervised in 2018 and in collaboration with M Brocchini (University of Ancona, Italy), it has been shown that the momentum decreases exponentially as a function of the bottom friction coefficient in the transverse direction, as for shallow wakes. A self-similar solution satisfying the full governing equation including bottom friction could not be obtained. Successive approximations permitted to solve analytically the problem in some basic cases. Two asymptotic cases have been distinguished: dominance of free turbulence and dominance of wall turbulence. Also perturbed solutions have been considered. This work is not concluded yet and needs further investigation.

Within the collaboration matured during the transnational access to the Coriolis Rotating Platform of F. De Serio and M. Mossa (Politecnico di Bari, Italy), the problem of jets in a rotating frame and interacting with vegetation (represented by rigid vertical plastic tubes) has been investigated (cf. figure 9.1). The effect of rotation on the turbulence induced by an obstructed pattern such as a jet is felt indirectly through the modification of the mean flow, and so the subsequent transport and spreading of turbulent kinetic energy and scalars (tracers). Rotation induces the development of Ekman boundary layers, which effectively increases bottom friction and could alter the turbulence characteristics within the jet. First, we have extended analytical solutions for a plane jet-like flow in quasi-geostrophic conditions issued in an obstructed flow field. Starting from the fundamental principles of mass conservation and momentum balance, the laws of variation of the jet momentum, length scale, velocity scale and centerline path have been derived, using the same method I used previously for shallow wakes/jets. In particular, the presented solution showed that (i) the jet transverse length scale varies linearly with the distance from the jet nozzle, (ii) the jet centerline velocity scale decreases as a function of both the distance from the jet nozzle and the main characteristics of the obstructions. The momentum deficit has been theoretically derived, leading to the conclusion that its decay is exponential and depends on the main parameters of the Coriolis and drag forces. Furthermore, an analytical model of the jet centerline path has also been derived. The presented solutions show that the velocity scale and momentum decrease faster in the case

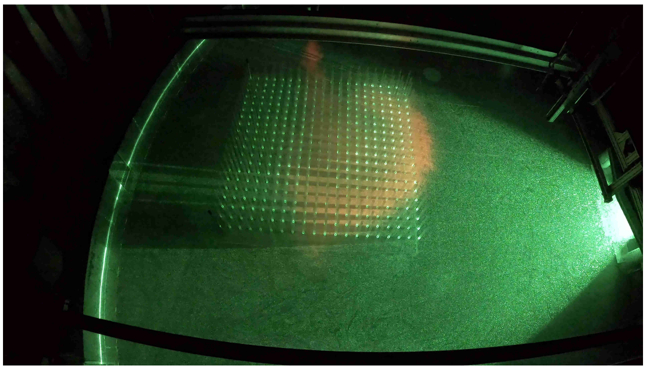
(a)

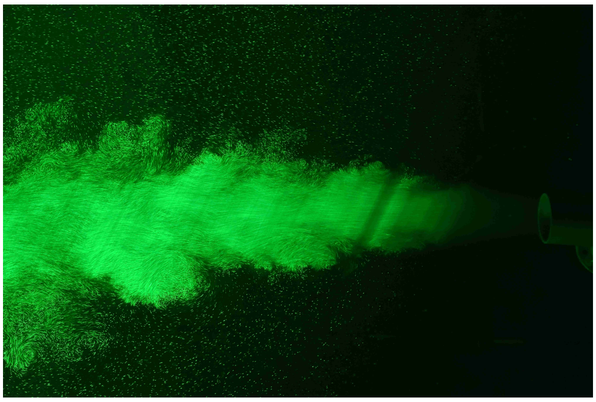
(b)

Figure 9.1: Jets interacting with Vegetation in Rotating Basin.

of obstructed flows. These analytical solutions have been compared with the experimental data collected in the Coriolis Rotating Platform, revealing a good agreement. Results are given in `publication [78]`.

A further article (`publication [? ]`) includes detailed experimental data of the jet development under various flow conditions and vegetation characteristics.

9.2 Western boundary currents interacting with a gap

Within the research project of S. Pierini (Parthenope University of Naples, Italy) accessing the Coriolis Rotating Platform within the Hydralab+ Program, a set of experiments have been performed to check if there is any evidence of self sustained intrinsic variability of western boundary currents (WBC) interacting with a lateral gap, as for example the Kuroshio current penetrating into the South China Sea through the Luzon Strait (figure 9.2a) or the Gulf Stream leaping from the Yucatan peninsula to Florida, called the Gulf of Mexico Loop Current.

A very important aspect is the different path followed by the jet when it penetrates west of the gap: the Kuroshio can assume a looping, leaping or leaking path (figure 9.2a). These states are accompanied by a notable variability and eddy shedding. It is worth noting that in all previous studies (including laboratory experiments) with a fixed flux, the states were steady. The lack of self sustained intrinsic variability was related to the strong dissipation (provided in this case by bottom friction) associated with the small dimension of the basin.

The experiments performed at the Coriolis Rotating Platform provided evidence, for the first time in laboratory experiments of rotating fluids, not only of self sustained intrinsic variability in an autonomous dissipative dynamical system, but also of the transition from small amplitude, almost periodic oscillations to large amplitude aperiodic oscillations as the forcing intensity of the WBC increases. The experiments illustrated how a real complex system can produce coherent time-dependent changes merely by virtue of intrinsic mechanisms are all internal to the system itself.

These results are given in `publication [92]`.

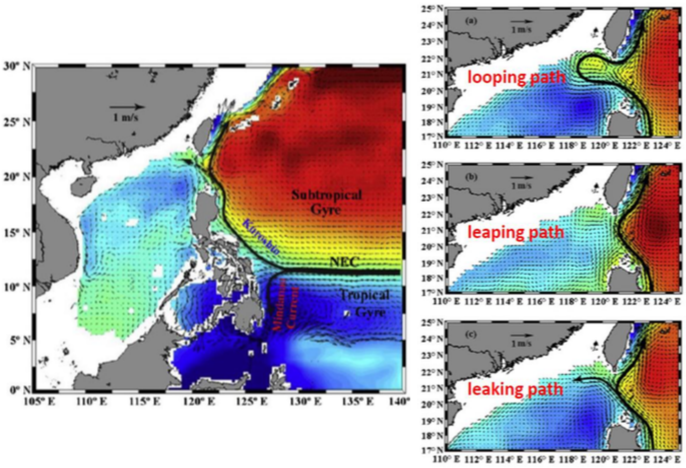

(a)

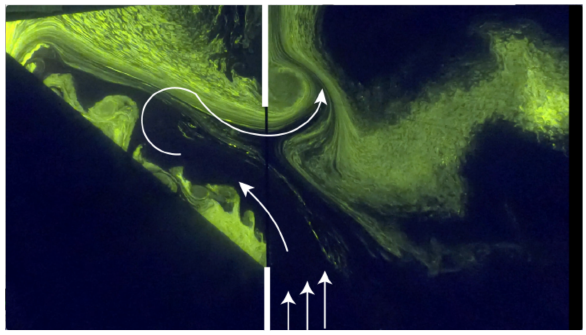

(b)

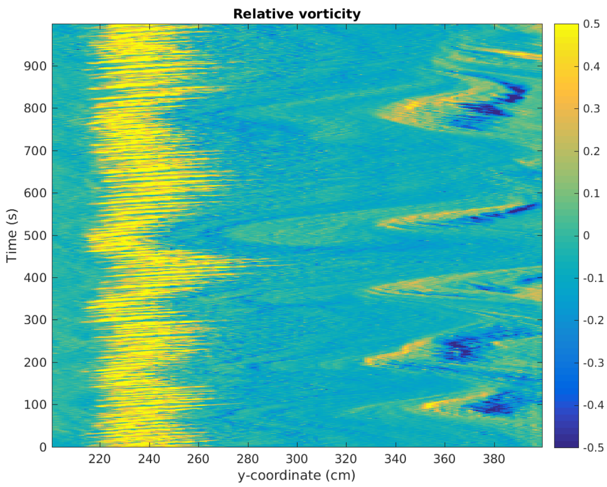

(c)

Figure 9.2: (a) Schema of the western boundary Kuroshio current interacting with the Luzon Strait, three patterns can arise: a leaping currrent without intrusion into the strait, a looping path with a partial intrusion and a bifuraction of the current from satelite image data reconstructed. (b) Visualization of gap-leaping and intruding western boundary currents experiments using Rhodamine fluorescent dye at the Coriolis Rotating Platform (c) relative vorticity characteristic plot highlighting self sustained oscillations.

Part III

Perspectives

Chapter 10

Perspectives: an overview

In this last part I will present my future research activities, which consist in both my own research projects and in projects related to collaborations which are born from the external access to the Coriolis Rotating Platform.

The main future research topic will be on rotating gravity currents and their role in the generation of turbulence in the ocean interior in collaboration with A. Wirth who will provide numerical simulations (team MEIGE, LEGI), continuing what already started in 2019 with the first experimental campaign TUBE I [88] and within the active contract (20CP03) with the SHOM Laboratory in Brest. I plan to submit an ANR ASTRID ('Gibraltar') proposal with the laboratory SHOM and LA (Toulouse) with focus on the exchange flow at the Gibraltar Strait. One Phd (S. Retif) started in October 2021 and will work on the data collected during the experimental campaign TUBE II. It is planned to employ a further PhD or Post-Doc to help with the project ANR-ASTRID 'Gibraltar'. This research topic will occupy 40% of my time.

I will also pursuit the collaboration with C. Brun (team MEIGE, LEGI) and G. Balarac (team MOST, LEGI) on the topic of stratified Görtler instabilities, with the promising results obtained from the PhD thesis of J. Dagaut concluded at the end of 2021. It is not planned to submit a research project for support in the immediate future, instead we will employ Master students to further analyze the performed simulations on stratified boundary layers over a concave bottom.

A further project on gravity currents is related to the collaboration with C. Adduce (University of Roma Tre, Italy) on gravity currents over complex topography (fixed roughness/sediment bottom) with the PhD M. R. Maggi which I co-supervise, who wishes to pursuit with a Post-Doc at LEGI, provided the proposal that will be submitted to the Call 2022 of the local LabEx Tec21 will be accepted.

In relation to the transnational access to the Coriolis Rotating Platform, one project on the barotropic Rossby waves and embedded vortices in the eastern Mediterranean south of Cyprus Island has been realized in summer 2021 in collaboration with A. Pirro from INOGS (Trieste) and will continue also in collaboration with A. Bosse from the MIO, Marseille, both providing observational data (Sea gliders and ACTP) in that region, to be compared to the experiments in the Coriolis Rotating Platform.

A further project on the Coriolis Rotating Platform will concern an ANR-PRCI with the TU Vienna (Austria) and with the EPFL (Switzerland) on the three-dimensional plunge flow initiated already in 2020, that will include turbidity currents and morphodynamical aspects. Additionally, the influence of background rotation, which may become

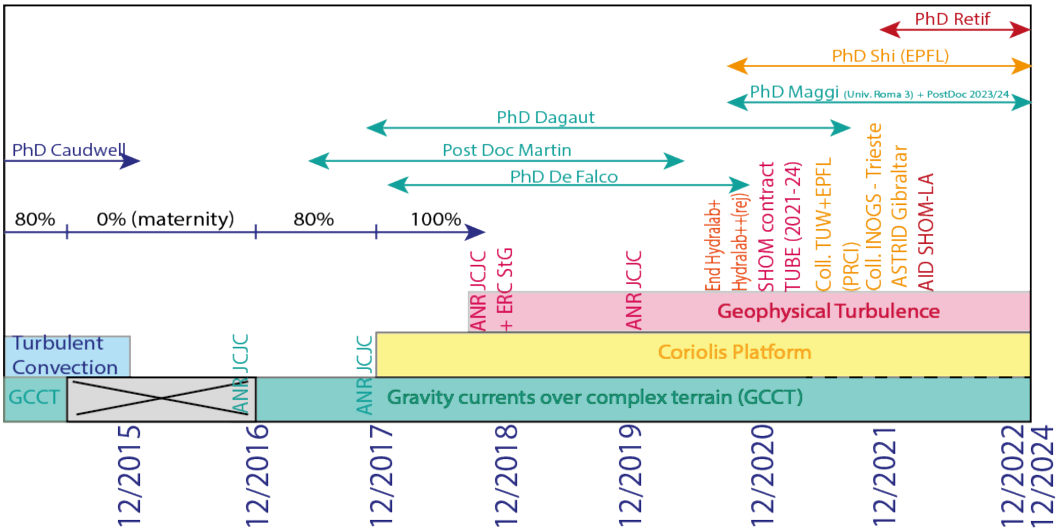

Figure 10.1: Overview of the research activity planned in the future. The different colors indicate the different research axes: Geophysical turbulence (red), the transnational access to the Coriolis Rotating Platform (yellow) and Gravity currents over complex terrain (green).

relevant in transitional environments such as plunge flows in estuaries, will complete the second experimental campaign. The EPFL and TU Vienna will provide the observational data taken in the plunge flow of the Rhone river into lake Geneva.
An ONR project is also planned in collaboration with J. Calantoni to investigate shear instabilities at high Reynolds numbers ($\geq 10^5$) to measure turbulent fluxes using the optical non-intrusive combined PIV/LIF measurement techniques.

Figure 10.1 gives an overview of the projects that will be realized in the near future.

Chapter 11

The turbulent life of downslope rotating intrusive gravity currents (TUBE)

As mentioned in sections 7.2.1 and 8, in 2019 I performed experiments at the Coriolis Rotating Platform to study the long term evolution of rotating gravity currents and to begin the exploration of the contribution to turbulence generation induced by boundary layers detaching from intrusive rotating gravity currents (TUBE I campaign). The promising results given in Negretti et al. [88] and the fruitful collaboration with the laboratories SHOM (F. Dumas, L. Bordois) and LA (F. Auclair) have motivated me to continue this research project as my primary research activity for the upcoming years (40%).

The data acquired from the experiments of TUBE I are still under processing, especially concerning the statistical analysis and accelerations of the surface generated baroclinic vortices [79].

The overall, long term, main objective of the future research on this topic is to help improving the quality of real-time ocean analysis and forecasting systems.

As already mentioned, the dynamics of oceanic gravity currents involve processes on a large range of scales: from the scale of the surrounding static (topography) and dynamic (mesoscale eddies) structures, from the current itself, to the boundary layers of about tenths of meters, to the dissipative scale of a few centimeters. It is impossible to resolve all these scales explicitly in current and near future numerical models of ocean dynamics [55]. These processes must therefore be parameterized in numerical codes. However, their parameterization is made difficult by the strong anisotropy of turbulence because horizontal scales are orders of magnitude larger than vertical scales. The incorrect parameterization of these submesoscale processes leads to unreliable predictions.

Despite the investment in more sophisticated observations, these remain limited in terms of spatial and temporal resolution. The Surface Water and Ocean Topography (SWOT) satellite to be launched in 2022 will provide images of the ocean surface on a band from which the sea surface height (SSH) can be calculated with an accuracy of [1cm] and a horizontal resolution of about [1km]. Large-scale SSH measurements have been used for decades to compute near-surface horizontal velocity using the geostrophic equilibrium, between the Coriolis force and the pressure gradient. The use of the new SWOT measurements on a band rather than a line only, could help to understand the dynamics at smaller scales, but only if a link between SSH information and deeper ocean dynamic processes can be established, which remains an unresolved scientific challenge.

./figs/DynamicalRegimesCor.jpg

(a)

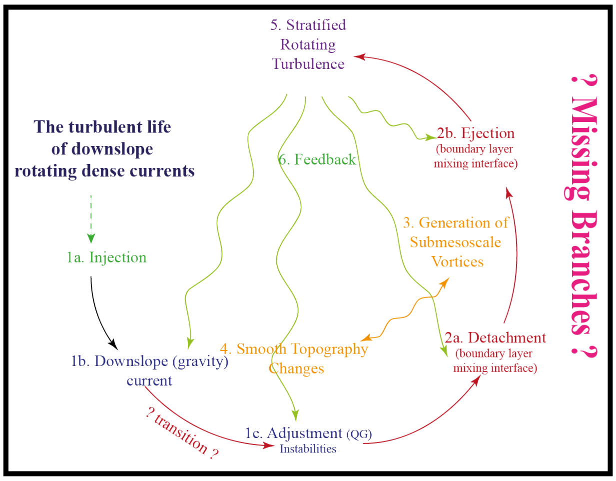

(b)

Figure 11.1: (a) Schematic view of the dynamical regimes in geophysical turbulence with focus on overflow processes. The regimes covered by realistic numerical simulations, experiments and the Coriolis Rotating Platform are highlighted by the shaded colored regions. (b) Schematic view of the scientific questions related to my main future research topic TUBE.

The national and international community has therefore turned its efforts towards the development of more sophisticated codes and parameterizations. In particular, the French national community that does regional and coastal ocean numerical modeling (Ifremer, IRD, INSU, INRIA, SHOM) is currently heavily involved in the development of a code, called CROCO.
CROCO (Coastal and Regional Ocean COmmunity model) is proposed as a new-generation community model for the next decade and gives priority to the study of very fine scales - whether oceanic, coastal or littoral - and their interactions with larger-scale processes.

At present, general ocean circulation codes are based on numerical models of deterministic and mechanistic ocean dynamics that solve the primitive equations under the Boussinesq and hydrostaticity hypotheses. CROCO, on the other hand, has a version capable of solving the dynamics under non-Boussinesq and non-hydrostatic conditions as encountered in gravity currents.

The CROCO model requires for its development that the existing parameterizations of the unresolvable processes be tested, on the one hand, and that the code be calibrated and validated under these more complex conditions (non-Boussinesq, non-hydrostatic) on the other hand, and that the dynamics of gravity currents be included.

Controlled laboratory experiments are therefore the only way to achieve this objective as they allow researcher to measure with a high temporal and spatial resolution all main characteristics of the flow (velocity, depth, entrainment, turbulent flow and mixing) by systematically varying key parameters (e.g. stratification, rotation, topography, initial flow conditions). The Coriolis Rotating Platform represents the ideal environment for this research topic since it permits the exploration a larger dynamical range of scales compared to smaller scale installations, as depicted in figure 11.1a.

Following the schema depicted in figure 11.1b, the future research aims at approaching

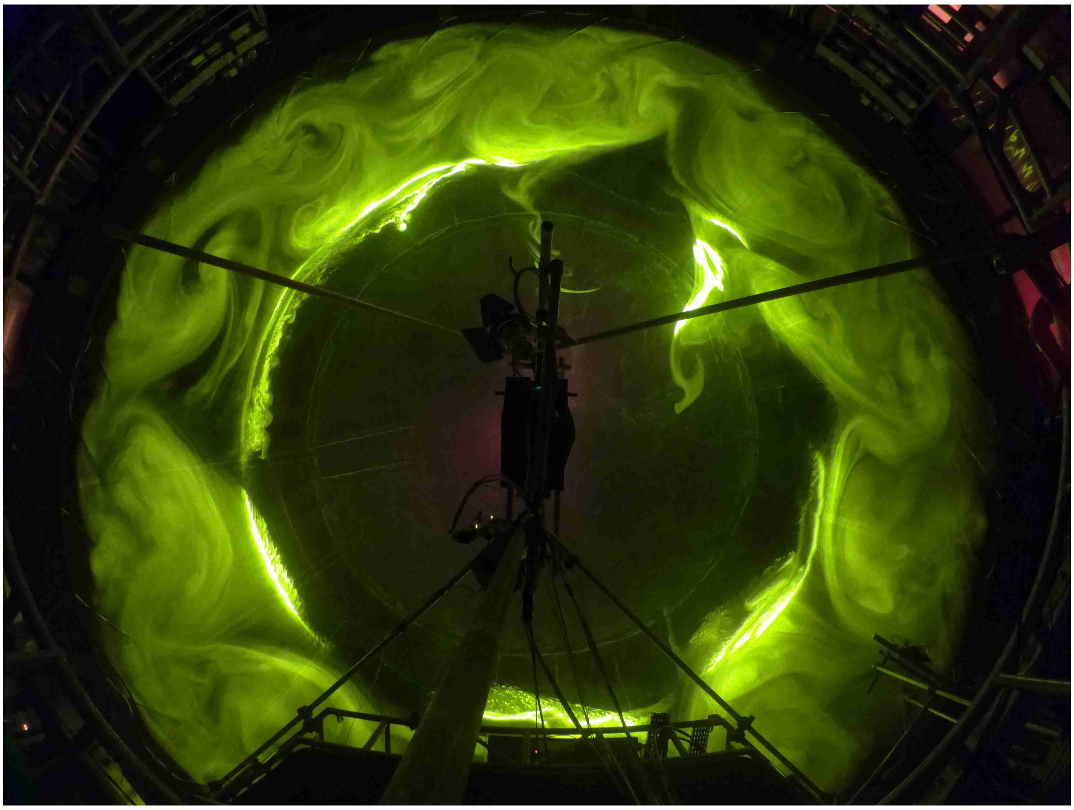

Figure 11.2: Top view of an experiment of the project TUBE in which the salt water injection is highlighted by the green dye (Rhodamine). Localized intrusions in form of dipoles can be clearly recognized.

and exploring the following aspects:

1. To characterize the transition from a downslope gravity current to a quasi-horizontal current under the effect of the Coriolis force: this is a form of geostrophic adjustment that leads to a horizontal current, where the downslope gravity force is balanced by the upslope Coriolis force, as long as friction is neglected ([119]).

2. To explore a possible new mechanism of turbulence generation in the ocean interior: turbulent advection of small scale turbulent structures generated at the boundary layer by frictional processes.

3. To understand the physical mechanisms that lead to the boundary layer detachment and propagation toward the ocean interior resulting in an intense turbulent environment;

4. To survey the evolution of the created turbulent environment, quantifying energy transfers and their route to dissipation and the feedback to the intruding current;

5. To explore the possibility of topographic generation of submesoscale vortices in the case of smooth topography changes.

This will be performed by conducting specially designed experiments that uses the configuration described in section 7.2.1. The first experimental campaign TUBE I realized in 2019 [88], captured the global flow with a high spatial resolution on a domain of the size of the Coriolis tank, at different depths. These measurements gave an overall view of the processes involved in the rotating gravity current, from the surface generated baroclinic vortices, to the current itself and to the global circulation induced in the central deep area. The recent experimental campaign realized in spring 2021 and hereafter called the TUBE II campaign, focused instead on the intrusion process using a 3D2C PIV measurement technique that will deliver more quantitative information about the detachment mechanisms and the turbulence characteristics. A PhD student (Sevan Retif) has been recruited in October 2021 to work specifically on this topic.

In particular, the main scientific questions to be answered using the full data set collected in both campaigns TUBE I and TUBE II are detailed below and grouped in different work packages.

1. WP. The transition from a slow (dominated by rotation) to a fast (dominated by gravity) current needs to be characterized. Rotating gravity currents are very different from their non rotating counter part. Under the effect of rotation, a downslope gravity current is subject to a geostrophic adjustment leading to a horizontal current, where the downslope gravity force is balanced by the upslope Coriolis force. The resulting distance before encountering the level of neutral buoyancy with respect to the Rossby radius of deformation will define a current more or less dominated by rotation or by gravity effects. A density front appears at the edge of this current, leading to specific instabilities and dissipation processes, which control the slow downward drift of the current and the final equilibrium location and density of the transported water mass. These small-scale dissipation and mixing processes are poorly represented in current ocean circulation models [**?**]. For different rotation rates and injected buoyancy fluxes at a given fixed slope, a range of currents dominated by gravity effects, to currents resulting in the baroclinic front in geostrophic balance that may grow baroclinic unstable will be studied.
   While for two-layers ambient stratification the current will interleave within the interface creating an intruding layer, the scenario is expected to change significantly when the ambient stratification is linear, similarly to the observations from the first experimental campaign TUBE I, where a set of experiments have been realized using as injection density the same as the bottom layer density in an initial two-layer stably stratified ambient.
   A further process that will be explored is the ratio between the injected buoyancy flux and the predicted Ekman transport. Once the current has reached its equilibrium, the flux through the Ekman layer is fixed. It is unknown how the current will react if the injected buoyancy flux exceeds the Ekman transport for the given current. One hypothesis based on observations from preliminary experiments performed at the Coriolis Rotating Platform, is that the current produces local scouring motions (i.e. avalanches) in order to evacuate the exceeding injected volume and to return in its original equilibrium state. Such process might lead to self-organized criticality and a pioneering paper revealed that such behaviour is observed for a stratified shear flow subject to the Holmboe wave instability [98].

2. WP. The small-scale processes and the turbulence production induced by boundary layers involved in rotating gravity currents will be explored; gravity currents are a common process encountered in the ocean, which includes boundary and shear layers with various types of flow instabilities, and which can produce baroclinic instabilities and may radiate internal waves. In particular we will focus on the

vorticity production induced by

- the current itself; this has been initiated already in TUBE I (cf. Muraro [79]), but needs further analysis and possibly further experiments for more robust statistics on their long term evolution.
- by small scale shear turbulence at the boundary layers (bottom, interfacial). Vorticity is ubiquitous in the ocean at all scales; its principal source is the wind shear at the surface, but it is also produced in boundary layers. The well resolved numerical simulation of Akuetevi and Wirth [3], showed that the western boundary layers are ejected from the boundary to the interior ocean, where the associated high vorticity values create a turbulent interior containing eddies, dipoles that propagate ballistically and vortex filaments of various sizes. Thin layers of high vorticity are also created at the sheared interface of gravity currents. The vorticity is then advected towards the interior when they interleave at the level of neutral buoyancy by boundary layer detachment. The formation of Heton like vortex structures (discrete, baroclinic geostrophic vortices [38, 43] may also be a possible mechanism for advecting vorticity, heat, salinity from boundaries into the ocean interior over long distances [39, 42, 59, 91].
- by topographic changes, i.e. local smooth variation of the slope that produce an unbalance between rotation and gravity. This induces a variation in the gravity force acting on the downslope current putting it out of equilibrium with respect to the Coriolis force, so that the current seeks for a new equilibrium. The regions in which the current feels the slope change are characterized by changes in the potential vorticity field and it is expected that large-scale, two-dimensional coherent vortices are formed. For this task, an elliptic cross section of the conical slope will be employed.

3. WP. Energy transfer processes in the resulting turbulent environment within the ocean interior and its route to dissipation will be determined and quantified using particularly the recently acquired data in the campaign TUBE II. In the interior, the mutual advection of vorticity constitutes the turbulent dynamics and is finally dissipated at smaller scales by dissipative processes [116]; mixing processes produced at the sheared interface contribute to modify the potential vorticity (PV) distribution, which is not conserved in these circumstances, and may generate vortices (as the cyclones observed at the Denmark strait, or the Meddies), dipoles and vortex filaments. The turbulent environment generated in this way will serve to characterize the energy transfers and deliver more robust interpretations of the energy spectra within regimes of higher buoyancy Reynolds numbers and in a different turbulence scenario such as those analyzed previously [31, 47, 54, 93**?**]. The background submesoscale eddy field in the interior, once the process of boundary layer detachment is launched, participates actively to the spreading of the density front, may interact with the topography generating a supplementary source of submesoscale vortices and alters the further boundary layer detachment of the current [114]. The feedback of the generated ambient eddy activity on the gravity current and the detachment process will be analyzed as well.

4. WP. Internal wave radiation emitted by the gravity current. Very little is known so far about the radiation of internal waves by gravity currents [33, 71]. In rotating downslope gravity currents, there may be two sources of perturbations which may

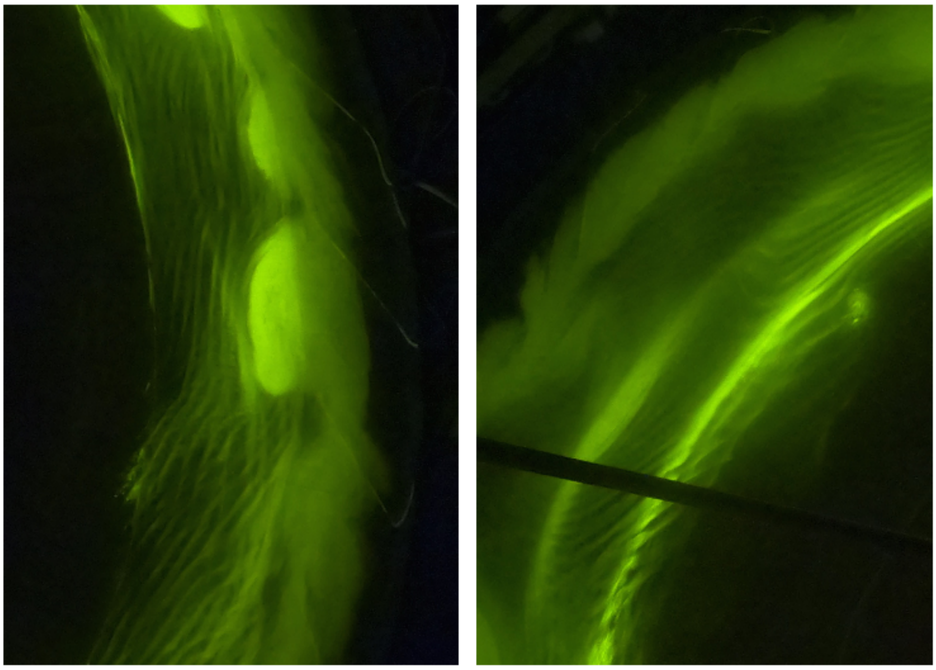

Figure 11.3: Two top views of TUBE I experiments with Rhodamine dye injected with the saline solutions to generate the gravity current. The Ekman boundary layer is highlighted by the well developed roll waves as already observed by Cenedese and Adduce [14].

lead to the production of internal waves: the first one is the front itself, both on the slope area and also once penetrating in the stratified ambient. The second mechanism may be represented by the roll waves that has been observed in the Ekman bottom layer (cf. figure 11.3). These roll waves may act as a sinusoidal bottom boundary, as in the case investigated by Aguilar and Sutherland [1], Aguilar et al. [2].

In this case, specific experiments will be performed using the PTV technique, to determine the acceleration fields within the receiving ambient water in the central area. This technique has been already explored in the Coriolis Rotating Platform. Specific Lagrangian statistics along particle tracks will be required to characterize the circulation patterns in the central deep area induced by the gravity current. This includes the velocity and acceleration statistics of individual particles, in particular the PDF of the acceleration will deliver information of the possible existence of internal waves or the presence of cyclostrophic components.

5. WP. A realistic implementation of the topography of the Gibraltar Strait including both the initial propagation of Atlantic Waters on the surface within the Western Mediterranean basin and the outflow from the Mediterranean in the Gulf of Cadiz, will be realized. Synoptic measurements will be performed by use of PIV/PLIF measurements techniques to obtain turbulent fluxes in the bottom boundary layer and the interface between the current and the ambient. Different hydraulic conditions (density difference, the relative flow rates in the upper/lower layers which mimic the tidal effect) will be explored in different areas of the exchange flow (over the Camarinal sill, initial acceleration region down the slope, hydraulic jumps and region where the current feels rotation within the gulf of Cadiz). The combined

measurements of PIV/LIF remain still a technical challenge in a large installation such as the Coriolis Rotating Platform, especially concerning the LIF technique, which requires a fine calibration procedure that is difficult to control for large scale experiments. The collected experimental data will be compared to in situ measurements, which will be collected in a sea campaign scheduled in September 2022 (at which my participation is planned) by the SHOM and will serve to test and calibrate the CROCO model in a realistic condition. This Work package is object of an ANR ASTRID 'Gibraltar' that will be submitted in the next call in winter 2022.

This research is conducted in close collaboration with A. Wirth who performs numerical simulations with CROCO on configurations similar to the laboratory experiments, that give complementary information to the experiments on a parameter range difficult to access in the laboratory. A publication is in progress on the obtained numerical results [122]. The new collected data in TUBE II and after those for the realistic configuration 'Gibraltar' will provide some of the quantities (velocity fields, concentration fields, accelerations, turbulent flows, energy transfer, entrainment and mixing) necessary to 1) test the parametrizations of the unresolved processes in the CROCO code related to the gravity flow (entrainment, mixing, turbulent flow) and 2) calibrate and validate the CROCO code under non-hydrostatic conditions, as produced in the ocean by gravity currents. A collaboration with Y. Morel at LEGOS and L. Gostiaux at LMFA is also planned. The data will be indeed used also for the theoretical PV diagnostic as outlined in Morel et al. [75], in particular for its further development, in order to identify and compare the diabatic sources (i.e. viscosity and diffusion effects) of potential vorticity modification in both physical and numerical experiments.

Proposals

A close collaboration with F Dumas and L Bordois at SHOM, with F Auclair at LA, Toulouse and A Wirth at LEGI having focus on a research contract with the SHOM over four years (20CP03, 2021-24, 80kE, PI LEGI: A Wirth). A proposal within the funding scheme of ANR-ASTRID will be submitted in 2021/22 with the same research group and including the collaborations with Y. Morel (LEGOS, Toulouse) and L Gostiaux, (LMFA Lyon) having focus on the realistic configuration of the Gibraltar Strait (WP 5). A conjoint request for a PhD fellowship between AID and the Doctoral school STEP will be submitted next spring 2022 to help working on this ANR-ASTRID project.

Chapter 12

Further research

12.1 Görtler instability with stratification

I plan to pursuit with C. Brun and G. Balarac the work initiated by the PhD of J. Dagaut, which includes results of numerical simulations of a Blasius boundary layer on a curved wall with background stratification. In the near future, we plan to continue the analysis of these data employing a Master student during the upcoming session in 2022, but wish to write a broader research project based on further simulations with different boundary/initial conditions and geometry (different inlet velocity profiles, concave/convex boundary) and to perform laboratory experiments in a specially designed apparatus. It is proposed to use a similar experimental set-up originally designed by Lawrence's group at the University of British Columbia (Canada) ([58]; [40]; [110]) and adapted after by [73] to study mixing in turbulent shear flows within an inclined tube. Instead of using the inclined tube, we will use a circular duct.

Moreover, we plan to include also observational data of katabatic winds that develop on the strong alpine slopes in the region of Grenoble. Two complementary applications will be considered: first, the analysis of databases of katabatic winds resulting from in situ measurements carried out within the framework of concluded OSUG2020 projects (Blein PhD Thesis 2016; LEGI / LTHE/ IGE collaboration). A campaign to measure stable winter episodes on the slopes of Grand Colon in the Belledonne massif has been carried out on a recurring basis since 2012 in collaboration with the IGE and with the support of INSU (LEFE 2012 project) and OSUG (LabEx OSUG AO2017 project). These data will allow us to check for the presence of Görtler vortices using a method for their recognition based on the anisotropy properties of the turbulence measured from the invariant of the Reynolds tensor [11]. Secondly, designing a new field campaign in an ideal configuration on the ski jumping hill of St. Nizier du Vercors (cf. figure 12.1. Katabatic wind measurements will be compared to simulations and laboratory experiments. This research topic will take 15% of my time. A research proposal is planned to be submitted to the LEFE support scheme (presumably in 2023).

12.2 Gravity currents over rough bottoms

As already mentioned in section 7.1.3, an active collaboration with C. Adduce at the University of Roma Tre is active on the topic of gravity currents on enhanced bottom roughness. At present, experimental data on fixed bottom roughness elements is conducted with the PhD student M.R. Maggi and results are given within a journal article

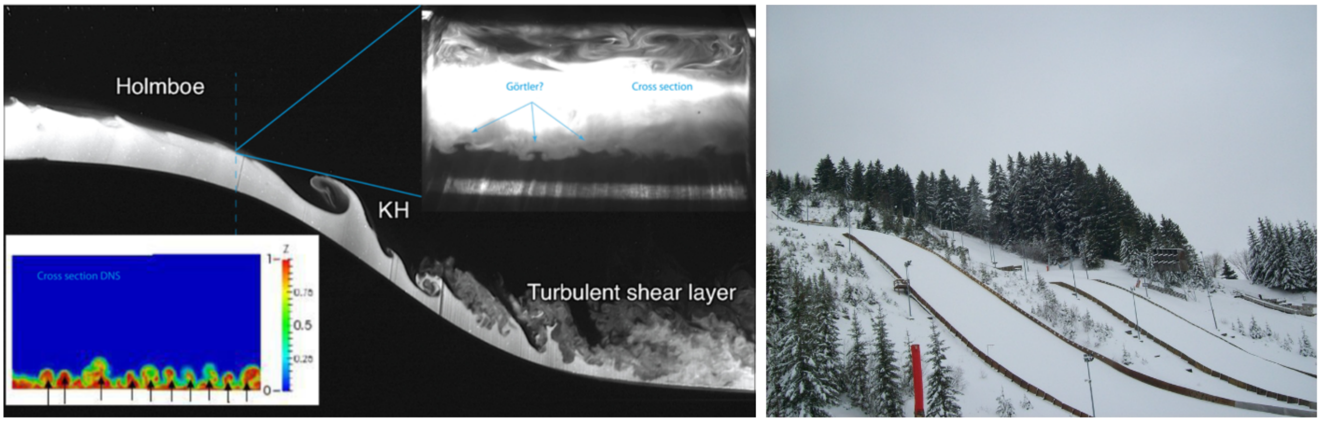

Figure 12.1: a) Visualizations from laboratory experiments of a gravity current with zoomed views of cross sectional areas from experiments (black/white square) and from DNS (colored square); (b) the ski springboard in St Nizier of Vercors, to be used for field experiments of katabatic winds over curved slopes.

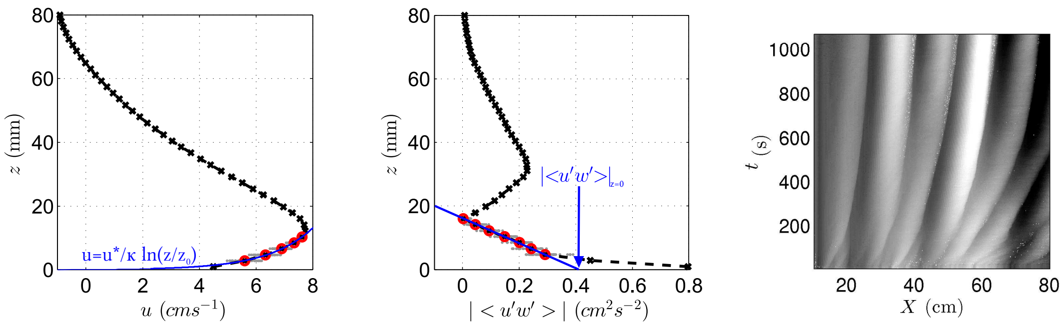

(a) (b) (c)

Figure 12.2: (a) Vertical profile of the along-slope velocity. (b) Vertical profile of the absolute value of the Reynolds stress. (c) Hovmöller diagram for the bed elevation anomaly.

currently in preparation `publication` [65]).

Explorative experiments of gravity currents on a sediment bed have been undertaken financed by the LabEx Tec21 from 2017 to 2020 with the post-doc A Martin and the PhD MC De Falco. The first set given experiments of continuously supplied gravity currents on a sediment bed to evaluate the impact of high bottom shear stress reported in the previous experiments on bottom erosion and sediment suspension. Preliminary results show that the bottom boundary layer is within a transitional state between a smooth and a rough regime with a roughness induced by the bed forms instead of the grain itself (cf. figure 12.2(a,b)). The performed bedform measurements combined with velocity measurements clearly show the formation of ripples-like bed waves that have never been observed previously in critical flow regimes under non-stratified conditions (cf. figure 12.2(c)). Hence, stratification may have a strong impact on bed morphology and sediment transport, which is of great relevance at present in transitional environments such as estuaries.

These are promising results and motivated the collaboration with C. Adduce at the

University of Roma Tre and M.R. Maggi now PhD, who wish to pursue with a Post-Doc on this topic. We plan to submit a Post-Doc funding request for one year at the LabEx Tec21 starting from 2023 to treat existent experimental data collected at LEGI (continuous supply) and INRAE (finite volume release) on downslope gravity currents over a sediment bottom. This project will take 15% of my research time in 2022-2023 (cf. figure 10.1).

Chapter 13

Access projects to the Coriolis Rotating Platform

The projects detailed below are considered as the access to the Coriolis Rotating Platform, that are complementary to my research and belong to collaborations born at the base of the interest of external researcher to access the Platform. A priori, they will take the remaining 30% of my time. The detailed time distribution between the future projects is not known a priori because it will also depend on the proposals that is accepted.

13.1 Barotropic Rossby waves in a homogeneous and a weakly stratified rotating flow

This research project to access the Coriolis Rotating Platform was proposed by the researchers A. Pirro and E. Mauri from the National Institute of Oceanography and Applied Geophysics (INOGS, Trieste, Italy). Previous oceanographic studies in the Levantine Basin including field campaigns, in-situ measurements and numerical simulations, revealed the presence of an anticyclonic eddy called Cyprus eddy which forms south of the island of Cyprus with a life time up to two years. Its center varies between $32° - 42.5°$ and the radius is approximately 50 km (figure 13.1a). Observations from gliders conducted in 2017 by the INOGS group along with other previous studies ([9, 126] have shown that the Cyprus eddy extends from the surface down to $\sim 800\,\mathrm{m}$ of depth and is located above the Eratosthenes seamount whose summit depth is $\sim 700\,\mathrm{m}$ over a surrounding water depth of $\sim 1200\,\mathrm{m}$. On the right side of the Cyprus eddy, a smaller cyclonic eddy (named South Shikmona Eddy - SSE) and an anticyclonic eddy (named North Shikmona Eddy - NSE) also appear (figure 13.1a). According to the analytical solution of [72], on a β-plane, when an eastward flow impinges over an isolated bump, an anticyclonic Taylor column will form over it and lee waves behind. If the height of the obstacle is tall enough, additional cyclonic end anticyclonic eddies will from in the wake downstream. For highly stratified flow, the solution gives bottom trapped waves (no wave-solution is given at the surface) while, for moderate stratified fluid the disturbances weaken towards the surface. The aim of the laboratory experiment was to prove that the Cyprus eddy observed in the Levantine Basin is a Taylor column trapped over the Eratosthenes seamount and it is generated by the eastward flow. Additionally, the SSE and NSE are associated to the wake that forms behind the Cyprus eddy, embedded in the generated Rossby waves.

An instantaneous top view visualization using Rhodamine dye of one of the experi-

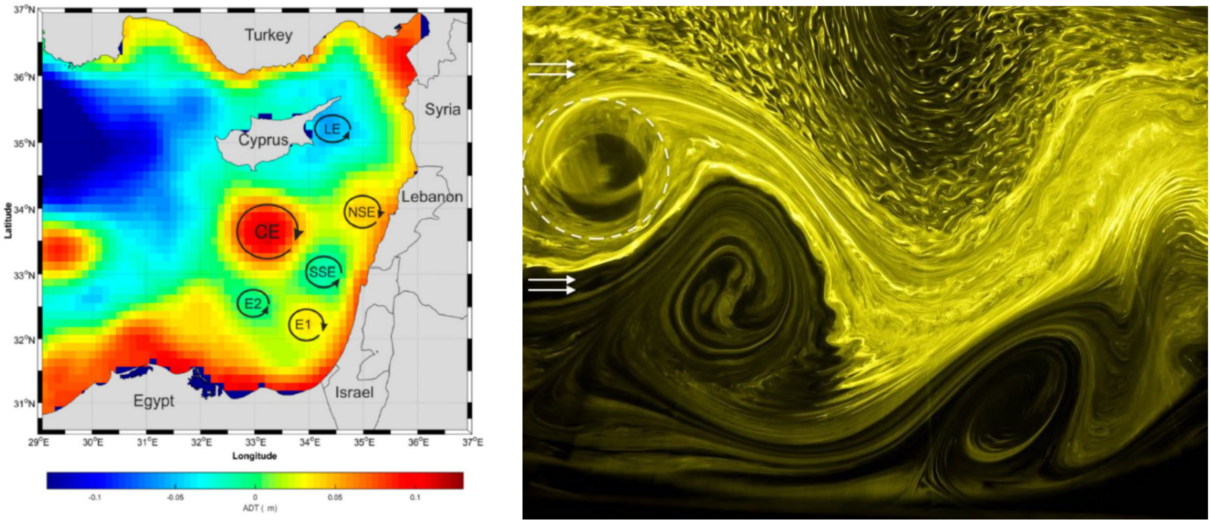

(a) (b)

Figure 13.1: (a) Mean Absolute Dynamic Topography for the period September 2016-August 2017, evidencing the Cyprus Eddy (CE), the north Shikmona eddy (NSE), the south Shikmona eddy (SSE), the anticyclone E1, a cyclone called E2, and the Latakia Eddy (LE). The color-scale units is in m. (From Mauri et al., 2019). (b) Top view visualization using Rhodamine dye of one of the experiments realized at the Coriolis Rotating Platform during summer 2021 highlighting the Rossby waves and formation of vortices. The circle represents the submerged bump.

ments realized is given in figure 13.1b, highlighting the Rossby waves and the formation of vortices in the wake. The circle represents the submerged bump, arrows the incoming flow direction produced by spin-up of the Coriolis tank.

The laboratory experiments have been conducted in June/July 2021 and the data is under analysis. Also, a collaboration with A. Bosse (MIO, Marseille) has born recently, interested in the experimental data to be compared to additional observational data collected in the levantine Mediterranean basin.

13.2 Three-dimensional plunging flows

Continuing the work initiated through the transnational access at the Coriolis Rotating Platform in collaboration with the EPFL in 2020 a collaborative research project within the funding scheme ANR-PRCI is planned to be submitted in the next session with the TUW (Austria) and with the EPFL (Switzerland) including complementary experiments. In particular, further improvements and novelties from the first experimental campaign realized in 2020, will be

- to perform detailed synoptic PIV/LIF measurements in order to better quantify the turbulence characteristics in the plunging flow region and underflow
- to consider turbidity currents and hence the suspension/deposition of suspended particles in the 3D plunge flow, including the presence of a sediment bed
- to vary the geometry, i.e. different slope angles and inlet channel widths
- to consider the added effect of the background rotation on the plunge flow

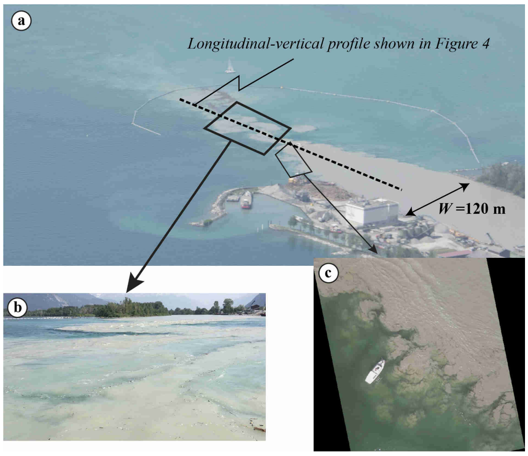

(i)

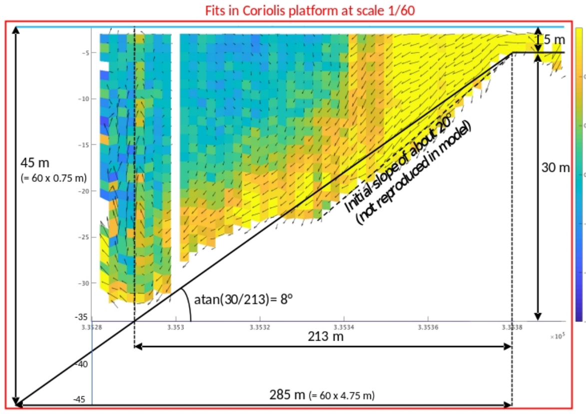

(ii)

Figure 13.2: (i) Geometrically unconfined plunging of the Rhone Rive into Lake Geneva illustrating the variety of vortical instabilities. (a) image from remote cameras on July 26, 2019 at 16.02; (b) Simultaneous image from a boat with focus on the vortical instabilities downstream of the plunge point; (c) Images from a boat-mounted balloon on July 9, 2019 with focus on the vortical instabilities at the edge of the plunge region.(ii) Velocity component in a longitudinal-vertical plane through along the axis of the Rhone inflow into Lake Geneva (cf. figure on the left) measured on November 23, 2017.

A large amount of observational data from lake Geneva are already available at both the EPFL and at the TUW. Numerical simulations using the OpenFoam code has been already tested and validated using the first experimental campaign data in 2020 and will accompany the experiments and observations. A PhD student and a post-doc fellowships will be requested to support the teams at LEGI/EPFL for the experimental laboratory data and at the TUW for the analysis of the observational data. An example of the already available observational data of the Rhone river plunge into the lake Geneva is given in figure 13.2: image view from remote cameras, from a boat on July 26, 2019 in (i) and velocity distribution in a longitudinal-vertical plane along the axis of the Rhone inflow into Lake Geneva measured on November 23, 2017 in (ii).

13.3 High Reynolds numbers shear instabilities

This research activity has been motivated by a visit of the ONR director in summer 2018. The correct parametrization of sub-grid turbulent processes related to gravity flows over topography are a problem of growing concern since predictions are often unreliable when the overflows themselves and the mixing processes induced by shear instabilities are not correctly included in coastal, oceanic and atmospheric circulation models. While previous laboratory experiments studied stratified shear instabilities and related mixing processes at low Reynolds numbers ($< 4,000$), this project aims at classifying the different flow regimes and quantifying the turbulent sub-grid processes (transport, fluxes and mixing) in the different regimes that arise by increasingly raising the Reynolds number up to values of 140,000, identifying the transition to turbulent shear instabilities, as observed and suggested in the field study of Geyer et al. [35] (see also Seim and Gregg [99], Smyth and Moum [104], van Haren and Gostiaux [113]). There are three objectives: (O1) To identify and characterize the possible different regimes (laminar, intermediate and turbulent) and transitions that can develop at the sheared interface of a propagating bottom gravity current as a function of the relevant non-dimensional parameters (Fr, Re, Ri, S) which take into account the density anomaly, the depth of the current, the shear strength and the slope. This will be realized by systematically varying the above mentioned variation parameters. (O2) To perform detailed measurements using synoptic PIV/PLIF for the velocity and density fields in such gravity currents within the different regimes. The detailed measurements in the different development regions of the shear layer and in the different regimes identified in O1 are needed to enable precise quantitative estimations of the turbulent transport, fluxes, entrainment, energy budgets and mixing efficiency, needed in numerical models for a correct parametrization. The main instability properties of Kelvin-Helmholtz and Holmboe, along with their route to a turbulent shear layer (see Geyer et al. [35]) will be identified and quantified, and compared to experimental, numerical/theoretical studies at lower Reynolds numbers.

Simultaneous PIV/LIF measurements using the equipment present at Coriolis will provide unprecedented measurements to validate regional scale ocean models such as NHWave [101].

An ONR Proposal in collaboration with J. Calantoni asking for 240,000$ has been submitted in October 2019 and is still awaiting a response due to the pandemic situation.

Chapter 14

Management of the Coriolis Rotating Platform: opportunities and risks

From its construction in 1960 to 1985, the Coriolis Rotating Platform has continuously received financial support from public/private institutions such as EDF, CEA, CNRS and the Institut Polytechnique of Grenoble. This insured over 25 years the maintenance and the regular improvement and optimization of the Platform (such as the big interventions in 1985 and 2002 supported by the CNRS) and its instrumentation. In 2010 the new Coriolis Rotating Platform has been entirely reconstructed on the Campus side following the demolition of the former Platform, financed by Grenoble INP and the CNRS. The CNRS contributes to sustaining the costs related to the Coriolis Rotating Platform with the two permanent engineer positions of S. Viboud (since 1999, IE, then IR from 2019) and the new position of T. Valran (IE since 2018).

Since 1992, the Coriolis Rotating Platform has been part of the European Consortium Hydralab led by the Dutch independent research institution DELTARES. The European contract assured a constant financial support (overheads) for the maintenance and the acquisition and replacement of the equipment and the instrumentation for the experiments, which was rapidly evolving, especially concerning optical non-intrusive measurement techniques. More recently, other projects funded by the European Union contributed to the financial support of the Coriolis Rotating Platform (EuHIT in 2015 and an ERC in 2015-2020).

However, in 2020 the last Hydralab contract ended and the new submitted proposal has been rejected for political reasons. Recently, there has been the possibility to join a much larger consortium called ENVRI-CLIM including more than 230 infrastructures in Europe for Climate Change research and in which the full Hydralab Consortium (made of 18 access platforms) was originally included. However, due to the huge number of participants, the main coordinators had to drastically reduce the number of participants, including the Coriolis Rotating Platform, and the Hydralab Consortium counted for two installations only.

At present, the access projects are directly financed by the external users institutions (e.g. the access of EPFL, Switzerland and INOGS, Trieste) using an indirect cost method for the invoices, which gives an access cost per day at the Coriolis Rotating Platform of 1,500Euros, a value estimated based on the expenses of the last 5 years Hydralab projects. However, these projects cannot support the maintenance of the Platform and its instrumentation and equipment.

The active project with the SHOM (20CP01) initiated in 2020, gives future perspectives of a continuous support, especially if combined with ANR-ASTRID funding schemes (such as the planned project 'Gibraltar', see section 11) aimed at the further development of the CROCO code, which permit us to invest in the rapidly evolving equipment used for the experiments. Other ANR projects (PRCI) requesting the access to the Platform and further international access projects (DFG, NSF, ONR) will additionally contribute in sustaining the equipment and instrumentation devices in the upcoming years.

The recent maturated cooperation with one of the ENVRI-CLIM coordinators, P. Laj (IGE, UGA), opens new perspectives for a possible participation in further European Consortia over longer periods in the future.

Bibliography

[1] D. Aguilar and B. Sutherland. Internal wave generation from rough topography. *Phys. Fluids*, 18:online, 2006.

[2] D. Aguilar, B. Sutherland, and D. Muraki. Laboratory generation of internal waves from sinusoidal topogaphy. *Deep-Sea Res. II*, 53:96–115, 2006.

[3] C. Akuetevi and A. Wirth. Dynamics of turbulent western-boundary currents at low latitude in a shallow-water model. *Ocean Sci.*, 11:471–481, 2015.

[4] V. Alavian, G. H. Jirka, R. A. Denton, M. C. Johnson, and H. G. Stefan. Density currents entering lakes and reservoirs. *J. Hydr. Eng.*, 118(11):1464–1489, 1992. doi: 10.1061/(ASCE)0733-9429(1992)118:11(1464).

[5] P. Augier, P. Billant, M. Negretti, and J.-M. Chomaz. Experimental study of stratified turbulence forced with columnar dipoles. *Phys. Fluids*, 26:046603, 04 2014.

[6] P. Baines. Mixing in flows down gentle slopes into stratified environments. *J. Fluid Mech.*, 443:237–270, 2001a.

[7] P. Baines. Two-dimensional plumes in stratified environments. *J. Fluid Mech.*, 471: 315–337, 2002.

[8] P. Billant and J.-M. Chomaz. Experimental evidence for a new instability of a vertical columnar vortex pair in a strongly stratified fluid. *J. Fluid Mech.*, 418: 167–188, 2000a.

[9] A. Bosse, P. Testor, L. Houpert, P. Damien, L. Prieur, D. Hayes, V. Taillandier, X. Durrieu de Madron, F. d'Ortenzio, L. Coppola, J. Karstensen, and L. Mortier. Scales and dynamics of submesoscale coherent vortices formed by deep convection in the northwestern Mediterranean sea. *J. Geophys. Res.: Oceans*, 121(10):7716–42, 2016. doi: 10.1002/2016JC012144.

[10] G. Brethouwer, P. Billant, E. Lindborg, and J.-M. Chomaz. Scaling analysis and simulation of strongly stratified turbulent flows. *J. Fluid Mech.*, 585:343–68, 2007.

[11] C. Brun and J. Chollet. Large eddy simulation of katabatic flow along a slope model. *CFM Marseille*, 173:431–471, 2009.

[12] F. Bryan. Parameter sensitivity of primitive equation ocean general circulation models. *J. Phys. Oceanorgr.*, 17:970–985, 1987.

[13] T. Caudwell, J.-B. Flór, and M. E. Negretti. Convection at an isothermal wall in an enclosure and establishment of stratification. *J. Fluid Mech.*, 799:448–475, 2016. doi: 10.1017/jfm.2016.360.

[14] C. Cenedese and C. Adduce. A new parameterization for entrainment in overflows. *J. Phys. Oceanogr.*, 40:1835–1850, 2010.

[15] C. Cenedese, J. Whitehead, T. Ascarelli, and M. Ohiwa. A dense current flowing down a sloping bottom in a rotating fluid. *J. Phys. Ocean.*, 34:188–203, 01 2004.

[16] J. Y. N. Cho, Y. Zhu, R. E. Newell, B. E. Anderson, J. D. Barrick, G. L. Gregory, G. W. Sachse, M. A. Carroll, and G. M. Albercook. Horizontal wavenumber spectra of winds, temperature, and trace gases during the Pacific Exploratory Missions: 1. climatology. *J. Geophys. Res.: Atm.*, 104(D5):5697–5716, 1999. doi: 10.1029/98JD01825.

[17] P. Choboter and G. Swaters. On the baroclinic instability of axisymmetric rotating gravity currents with bottom slope. *J. Fluid. Mech.*, 408:149–77, 2000. doi: 10.1017/S0022112099007661.

[18] J. Dagaut. *Görtler instability in (non) stratified flows*. PhD thesis, LEGI, University Grenoble Alpes, 12 2021.

[19] J. Dagaut, M. Negretti, G. Balarac, and C. Brun. Laminar to turbulent Görtler instability transition. *Phys. Fluids*, 33(1).

[20] G. Danabasoglu, W. Large, and B. Briegleb. Climate impacts of parametrized nordic sea overflows. *J. Geophys. Res.*, 115:C11005, 2010.

[21] M. De Falco, C. Adduce, M. Negretti, and E. Hopfinger. On the dynamics of quasi-steady gravity currents flowing up a slope. *Advances in Water Resources*, 147: 103791, 2021.

[22] M. C. De Falco, C. Adduce, A. Cuthbertson, M. E. Negretti, J. Laanearu, D. Malcangio, and J. Sommeria. Experimental study of uni- and bi-directional exchange flows in a large-scale rotating trapezoidal channel. *Phys. Fluids*, 33(3):036602, 2021. doi: 10.1063/5.0039251.

[23] F. De Serio, E. Armenio, G. Badin, A. Di Leonardo, R. Hilel, D. Liberzon, M. Mossa, M. Negretti, G. Pisaturo, M. Righetti, J. Sommeria, D. Termini, T. Valran, B. Vermeulen, and S. Viboud. Experiments on rotating jets interacting with vegetation. *Exp. Fluids*, 62:218–33, 2021. doi: 10.1007/s00348-021-03297-2.

[24] S. Decamp and J. Sommeria. Scaling properties for turbulent gravity currents deviated by coriolis effects on a uniform slope. unpublished, 2009.

[25] A. Deloncle, P. Billant, and J.-M. Chomaz. Nonlinear evolution of the zigzag instability in stratified fluids: a shortcut on the route to dissipation. *J. Fluid Mech.*, 599:229–239, 2008.

[26] R. R. Dickson and J. Brown. The production of north Atlantic deep water: Sources, rates, and pathways. *J. Geophys. Res.: Oceans*, 99(C6):12319–41, 1994. doi: 10.1029/94JC00530.

[27] S. Décamp. *Etude en laboratoire d'un courant de gravité turbulent sur un talus continental*. PhD thesis, 2005. URL `http://www.theses.fr/2005GRE10236`. dir.: J. Sommeria, Océan, atmosphère, hydrologie, Grenoble 1 2005.

[28] T. H. Ellison and J. S. Turner. Turbulent entrainment in stratified flows. *J. Fluid Mech.*, 6(3):423–448, 1959.

[29] D. Etling, F. Gelhardt, U. Schrader, F. Brennecke, G. Kühn, G. d'Hieres, and H. Didelle. Experiments with density currents on a sloping bottom in a rotating fluid. *Dynamics of Atmospheres and Oceans*, 31:0–164, 2000. ISSN 0377-0265.

[30] D. Farmer and L. Armi. Stratified flow over topography: the role of small scale entrainment and mixing in flow establishment. *Proc. R. Soc. Lond.*, A455:3221–58, 1999.

[31] A. Fincham, T. Maxworthy, and G. Spedding. Energy dissipation and vortex structure in freely decaying sratified grid turbulence. *Dyn. Atm. Oceans*, 23:155–169, 1996.

[32] J. Floryan and W. Saric. Stability of Görtler vortices in boundary layers. *AIAA journal*, 20(3):316–324, 1982.

[33] M. Flynn and B. Sutherland. Intrusive gravity currents and internal gravity wave generation in stratified fluid. *J. Fluid Mech.*, 514:355 – 383, 2004. doi: 10.1017/S0022112004000400.

[34] M. Gacic, A. Rubino, L. Ursella, V. Kovacevic, M. Menna, V. Malacic, M. Bensi, M. Negretti, V. Cardin, M. Orlic, J. Sommeria, R. Viana Barreto, S. Viboud, T. Valran, B. Petelin, and G. Siena. Impact of the dense water flow over the sloping bottom on the open-sea circulation: Laboratory experiments and the Ionian Sea (Mediterranean) example. *Ocean Sci.*, 17:975–96, 2021. doi: 10.5194/os-17-975-2021.

[35] W. Geyer, A. Lavery, M. E. Scully, and J. Trowbridge. Mixing by shear instability at high reynolds number. *Geophysical Research Letters*, 37, 2010.

[36] M. Gibert. *Convection thermique turbulente: Panaches et Fluctuations*. PhD thesis, ENS LYON, 2007. URL `https://tel.archives-ouvertes.fr/tel-00268361`.

[37] F. S. Godeferd and C. Cambon. Detailed investigation of energy transfers in homogeneous stratified turbulence*. *Phys. Fluids*, 6(6):2084–2100, 1994. doi: 10.1063/1.868214.

[38] V. M. Grianik. The dynamics of singular geostrophic vortices in a two-level model of the atmosphere (ocean). *Akademiia Nauk SSSR Fizika Atmosfery i Okeana*, 19: 227–40, 1983.

[39] R. W. Griffiths and E. J. Hopfinger. Gravity currents moving along a lateral boundary in a rotating fluid. *J. Fluid Mech.*, 134:357–399, 1983. doi: 10.1017/S0022112083003407.

[40] L. Gu and G. Lawrence. Analytical solution for maximal frictional two-layer exchange flow. *J. Fluid Mech.*, 543:1–17, 2014.

[41] J. Gula, M. J. Molemaker, and J. C. McWilliams. Topographic generation of submesoscale centrifugal instability and energy dissipation. *Nat. Commun.*, 7:12811, 2016. doi: https://doi.org/10.1038/ncomms12811.

[42] K. Helfrich and U. Send. Finite-amplitude evolution of two-layer geostrophic vortices. *J. Fluid Mech.*, 197:337–48, 1988.

[43] N. Hogg and H. Stommel. Hetonic explosions: The breakup and spread of warm pools as explained by baroclinic point vortices. *J. Fluid Mech.*, 397:1–20, 1985a.

[44] J. Holyer and H. Huppert. Gravity currents entering a two-layer fluid. *J. Fluid Mech.*, 100:739–767, 1980.

[45] E. Hopfinger. Snow avalanche motion and related phenomena. *Ann. Rev. Fluid Mech.*, 15:47–76, 1983.

[46] J. Imberger and G. N. Ivey. On the nature of turbulence in a stratified fluid. part ii: Application to lakes. *Journal of Physical Oceanography*, 21(5):659 – 80, 1991. doi: 10.1175/1520-0485(1991)021¡0659:OTNOTI¿2.0.CO;2.

[47] E. C. Itsweire, K. N. Helland, and C. W. Van Atta. The evolution of grid-generated turbulence in a stably stratified fluid. *J. Fluid Mech.*, 162:299–388, 1986. doi: 10.1017/S0022112086002069.

[48] L. Jiang and R. Garwood. Three-dimensional simulations of overflows on continental slopes. *J. Phys. Ocean.*, 26(7):1214–33, 1996. doi: 10.1175/1520-0485(1996)026¡1214:TDSOOO¿2.0.CO;2.

[49] H. Johnson, A. Cuthberson, C. Adduce, M. Negretti, and J. Sommeria. Sediment transport and morphological implications for two-layer stratified rotating exchange flows. *J. Hydr. Res.* in preparation.

[50] J. Jungclaus and J. Backhaus. Application of a transient reduced gravity plume model to the Denmark Strait overflow. *J. Geophys. Res. Oceans*, 99C6:12375–96, 1994.

[51] R. Käse, J. Girton, and T. Sanford. Structure and variability of the Denmark Strait overflow: Model and observations. *J. Phys. Ocean.*, 108(12):15, 2003.

[52] Y. Kitamura and Y. Matsuda. Energy cascade processes in rotating stratified turbulence with application to the atmospheric mesoscale. *Journal of Geophysical Research: Atmospheres*, 115(D11), 2010. doi: 10.1029/2009JD012368.

[53] R. Kostaschuk, M. M. Nasr-Azadani, E. Meiburg, T. Wei, Z. Chen, M. E. Negretti, J. Best, J. Peakall, and D. Parsons. On the causes of pulsing in continuous turbidity currents. *J. Geophysi. Res.: Earth Surface*, 123(11):2827–2843, 2018. doi: https://doi.org/10.1029/2018JF004719.

[54] Y. Kyunghwan and Z. Warhaft. The evolution of grid-generated turbulence under conditions of stable thermal stratification. *J. Fluid Mech.*, 215:601–38, 1990. doi: 10.1017/S0022112090002786.

[55] N. Laanaia, A. Wirth, J.-M. Molines, B. Barnier, and J. Verron. On the numerical resolution of the bottom layer in simulations of oceanic gravity currents. *Ocean Sci.*, 6:563–572, 2010.

[56] G. F. Lane-Serff and P. G. Baines. Eddy formation by dense flows on slopes in a rotating fluid. *J. Fluid Mech.*, 363:229–252, 1998.

[57] G. F. Lane-Serff and P. G. Baines. Eddy formation by overflows in stratified water. *J. Phys. Ocean.*, 30(2):327–337, 2000.

[58] G. Lawrence, F. Browand, and L. Redekopp. The stability of a sheared density interface. *Phys. Fluids*, 3:2360–2370, 1991.

[59] S. Legg and J. Marshall. A heton model of the spreading phase of open-ocean deep convection. *J. of Phys. Ocean.*, 23(7):1040 – 1056, 1993.

[60] S. Legg, R. W. Hallberg, and J. Girton. Comparison of entrainment in overflows simulated by z-coordinate, isopycnal and non-hydrostatic models. *Ocean Modell.*, 11:69–97, 2006. doi: 10.1016/j.ocemod.2004.11.006.

[61] D. Lilly. Stratified turbulence and the mesoscale variability in the atmosphere. *J. Atm. Sci.*, 40:749, 1983.

[62] E. Lindborg. Can the atmospheric kinetic energy spectrum be explained by two-dimensional turbulence? *J. Fluid Mech.*, 388:259–88, 1999.

[63] E. Lindborg. Strongly stratified turbulence: An explanation to the energy spectra of the stratosphere. In *AGU Fall Meeting Abstracts*, volume 2002, pages NG71A–02, Dec. 2002.

[64] E. Lindborg. The energy cascade in a strongly stratified fluid. *J. Fluid Mech.*, 550: 207–242, 2006. doi: 10.1017/S0022112005008128.

[65] M. Maggi, M. Negretti, and C. Adduce. Lock-exchange gravity currents over a rough bottom. *Special Issue Env. Fluid Mech.*, 2021. submitted.

[66] M. Maggi, M. Negretti, and C. Adduce. On the formation of ripples in downslope gravity currents over a sediment floor. *Env. Fluid Mech.*, 2021. in preparation.

[67] M. M. Maqueda, A. Willmott, and N. Biggs. Polynya dynamics: a review of observations and modeling. *Rev. Geophys.*, 42(1):–, 2004.

[68] A. Martin, M. E. Negretti, and E. J. Hopfinger. Development of gravity currents on slopes under different interfacial instability conditions. *J. Fluid Mech.*, 880:180–208, 2019.

[69] A. Martin, M. E. Negretti, M. Ungarish, and T. Zemach. Propagation of a continuously supplied gravity current head down bottom slopes. *Phys. Rev. Fluids*, 5: 054801, 2020.

[70] T. Maxworthy and R. Nokes. Experiments on gravity currents propagating down slopes. part 1. the release of a fixed volume of heavy fluid from an enclosed lock into an open channel. *J. Fluid. Mech.*, 584:433–453, 2007.

[71] T. Maxworthy, J. Leilich, J. Simpson, and E. Meiburg. The propagation of a gravity current into a linearly stratified fluid. *J. Fluid Mech.*, 453:371–394, 2002.

[72] M. McCartney. The interaction of zonal currents with topography with applications to the southern ocean. *Deep Sea Res.*, 23:413–27, 1976.

[73] C. Meyer and P. Linden. Stratified shear flow: experiments in an inclined duct. *J. Fluid Mech.*, 753:242–253, 2014.

[74] M. Molemaker, J. McWilliams, and W. Dewar. Submesoscale instability and generation of mesoscale anticy- clones near a separation of the california undercurrent. *J. Phys. Ocean.*, 45:613, 2015.

[75] Y. Morel, J. Gula, and A. Ponte. Potential vorticity diagnostics based on balances between volume integral and boundary conditions. *Ocean Mod.*, 138:23–35, 2019. ISSN 1463-5003. doi: https://doi.org/10.1016/j.ocemod.2019.04.004.

[76] B. R. Morton, G. I. Taylor, and J. S. Turner. Turbulent gravitational convection from maintained and instantaneous sources. *Proc. the Roy. Soc. London. A*, 234 (1196):1–23, 1956. doi: 10.1098/rspa.1956.0011.

[77] M. Mory, M. Stern, and R. Griffiths. Coherent baroclinic eddies on a sloping bottom. *J. Fluid. Mech.*, 183:45–62, 1987. doi: 10.1017/S0022112099007661.

[78] M. Mossa, R. Goldshmid Hilel, D. Liberzon, M. Negretti, J. Sommeria, D. Termini, and F. De Serio. Quasi-geostrophic jet-like flow with obstructions. *J. Fluid Mech.*, 921:112, 2021. doi: 10.1017/jfm.2021.501.

[79] A. Muraro. Dynamics and structure of coherent eddies generated by gravity currents. Master's thesis, LEGI, CNRS, Grenoble, France, 2021. dir.: A. Wirth and M.E. Negretti, LEGI.

[80] M. Negretti, A. Rummel, S. Socolofsky, and G. Jirka. Stabilization of cylinder wakes inshallow water flows by means of roughness elements : an experimental study. *Exp. Fluids.*, 38:403–14, 2005.

[81] M. Negretti, A. Martin, and F. Naaim Bouvet. On the propagation of the front speed of lock released density clouds. *Env. Fluid Mech.*, October 2021.

[82] M. E. Negretti and P. Billant. Stability of a gaussian pancake vortex in a stratified fluid. *J. Fluid Mech.*, 718:457– 480, 2013.

[83] M. E. Negretti, G. Vignoli, M. Brocchini, and M. Tubino. On shallow wakes: an analytical study. *J. Fluid Mech.*, 567:457–75, 2006.

[84] M. E. Negretti, D. Zhu, and G. Jirka. Barotropically induced interfacial waves in a two-layer stratified exchange flow down a sill. *J. Fluid Mech.*, 592:135–154, 2007.

[85] M. E. Negretti, S. Socolofsky, and G. Jirka. Linear stability analysis of inclined two-layer stratified flows. *Phys. Fluids.*, 20:094104, 2008.

[86] M. E. Negretti, D. Zhu, and G. Jirka. The effect of bottom roughness in two-layer flows down a slope. *Dyn. Oceans Atm.*, 45:46–68, 2008.

[87] M. E. Negretti, E. Hopfinger, and J.-B. Flor. Development of a gravity current on rapidly changing slopes. *J. Fluid Mech.*, 833:70–97, 2017.

[88] M. E. Negretti, F. L. Tucciarone, and A. Wirth. Intruding gravity currents and re-circulation in a rotating frame: Laboratory experiments. *Phys. Fluids*, 33(9): 096607, 2021. doi: 10.1063/5.0058629.

[89] G. Parker, Y. Fukushima, and H. Pantin. Self accelerating turbidity currents. *J. Fluid Mech.*, 171:145–181, 1986.

[90] G. Pawlak and L. Armi. Mixing and entrainment in developing stratified currents. *J. Fluid Mech.*, 424:45–73, 2001.

[91] J. Pedlosky. *Geophysical Fluid Dynamics*. Springer, 1987.

[92] S. Pierini, P. De Ruggiero, M. Negretti, J. Sommeria, I. Schiller Weiss, J. Weiffenbach, and H. Dijkstra. Laboratory experiments reveal self-sustained intrinsic oscillations in ocean relevant rotating fluid flows. *Nature Sci. Rep.*, 2022. in press.

[93] O. Praud, A. Fincham, and J. Sommeria. Decaying grid turbulence in a strongly stratified fluid. *J. Fluid. Mech.*, 522:1–33, 2005. doi: 10.1017/S002211200400120X.

[94] M. Rastello and E. Hopfinger. Sediment-entraining suspension clouds: a model of powder-snow avalanches. *J. Fluid Mech.*, 509:181–206, 2004.

[95] J. Riley and S. M. DeBruynKops. Dynamics of turbulence strongly influenced by buoyancy. *Phys. Fluids*, 15:2047–2059, 2003.

[96] A. Rubino, M. Gačić, M. Bensi, V. Kovačević, V. Malačič, M. Menna, M. E. Negretti, J. Sommeria, D. Zanchettin, R. V. Barreto, L. Ursella, V. Cardin, G. Civitarese, M. Orlić, B. Petelin, and G. Siena. Experimental evidence of long-term oceanic circulation reversals without wind influence in the North Ionian Sea. *Sci. Rep.*, 10:1905, 2020. doi: https://doi.org/10.1038/s41598-020-57862-6.

[97] B. S. and S. S. Dynamics of a stratified shear layer with horizontal shear. *J. Fluid Mech.*, 568:19–54, 2006.

[98] H. Salehipour, W. Peltier, and C. Caulfield. Self-organized criticality of turbulence in strongly stratified mixing layers. *J. Fluid Mech.*, 856:228–256, 12 2018. doi: 10.1017/jfm.2018.695.

[99] H. E. Seim and M. C. Gregg. Detailed observations of a naturally occurring shear instability. *J. Geophys. Res.: Oceans*, 99(C5):10049–10073, 1994. doi: 10.1029/94JC00168.

[100] G. Shapiro and A. Hill. Dynamics of dense water cascades at the shelf edge. *J. Phys. Ocean.*, 27:2381–2394, 11 1997.

[101] F. Shi, C. Chickadel, and T. e. a. Hsu. High-resolution non-hydrostatic modeling of frontal features in the mouth of the columbia river. *Estuaries and Coasts*, 40: 296–309, 2017.

[102] H. Shi, M. Negretti, J. Chauchat, K. Blanckaert, U. Lemmin, and D. Barry. Unconfined plunging process of a hyperpycnal river flowing into a lake: Laboratory experiments and numerical modelling. *Water Res. Research*, 2021. submitted October 2021.

[103] J. S. Simpson. Gravity currents in the laboratory, atmosphere and ocean. *Ann. Rev. Fluid Mech.*, 14:213–234, 1982.

[104] W. D. Smyth and J. N. Moum. Ocean mixing by Kelvin-Helmholtz instability. *Oceanography*, 25(2):140–149, 2012.

[105] M. Spall. Dynamics of downwelling in an eddy-resolving convective basin. *J. Phys. Ocean.*, 10:2341, 2010. doi: 10.1175/2010JPO4465.1.

[106] C. Staquet and J. Sommeria. Internal gravity waves: From instabilities to turbulence. *Annual Review of Fluid Mechanics*, 34(1):559–593, 2002. doi: 10.1146/annurev.fluid.34.090601.130953.

[107] H. G. Stefan and T. R. Johnson. Negatively buoyant flow in diverging channel. iii: Onset of underflow. *J. Hydr. Eng.*, 115(4):423–436, 1989. doi: 10.1061/(ASCE)0733-9429(1989)115:4(423).

[108] G. E. Swaters. Numerical simulations of the baroclinic dynamics of density-driven coupled fronts and eddies on a sloping bottom. *J. Geophys. Res. Oceans*, 103(C2): 2945–61, 1998. doi: https://doi.org/10.1029/97JC02441.

[109] I. Tani. Production of longitudinal vortices in the boundary layer along a concave wall. *J. Geophys. Res.*, 67:3075?80, 1962.

[110] E. Tedford, J. Carpenter, R. Pieters, and G. Lawrence. Instabilities in a tilting channel with open ends. *Proceedings of the 7th Int Symp. Strat Flows Rome*, -:–, 2011.

[111] S. Thorpe. The stability of statically unstable layers. *J. Fluid Mech.*, 260:315–331, 1994.

[112] J. Turner. In *Buoyancy effects in fluids*, pages –. Cambridge University Press, 1973.

[113] H. van Haren and L. Gostiaux. A deep-ocean Kelvin-Helmholtz billow train. *Geoph. Res. Lett.*, 37:3605, 2010.

[114] C. Vic, G. Roullet, X. Capet, X. Carton, M. Molemaker, and J. Gula. Eddy-topography interactions and the fate of the Persian Gulf Outflow. *J. Geophys. Res. Oceans*, 120:6700–17, 2016. doi: 10.1002/2015JC011033.

[115] M. Waite and P. Bartello. Stratified turbulence dominated by vortical motion. *J. Fluid Mech.*, 517:281–308, 2004.

[116] M. L. Waite and P. Smolarkiewicz. Instability and breakdown of a vertical vortex pair in a strongly stratified fluid. *J. Fluid Mech.*, 606:239–273, 2008.

[117] V. Weitbrecht, D. Seol, M. Negretti, M. Detert, G. Kuehn, and G. Jirka. Piv measurements in environmental flows. *J. Hydr. Res.*, 5(4):231–45, 2011.

[118] J. Wenegrat, J. Callies, and L. Thomas. Submesoscale baroclinic instability in the bottom boundary layer. *J. Phys. Ocean.*, 48:2571–92, 2018.

[119] A. Wirth. On the basic structure of oceanic gravity currents. *Ocean Dynamics*, 59: 551–563, 08 2009.

[120] A. Wirth. Estimation of friction parameters in gravity currents by data assimilation in a model hierarchy. *Ocean Sci.*, 7:245–255, 2011.

[121] A. Wirth. Laminar and weakly turbulent oceanic gravity currents performing inertial oscillations. *Ocean Sci.*, 8:301–307, 2012.

[122] A. Wirth and M.-E. Negretti. The circulation of (non) intruding gravity currents and their re-circulation in a rotating frame. *Ocean Model.*, 2021. submitted.

[123] M. Worster and A. M. Leitch. Laminar free convection in confined regions. *J. Fluid Mech.*, 156:301–19, 1985.

[124] E. Yankovsky and S. Legg. Symmetric and baroclinic instability in dense shelf overflows. *J. Phys. Ocean.*, 49:39, 2019. doi: 10.1175/JPO-D-18-0072.1.

[125] T. Zemach, M. Ungarish, A. Martin, and M. E. Negretti. On gravity currents of fixed volume that encounter a down-slope or up-slope bottom. *Phys. Fluids*, 31(9): 096604, 2019. doi: 10.1063/1.5121290.

[126] G. Zodiatis, P. Drakopoulos, S. Brenner, and S. Groome. Variability of the Cyprus warm core eddy during the CYCLOPS project. *Deep Sea Res. Part II*, 52(22): 2897–2910, 2005. doi: 10.1016/j.dsr2.2005.08.020.